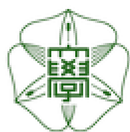
HOKKAIDO UNIVERSITY

Title	Studies on Photoacid Generators for the Next-generation Photolithography
Author(s)	朝倉, 敏景
Citation	北海道大学. 博士(理学) 甲第11581号
Issue Date	2014-09-25
DOI	10.14943/doctoral.k11581
Doc URL	http://hdl.handle.net/2115/59838
Type	theses (doctoral)
File Information	Toshikage_Asakura.pdf

Instructions for use

Hokkaido University Collection of Scholarly and Academic Papers : HUSCAP

Studies on Photoacid Generators for the Next-generation Photolithography

次世代フォトリソグラフィーのための光酸発生剤の研究

Toshikage Asakura

2014

Chapter 1
General Introduction

Photolithography is a technique to transfer a circuit pattern drawn on a mask to a photo-reactive material coated on a silicon wafer and is currently indispensable in fabrication of semiconductor devices (Fig. 1). In this technology, circuit patterns are created on the surface of silicon wafer in the following manner: (1) coating a formulation including photo-sensitive compounds (photoacid generator, PAG) and reactive polymeric material that changes solubility on reaction with acid, (2) photo irradiation to promote acid generation and polymer reaction, and (3) washing the surface with an alkaline developer (development).[1]

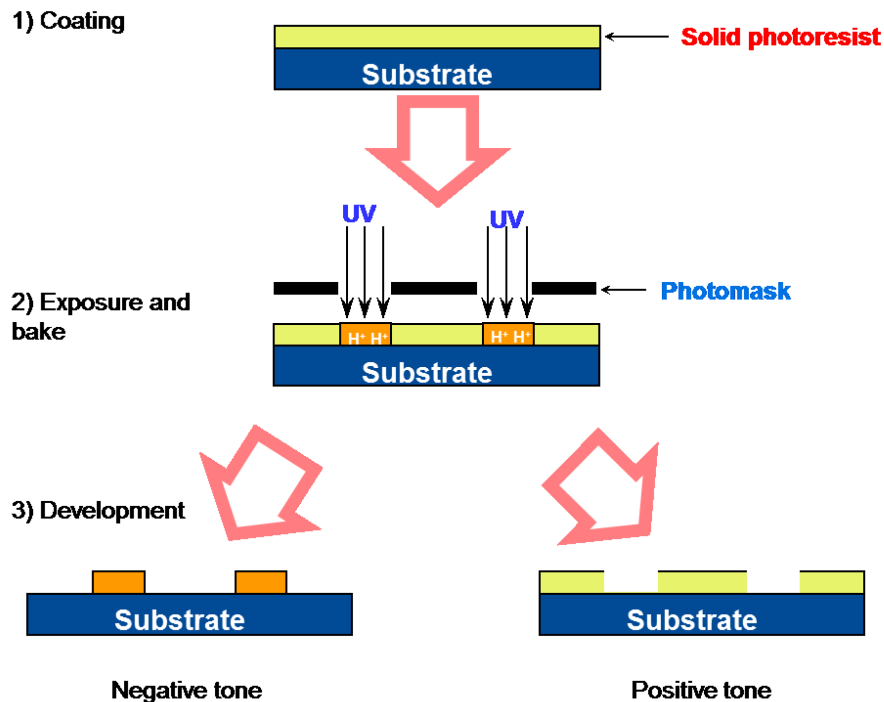

Fig. 1. A conceptual diagram of photolithography.

One of the most important issues in photolithography technology is "miniaturization" making the size of circuit patterns as thin or narrow as possible. In general, a narrower line width in circuit patterns can realize a higher degree of circuit integration of semiconductor devices.[2] The main factor limiting the wire width is energy of the light source irradiating the masked silicone substrate. As for this aspect, in 1878, Abbe (Jena University) established for optical microscopes that special

resolution is principally decided by the wavelength of the incident light for observation and is expressed by the following equation:

$$d = \lambda / 2\ NA$$

where d is resolution or minimal size that can be observed (the Abbe limit) and NA is NA is numerical aperture of the lens of a microscope. In case NA can reach about 1.4 in modern optics, the Abbe limit is $d = \lambda / 2.8$.

The Abbe limit concept has been extended to photolithography. A widely accepted, general understanding in photolithography technology is that the minimal size of a developed wire line (d) is half the wavelength of the irradiating light (λ) where the maximum number of numerical aperture (NA) of the optics is 1.[3]

More precisely and specifically to photolithography, resolution in photolithography is determined by the Reyleigh's equation:

$$R = k_1 \times \lambda / NA$$

where k_1 is "process factor" which sums up various factors involved in industrial processing affecting resolution, l is wavelength of light, and NA is numerical aperture of the lens used in photolithography apparatus. Though through several factors including surface light scattering properties and resist and matrix polymers' properties that are expressed as k_1 in this equation, the size of wire line is critically dependent of the wavelength the source light. Due to this reason, wavelength of source light kept becoming shorter since the early commercial development of photolithography in 1980's using g-line (435 nm) and i-line (365 nm) which are obtained from a high pressure mercury lamp. With g-line irradiation, resolution down to 0.8 μm can be realized while with i-line processing line width of down to 0.5μm was initially possible. Through developments of resist polymers and highly-transparent lens materials leading to a high NA, 0.28 μm line width has been achieved by now with i-line irradiation.

As a next major improvement of shortening wavelength to the DUV region (< 300 nm), KrF excimer laser (248 nm) irradiators were commercialized. With KrF irradiation, a problem came up with Novolac resin-diazonaphthoquinone resist materials, which had been the most-often chosen before the KrF development, that is, the resist material cannot be sufficiently excited as the resin strongly absorbs. In order to overcome this point with KrF irradiation, "chemically amplified photoresist (CAPR)" technique was developed. CAPR's generally consist of a matrix polymer having an acid-sensitive side chain group, a "photoacid generator (PAG)", and a solvent dissolving the aforementioned two.

Further advances aiming at narrower circuit lines, ArF excimer laser (193 nm) developers have been commercialized since early 2000's. With ArF, similarly to KrF, positive-type resist is the main stream. Technologies accumulated for light sourced up to KrF are believed to be applicable also to ArF. As a future light source for photolithography, extreme UV (EUV) (13.5 nm) light irradiation is currently under development but it is not yet on the practical level.

This thesis work focuses on developments of novel PAG's for practical usages. PAG's studied here are oxime sulfonates including 2,2,2-trifluoro-1-{4-(3-[4-{2,2,2-trifluoro-1-(1-propanesulfonyloxyimino)-ethyl}-phenoxy]-propoxy)-phenyl}-ethanone oxime 1-propanesulfonate. In the CAPR technique, a PAG generates an acid on photo irradiation (Scheme 1).[4] The acid hydrolyzes the side chain of the matrix polymer in the following thermal processes, leading to a drastic change in polarity of the resist material from hydrophobic to hydrophilic (Fig. 2).

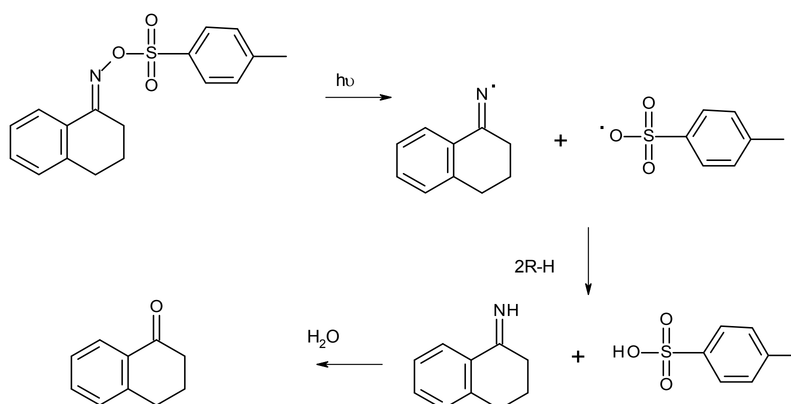

Scheme 1. General reaction diagram for PGA degradation leading to formation of acid.

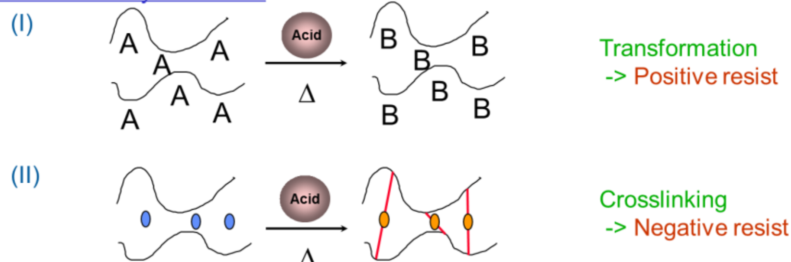

Fig. 2. Acid generation (1) and positive and negative resist reactions (2).

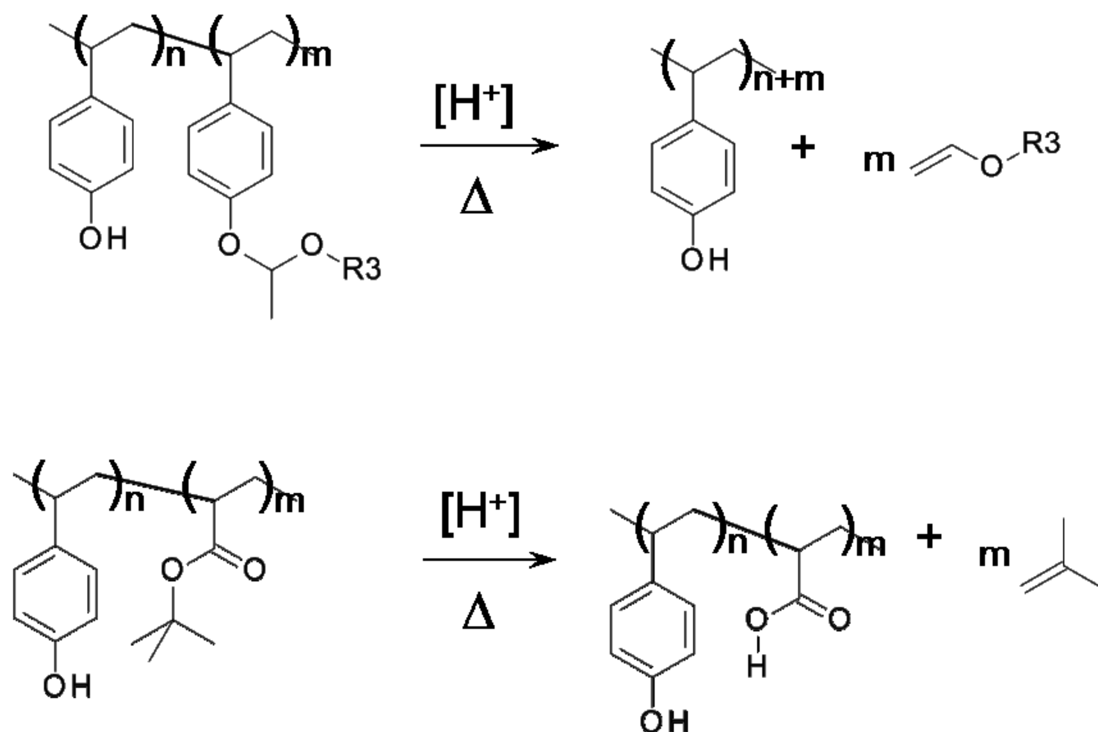

Scheme 2. Examples of reaction chemistry in positive-tone chemically amplified photo resists. (Upper: deprotection of acetal protection group, lower: decomposition of tertiary ester group)

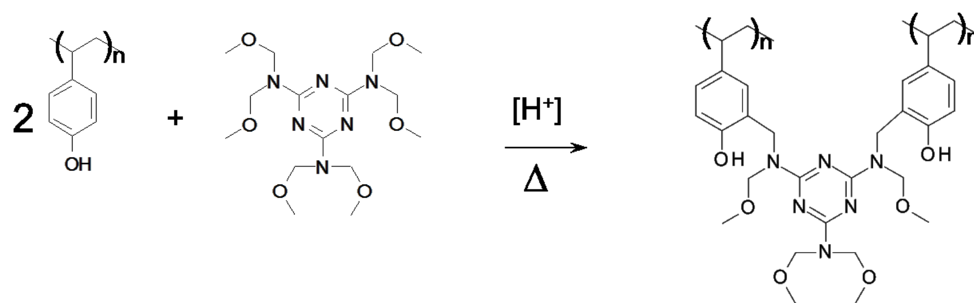

Scheme 3. An example of reaction chemistry in negative-tone chemically amplified photo resist. (crosslinking reaction with hexamethoxymethyl melamine)

Due to this change, the irradiated (exposed) part can be dissolved in and washed by a basic developer (positive-type photoresist). As a matrix polymer, poly(4-hydroxystyrene) with an acetal-type protecting group on the hydroxyl group and copolymers of 4-hydroxystyrene with tertiary alkyl methacrylate including *t*-butyl methacrylate are often used. These polymers show excellent photo-reactivity.

A general issue about PAG development is its sensitivity (reactivity). The shorter the light source wavelength is, the fewer photons are emitted at the same exposure energy level. More advanced exposure techniques hence require more sensitive PAG's. Therefore, studies aiming at highly reactive, practical PAG's are important. Prior to this thesis work, chloromethyltriazines as PAG's which are sensitive in a wide wavelength range including g-line and i-line and onium salts as PAG's which are sensitive in the DUV region had been developed and studied in detail. However, chloromethyltriazines photochemically generate hydrochloric acid which is highly volatile and corrosive, and this may be a concern regarding substrate compatibility, device reliability and potential damage of the manufacturing equipment. As for onium salts, their low solubility in organic solvents due to high polarity hampers their practical usage. In addition, onium salts are often not stable enough as a part of a CAPR mixture on storage from a practical view.

In this work, the author synthesized oxime sulfonates as novel PAGs, studied their properties such as absorbance, photo-sensitivity, heat-resisting properties, and solubility and found that the new PAG's are suitable, not only for g-line and i-line but also are applicable to KrF and ArF exposures.

The ultimate goal of this work was to increase "photosensitivity" of photolithography system. Photosensitivity is defined as follows:

Photosensitivity = (absorbance of PAG) x (quantum yield of PAG photo reaction) x (acid strength) x (acid mobility in matrix)

Among the five elements in this equation, it was reported that quantum yield of acid generation in photo reaction from ionic PAG, i.e., triphenylsulfonium salt, is in the range of 0.26 - 0.4 in solid state and 0.74 - 0.8 in solution.[5] Strength of generated acids is in the range of -2 - -13 in pKa.[6] Acid mobility in matrix is also an important factor for "amplification" of reaction with polymer side chain. Although a low mobility is necessary in creating a narrower circuit pattern, it generally leads to a low sensitivity in photoresist. Hence, an optimal (compromised) mobility has to be achieved for a target resolution. As absorbance of PAG varies depending sensitively on its chemical structure, a focus in this thesis work was to modify PAG chemical structure in order to optimize absorbance properties of PAGs. In the model formulations employed in this thesis, PAG loading against solid contents was in the range of 2 - 5 to achieve reasonable photo-sensitivity and concentrations of solid contents in model formulations were varied in the range of 3.4% for EUV exposure to 28% for g-line due to the differences of target resolution and thickness.

[Survey of this thesis]

This thesis is composed of seven chapters:

Chapter 1 is General Introduction describing background of this thesis work and summarizing problems and solutions.

Chapter 2 describes properties of newly developed oxime sulfonates PAGs which are non-ionic and halogen-free. While they were originally developed for the exposure under i-line (365 nm), they were found to be sensitive enough not only under i-line but also g-line (436 nm) and DUV (254 nm) due to its broad absorption profile. In addition, they exhibited high solubility in propylene glycol monomethyl ether acetate (PGMEA), which is one of the most frequently-used solvents in practical applications. Further, they were thermally stable up to 140 °C in a phenolic matrix (poly(hydroxystyrene): PHS); based on this character, they had enough storage stability for industrial applications. It was possible to store them without any deterioration at 40 ºC for more than a year. Moreover, chemically amplified (CA) negative tone photoresist formulations comprising the novel compounds were examined.

Chapter 3 deals with oxime sulfonate-type PAGs developed for the CA photoresist application under the exposure at DUV (254 nm). The PAG described in this chapter are all non-ionic, and they effectively generated propanesulfonic acid, octanesulfonic acid, camphorsulfonic acid and toluenesulfonic acid under DUV exposure and trifluoromethanesulfonic acid under ArF exposure, in CA photoresist formulations. The application-relevant properties of the non-ionic PAGs, *i.e.,* solubility in frequently used solvents, such as PGMEA, ethyl lactate, and 2-heptanone, UV absorption, thermal stability with or without poly(4-hydroxystyrene), volatility, and photosensitivity in model photoresists were studied and discussed. Furthermore, the microlithography simulation was conducted to predict the resolution limit.

Chapter 4 discusses structures and properties of PAGs for ArF (193 nm) exposure. As this type of PAGs, 2-[2,2,3,3,4,4,5,5,-6,6,7,7-dodecafluoro-1-(nonafluorobutylsulfonyloxyimino)-heptyl]fluorene (DNHF), 2-[2,2,3,3,4,4,4-heptafluoro-1-(nonafluorobutylsulfonyloxyimino)-butyl]fluorene (HNBF), and 2-[2,2,3,3,4,4,-5,5-octaf1uoro-l-(nonafluorobutylsulfonyloxyimino)pentyl]fluorene (ONPF) were developed and were found to be applicable to ArF photoresist. For these three PAGs, DNHF, HNBF and ONPF, in order to evaluate photo efficiency, quantum yields in solution and in a model formulation under ArF exposure were measured and compared with those of conventional ionic PAGs, *i.e.,* triphenylsulfonium perfluorobutanesulfonate (TPSPB) and bis(4-*tert*-butylphenyl)iodonium perfluorobutanesulfonate (BPIPB). On the basis of the fact that fluorinated alkyl chains led to differences not in transparency and photo efficiency at 193 nm but also in coating property and

contact angle of the coated formulation, the author concluded that one terminal hydrogen atom of fluoroalkyl chains of DNHF and ONPF played an important role in the coating of photoresist.

Chapter 5 discusses photoresist applications of DNHF and HNBF as non-ionic PAGs under an ArF immersion lithography which is one of the latest exposure techniques. PAG leaching from a coated model photoresist formulation into water as an immersion media was investigated in detail during the process of immersion lithography. DNHF and HNBF showed no clear leaching under the process while significant amount of TPSPB as a reference sample was significantly eluted. These results indicate that a risk of contamination onto the surface of the objective lens under immersion exposure process can be minimized by using this type of non-ionic PAG chemistry. Through dissolution rate monitoring (DRM) which gives information on the fundamental dissolution properties of photoresists, no significant difference was confirmed on dry and immersion exposures, strongly suggesting that the resolution limit achievable in dry photoresist can be expected also under immersion lithography conditions.

Chapter 6 deals with investigations on fundamental aspects of traditional PAG additive approach in EUV lithography, the next generation exposure system. Four sulfonium nonafluorobutanesulfonate-type PAGs, *i.e.*, triphenylsulfonium nonafluorobutanesulfonate (TPS), tri(4-methoxy-3,5-dimethyl-phenyl) sulfonium nonafluorobutanesulfonate (MDP), tri(4-methoxy-3-methylphenyl)sulfonium nonafluorobutanesulfonate (MMP), and tri(4-methoxy-3-phenylphenyl)sulfonium nonafluorobutanesulfonate (MPP) were compared in two different polymer platforms, PHS type and poly(methacrylates) type, and under two different exposure techniques, ArF and EB exposures. Through these investigations, influences of PAG structure on photoresist fundamental properties, such as sensitivity, photo efficiency, and lithographic achievements were discussed.

Chapter 7 concludes this thesis. The author concludes the properties of newly synthesized PAGs in this study, discusses overall relationships between PAG structures and characters, and comments further development of the studies in future.

References

1. For example, H. Ito, *Resist Materials*, Chapter 1, Kyoritsu Shuppan, Tokyo, **2005**.
2. *"PROCESS INTEGRATION, DEVICES, AND STRUCTURES"*, **2011** edition, The International Technology Roadmap for Semiconductors.
3. E. Abbe, *Archiv für Mikroskopische Anatomie*, **1878,** *9* (1), 413 - 468.
4. M. Shirai, et al., *Makromol. Chem., Rapid Commun*., **1984**, *5*,689 - 693.
5. J-P Fouassier, et al., *Radiation curing in polymer science and technology: practical aspect and application, Page 273,* Springer, Berlin, **1993**.
6. *"Ionization Constants of Heteroatom Organic Acids"* published from Michigan State University at http://www.cem.msu.edu/~reusch/OrgPage/acidity2.htm.

Chapter 2

Studies on novel photoacid generator for i-line exposure

Abstract

A new class of compounds, (2-alkylsulfonyloxyimino-2*H*-thiophen-3-ylidene)-2-methylphenyl-acetonitriles, characterized as non-ionic and halogen-free photoacid generators (PAG's) was developed. The compounds generate various kinds of sulfonic acids, such as methane, n-propane, and camphor sulfonic acid under the g-line (436 nm), i-line (365 nm) and Deep UV (DUV, 248 nm or shorter) exposure and are applicable for chemically amplified (CA) photoresists. The application-relevant properties of the compounds such as solubility in propylene glycol monomethyl ether acetate (PGMEA), UV absorption, thermal stability with or without poly (4-hydroxystyrene), storage stability in a neat form, sensitivity in some model resist formulations and dissolution inhibition efficiency during development process were evaluated. The compounds exhibit enough solubility in PGMEA, red-shifted UV absorption (λ_{max}: 405 nm), good thermal stability up to 140 °C in a phenolic matrix, effective acid generation in terms of quantum yield in an acetonitrile solution and high sensitivity in negative tone and positive tone CA resist formulations, such as *tert*-butylester type and *t*-BOC type formulations, with g-line, i-line, and DUV exposure. The photochemical decomposition reaction of the compound was also studied. Additionally a scanning electron microscope (SEM) photography as an application example of microlithography by the CA negative tone resist with the PAG is presented.

Introduction

CA resist technology is predominantly driven by the demand for ultra-high resolution required for advanced memory chips and microprocessors. DUV exposure and specifically designed resist materials are usually required for such applications. For lower resolution, conventional diazonaphthoquinone positive resist technology is well established and utilizes exposure at i-line and g-line.[1] Although not yet widely applied, CA negative resists suitable for i-line and g-line exposure are expected to show advantages over conventional positive resists in certain applications. For example, they do not require overexposure to remove an edge bead and would be preferable for isolated features and patterns which cover only a minor area of the substrate. Also reduced defect densities, due to less particle contamination impact on lithographic patterning, are expected with negative resists in such cases. One example where these preconditions apply might be the thin-film-transistor (TFT) manufacturing process for flat panel displays. Other advantages are the high thermal and chemical resistance of cross-linked CA negative resists. For example, they withstand harsh ion-implantation conditions without additional thermal or DUV hardening processing steps. It is therefore desirable to make new PAG's available, which fulfill the requirements for use in CA resists not only for DUV exposure but also for i-line and g-line.

Chloromethyl triazines with extended conjugation are known as suitable PAG's for i-line and particularly for g-line exposure.[2] However hydrochloric acid photochemically generated from chloromethyl triazines is highly volatile and corrosive and can be a concern regarding substrate compatibility, device reliability and potential damage of the manufacturing equipment.

Sulfonic acids are less volatile, less mobile, and less corrosive and are therefore preferred over hydrochloric acid in resist applications.

A few sulfonic acid generators sensitive up to g-line are known. Brunsvold and coworkers reported N-sulfonyloxy-2,3-diphenylmaleimide derivatives suitable as near-UV sensitive PAG's which, however, suffered from low g-line sensitivity due to its low absorption.[3] 4-Nitrobenzyl-9,10-dimethoxyanthracene-2-sulfonate (NBAS) reported by Yamaoka and coworkers showed relatively good quantum yield at g-line.[4] However this type of compounds offers the limited structural variation because the photodissociation reaction of this compound depends on the intramolecular energy transfer from its dimethoxyanthracene moiety to *p*-nitrobenzyl moiety.

The author has been investigating oxime sulfonates type PAG's[5] which can be adjusted to the target applications and exposure wavelength range by selection from a wide range of chromophores and acid moieties. Additionally, non-ionic oxime sulfonates show good solubility in various solvents and compatibility with a wide range of polymers in various formulations.

In this chapter, examples of a novel class of non-ionic and halogen-free PAG's, (2-methylsulfonyloxyimino-2*H*-thiophen-3-ylidene)-2-methylphenyl-acetonitrile (MTMA), (2-camphorsulfonyloxyimino-2*H*-thiophen-3-ylidene)-2-methylphenyl-acetonitrile (CTMA), and (2-propylsulfonyloxyimino-2*H*-thiophen-3-ylidene)-2-methylphenyl-acetonitrile (PTMA) are reported. It has been evaluated application-relevant properties such as solubility, thermal stability, storage stability in neat form, UV absorption, photochemistry, sensitivity in model photoresists with g-line, i-line and 254 nm (DUV region) exposure, dissolution inhibition in a poly(*tert*-butylacrylate-co-hydroxystyrene)-type model formulation, and feasibility for use in microlithography.

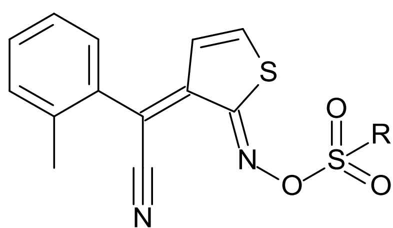

R = Methyl Propyl Camphor

MTMA PTMA CTMA

Experimental

Materials. In polymers, poly(4-hydroxystyrene) and a copolymer of 4-hydroxystyrene, styrene and *tert*-butyl acrylate (69/22/9 mol-%, Mw=9850) were purchased from Maruzen Petrochemical Co., Ltd and employed as received.

In solvents and developers, propyleneglycol monomethyl ether acetate (PGMEA, from Tokyo Kasei Kogyo Co., Ltd), acetonitrile (from Wako Pure Chemical Industries, Ltd.), and 2.38 % aqueous tetramethyl ammonium hydroxide solution (TMAH, from Tokyo Ohka Kogyo Co., Ltd.) were purchased and employed as received.

In chemicals: hexa(methoxymethyl)melamine (from Dyno-Cytec), Rhodamine B base (from Aldrich), methane sulfonic acid (from Tokyo Kasei Kogyo Co., Ltd), triphenylsulfonium trifluoromethane sulfonate (from Midori Kagaku Co., Ltd.), and 2-[2-(5-methylfuran-2-yl)vinyl]-4,6-bis(trichloromethyl)-1,3,5-triazine (from Midori Kagaku Co., Ltd.) were purchased and employed as received. Bis(cyclohexylsulfonyl)diazomethane, MTMA, PTMA, and CTMA were synthesized internally by the know procedures.[6]

Solubility. Solubility of the compounds was determined by UV absorption measurement of the saturated solution in PGMEA. By comparing the absorption with that of the standard concentration, 0.01 g/L, the solubility was determined.

Thermal properties. DSC analysis was carried out under nitrogen to evaluate melting points (Tm) and decomposition temperatures (T_d) with a Mettler DSC 30 system.

T_d was determined as the onset value of the exothermic reaction at a scanning rate of 10 °C/min. These measurements were performed for the neat compounds and also in the presence of the same amount of partially hydrogenated poly(4-hydroxystyrene) (PHS), MARUKA LYNCUR PHMC, obtained from Maruzen Petrochemical Co., Ltd.

Storage stability in neat form. MTMA was stored as a solid at 60 °C, 40 °C, room temperature (ca. 23 °C), and 4 °C for one year and tested for trace acid in frequent intervals. A solution of the MTMA in acetonitrile at a concentration of 10 g/L was prepared. 0.35 mL of a 1 g/L solution of Rhodamine B base, which was employed as an acid indicator,[7] in acetonitrile was added to 3.15 mL of the MTMA solution. The acid concentration in the sample was determined by measuring the absorption at 575 nm of the protonated form of Rhomaine B. For calibration, a solution of methane sulfonic acid in acetonitrile was used.

UV absorption. UV absorption of the compounds was measured in acetonitrile solutions at concentration of 0.01 and 0.50 g/L with a Hitachi U-3300 spectrometer.

Photochemistry. MTMA was dissolved in acetonitrile at a concentration of 0.01 g/l and irradiated with a Xenon lamp (USHIO UI-501) through a g-line narrow bandpass filter. Samples of the irradiated solution were taken after 0, 10, 30, 60, 120, 240, and 360 min exposure time and the UV absorption of each sample was measured. The amount of the generated acid in the samples was determined by the indicator dye method described above.

To determine the photolysis quantum yield, Φ_d, the stirred PAG solution in acetonitrile was monochromatically irradiated through a g-line bandpass filter for 10 min in an optical cuvette. The exposure light intensity was measured with an Oak UV- MO2 intensity probe**.**

The Φ_d of the PAG is defined by Equation I.

$$\Phi_d = N_{Dec} / N_{Abs} \qquad \text{[Equation I]}$$

Where

$$N_{Abs} = (1-10^{-A})\, W\, S\, t\, \lambda / h\, c$$

$$N_{Dec} = (1-B)\, C\, V\, L$$

$$A = (A_0 + A_f) / 2$$

$$B = A_f / A_0$$

The definitions of abbreviations in the above equations are; N_{Dec}, number of dissociated molecules; W, intensity of the exposure (W); S, exposed area (cm^2); t, exposure time (sec); λ, wavelength of exposed light (nm); *h,* Planck constant; *c,* the light speed; N_{Abs}, number of absorbed photon; C, concentration of the solution (M); V, volume of the sample (L); *L,* Avogadro number; A_0, absorbance of the sample before exposure; A_f, absorbance of the sample after exposure; and A, approximate average absorbance of the sample during irradiation.

The quantum yield for acid generation, Φ_a, was derived from the measured acid concentration and exposure dose.

Photosensitivity. Photosensitivity was measured in three different formulations with two different exposure tools, a Canon mask aligner PLA 501 for i-line and g-line exposure and a Canon mask aligner PLA 521 for 254 nm (DUV) exposure. Melamine-cross-linker-based acid catalyzed negative resist formulations were used with i-line and g-line exposures. *t*-BOC as well as poly(*tert*-butyl acrylate-co-4-hydroxystyrene)-type chemically amplified positive tone resists were DUV exposed at

254 nm. The negative tone resists were based on 10 mol-% hydrogenated poly-(4-hydroxystyrene) (MARUKA LYNCUR PHMC). The positive tone resists utilized 40 mol% *tert*-butoxycarbonylated poly-(4-hydroxystyrene) as the polymer binder for *t*-BOC type resist and a copolymer of 4-hydroxystyrene, styrene and tert-butyl acrylate (69/22/9 mol-%, Maruzen Petrochemical Co., Ltd) having a weight average molecular weight of 9850 in the *tert*-butyl acrylate type resist formulation, respectively. In the negative tone resist, hexa(methoxymethyl)melamine (Cymel 301 from Dyno-Cytec) served as a crosslinker. In all cases the resist solvent was PGMEA (Tokyo Kasei Kogyo Co., Ltd). The compositions of the formulations are described in the Table 1.

The resists were spin-coated on silicon wafers and prebaked at 110 °C for 60 sec. After exposure through a multi density mask, a post exposure bake was applied at 110 °C for 60 sec. and the resists were then developed in 2.38 % aqueous tetramethyl ammonium hydroxide solution for 60 sec and rinsed 30 seconds in water. Thickness was measured mechanically with an Alpha Step 200 profiler (Tencor Instruments), or optically with an Axiospeed film thickness measurement instrument from Zeiss. Only in the case of *tert*-butyl acrylate-type resist formulations, baking process was carried out at 140 °C for 90 seconds. In the latter cases the developer concentration was additionally reduced to 1.78 % in order to adjust the polymer dissolution rate to a suitable level of 100 nm/min.

For comparison, three PAG's were investigated in terms of sensitivity and dissolution inhibition property, triphenylsulfonium trifluoromethane sulfonate (TPST) as a typical ionic DUV PAG, bis(cyclohexylsulfonyl)diazomethane (BCSD) as a representative non-ionic DUV PAG and 2-[2-(5-methylfuran-2-yl)vinyl]-4,6-bis(trichloromethyl)-1,3,5-triazine (MFVT), representing a well known class of i-line and g-line PAGs.

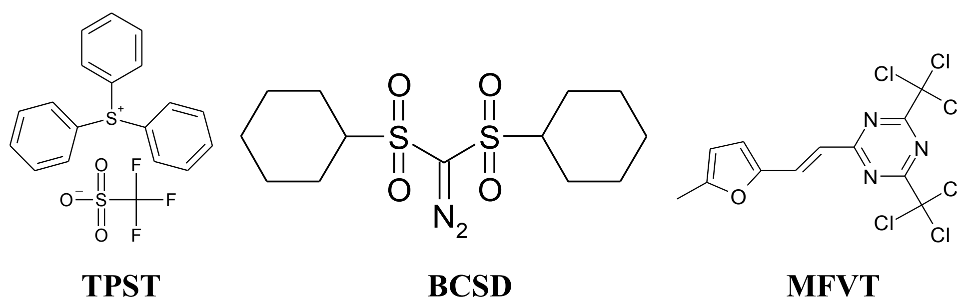

Table 1. Composition of the formulations

Composition	1	2	3
wavelength (nm)	356, 436	254	254
binder polymer (parts)	65	100	100
PAG (parts)	5	4	4
cross-linker (parts)	30	-	-
solvent (parts)	257	400	475

Dissolution inhibition for positive resists. The resist dissolution rate, R_{min}, for unexposed resist was determined from the slope of the remaining thickness vs. development time plot. A normalized R_{min} , NR_{min}, was calculated by dividing R_{min} by the polymer dissolution rate. NR_{min}, is used in this work as a measure for the PAG's dissolution inhibition. The smaller NR_{min} is the better for the inhibition of polymer dissolution by the PAG in the unexposed resist regions.

Microlithography. To demonstrate the microlithographic feasibility of MTMA, a negative tone model photoresist formulation was prepared with a ratio of PHMC/ PAG/cross-linker of 70/5/25 by weight and coated on a 4 inch silicon wafer at a thickness of 4.2 µm. A 1.5µm dense line pattern was contact printed with Canon PLA 501 mask aligner equipped with a g-line narrow band filter. As for the scanning electron microphotograph observation, JEOL JSM 5200 was employed.

Results and discussion

Solubility. As shown in Table 2, all new non-ionic compounds exhibited superior solubility (8.3 - 20.1%) in PGMEA compared to TPST (1.2%) which is a representative ionic PAG. Good solubility minimizes the risk of particle generation during resist storage and improves formulation flexibility.

Table 2. Solubility in PGMEA

Compound	Solubility (%)
MTMA	9.4
PTMA	20.1
CTMA	8.3
TPST	1.2

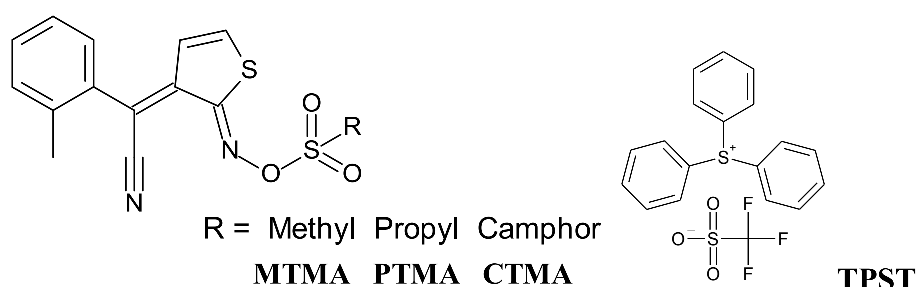

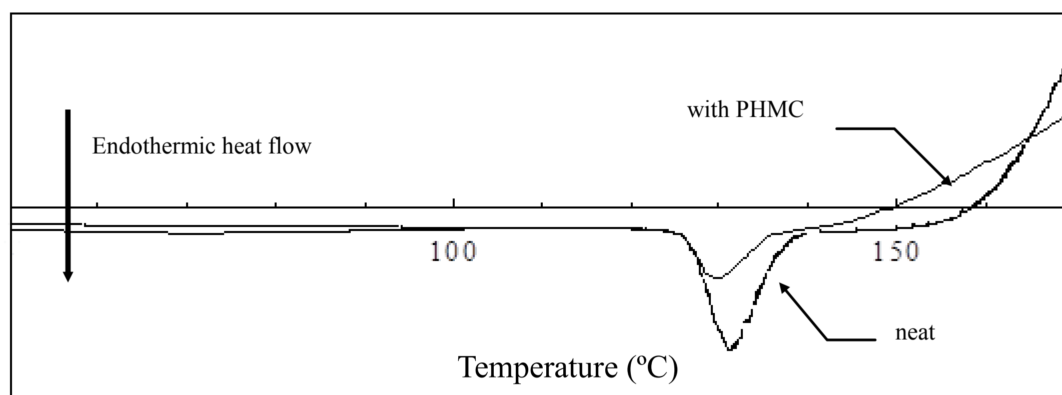

Fig. 1. DSC curves of the MTMA in neat state or with PHMC

Thermal stability. The DSC curves of MTMA, with and without PHMC, are plotted in Fig. 1. PAG melting was observed at 133 °C. Neat MTMA exhibits its T_d at 155 °C. In the presence of PHMC a reduction of T_d by 15 °C was observed. This reduced thermal PAG stability in the presence of phenolic resins is well known and documented for a variety of PAG's, independent of their chemical structure.[8] Even if blended with phenolic resin, MTMA exhibits sufficiently high thermal stability (140 °C) for resist pre- and post-bake processes typically performed in the 100 - 120 °C

temperature range.

The acquired data are summarized in Table 3. No acid size effect was observed on Td in neat state and in phenolic (PHMC) polymer matrix.

Table 3. Melting point (T_m) and decomposition point (T_d)

Compound	T_m (° C)	T_d neat (° C)	T_d in PHS (° C)
MTMA	133	155	140
PTMA	96	155	140
CTMA	139	155	141

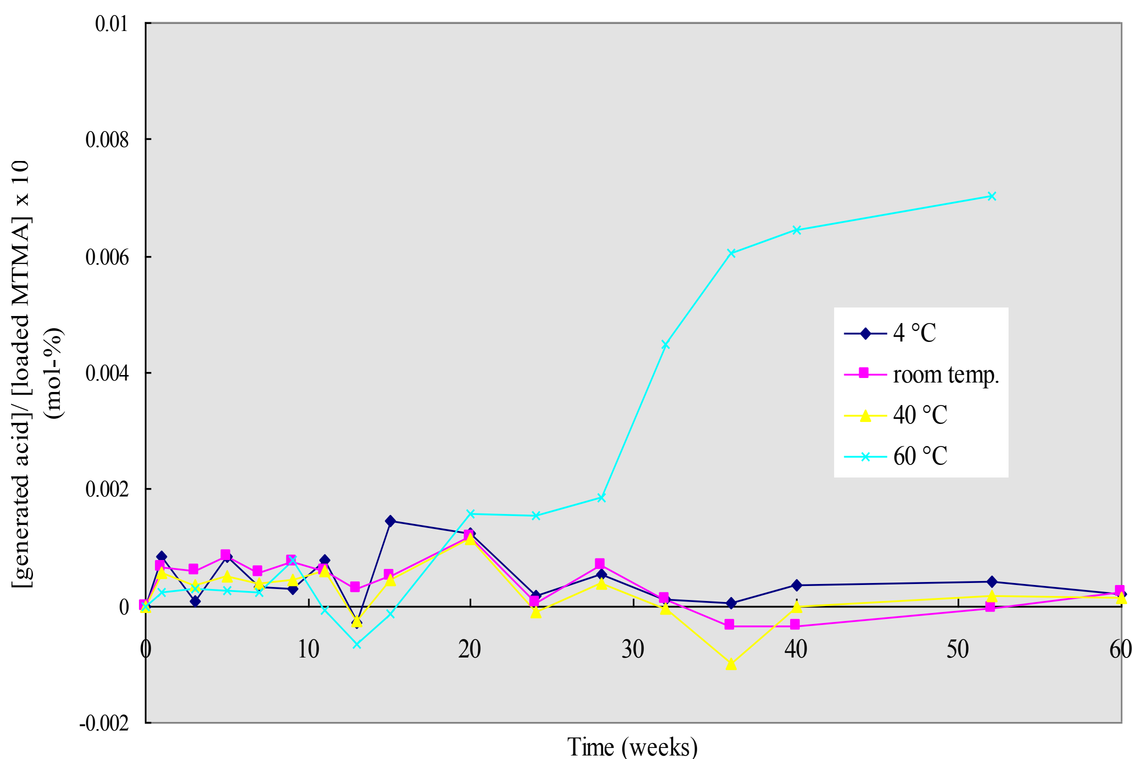

Fig. 2. Storage stability of MTMA

Storage stability in neat form. As even catalytic concentration of acid can cause degradation of CA photoresists, it is important that the PAG is stable and does not thermally decompose to form acid under ambient conditions. The amount of acid formed during storage of the neat PAG at different temperatures and prolonged storage time was measured. In Fig. 2 the relative (normalized to initial PAG concentration) acid amount is plotted against storage time up to 60 weeks at temperatures up to 60 °C. No acid formation was observed after more than 1 year storage if the temperature did not exceed 40 °C. Only stored at 60 °C, less than 0.008 mol-% of acid (relative to

100 mol% of PAG) was generated during this period.

UV absorption. Fig. 3 shows UV absorption of MTMA. Its enlarged conjugation chain length shifted λ_{max} to 405 nm (ε = 9340). Brunsvold and coworkers reported *N*-sulfonyloxy-2,3-diphenylmaleimide derivatives suitable as near-UV sensitive PAG's which, however, suffered from low g-line sensitivity due to low absorption at g-line.[3] The absorption of MTMA, as well as of PTMA and CTMA are sufficiently red-shifted. Their long-wavelength absorption is close to that of the red-shifted triazine, MFVT. Additionally, the absorption at i-line is significantly lower than that of MFVT, which allows good light penetration of thick resist films. The absorption spectrum extends into the DUV, which provides sensitivity over a wide spectral range.

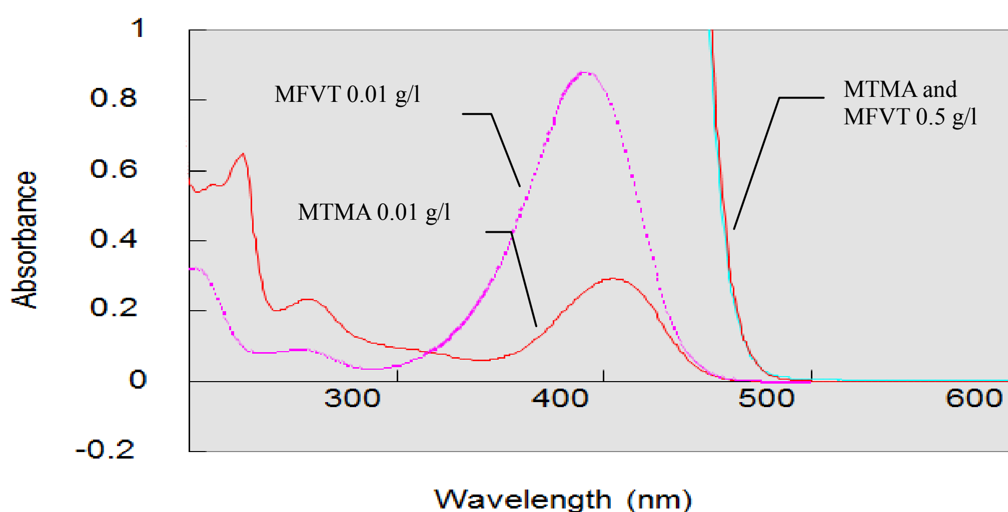

Fig. 3. UV absorption spectra

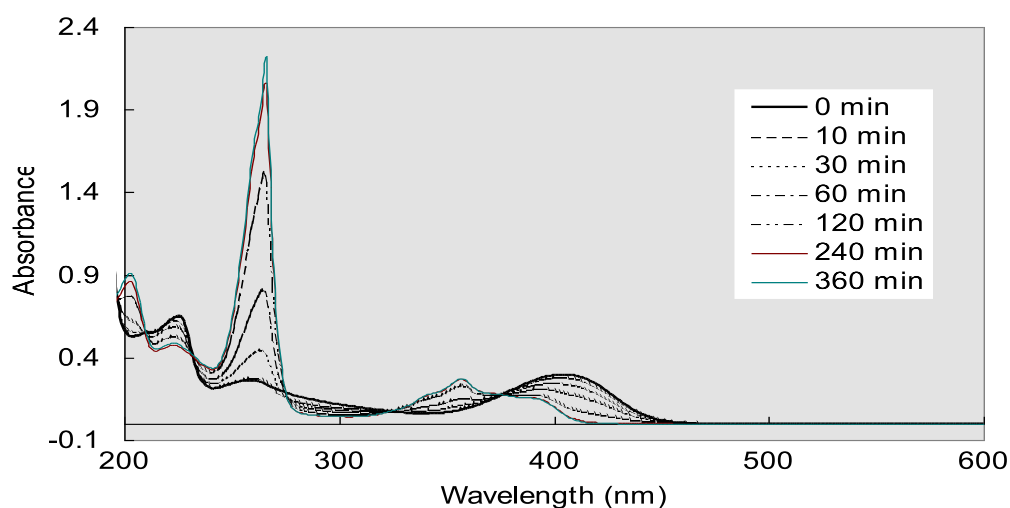

Fig. 4-a. Change of UV absorption in the area from 200 to 600 nm

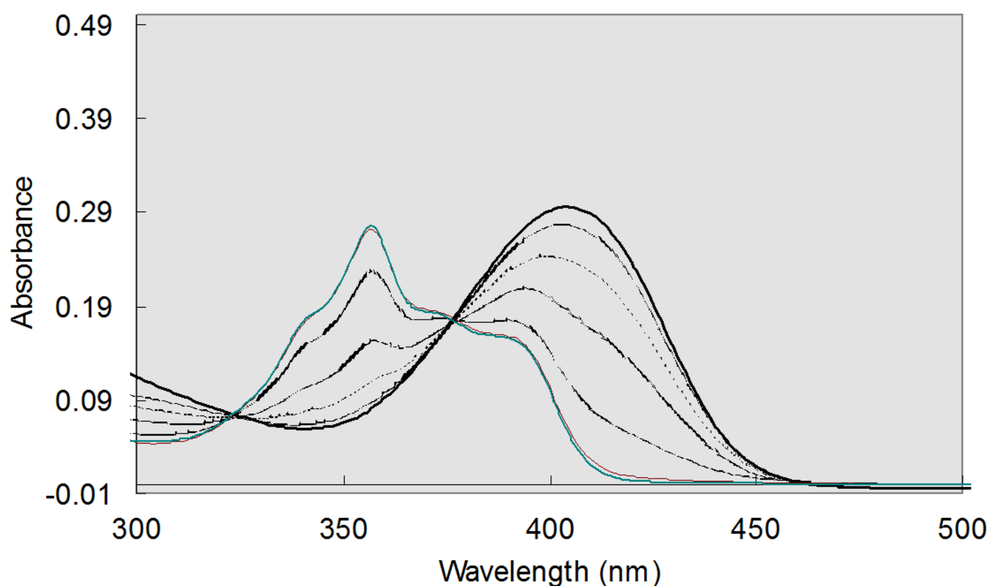

Fig. 4-b. Change of UV absorption in the area from 300 to 500 nm

Photochemistry. Fig. 4-a and Fig. 4-b show the change of the UV absorption of MTMA in acetonitrile solution upon exposure to g-line monochromatic light. A distinctive absorption at 255 nm was generated during exposure (Fig. 4-a). The change clearly indicates that the MTMA is photochemically converted to other species. The absorption above 375 nm decreased with exposure time and the one above 420 nm completely disappeared at high exposure dose (Fig. 4-b).

The quantum yield of photolysis, Φ_d, was determined from the absorption decrease at g-line according to Equation I as shown in the Table 4.

Table 4. Photolysis Quantum Yield (Φ_d)

Compound	Φ_d
MTMA	0.15
PTMA	0.13
CTMA	0.12

The observed differences in quantum yield among compounds comprising different size of acid moiety were less than 20 %. As reported by Neenan and coworkers in a quantum yield study for a different class of PAG's, the size of the acid group did not much affect the quantum yield here as well.[9]

Yamaoka and coworkers reported that NBAS can be photochemically cleaved with g-line exposure (Φ_d = 0.12).[4] The evaluated new PAG's exhibited at least equivalent quantum yields to that of NBAS.

The experiments for quantum yield determination were carried out under air and nitrogen. No differences of the quantum yields were observed between these two. This result suggests that oxygen does not play a significant role under the experiment conditions.

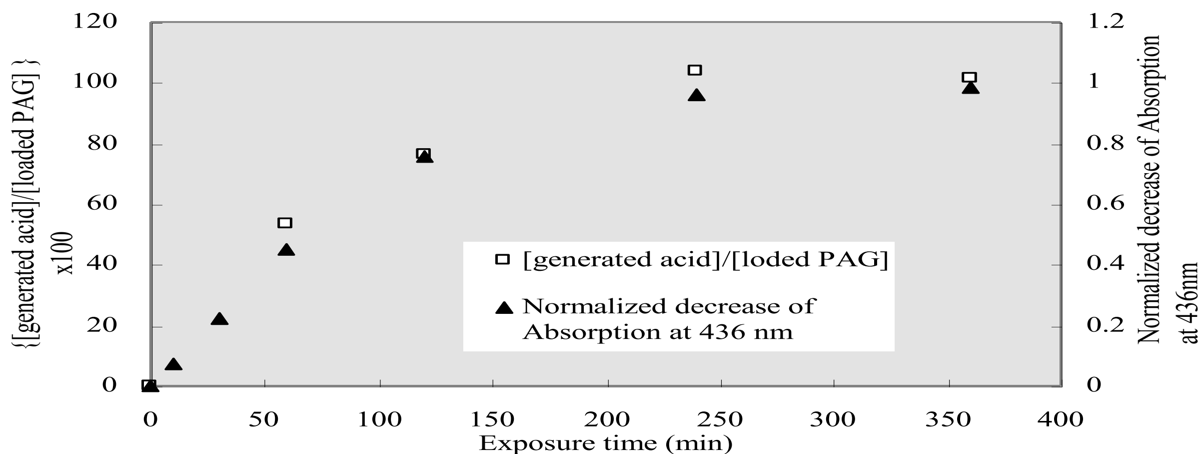

Fig. 5. The ratio of the generated acid concentration against the loaded PAG concentration and normalized decrease of absorption at g-line vs. exposure time plot.

In Fig. 5, the decrease of the normalized absorption at g-line and the normalized molar acid concentration (relative to initial molar PAG concentration) of the photochemically generated acid were plotted against exposure time. It was found that the decrease of absorption at g-line (photobleaching) was - within the error of measurement - equal to the generated acid concentration when both were normalized to the initial molar PAG concentration. This result suggests that the PAG is quantitatively photo-decomposed into acid. Therefore, the quantum yield for photolysis of MTMA, Φd, corresponds directly to that for acid formation, Φ_a, thus

$$\Phi_a / \Phi_d = 1$$

The reported Φ_a / Φ_d ratios for oxime sulfonates were found in the range of 0.6 - 0.8.[10] As a consequence, it was found that MTMA provides good or superior photoacid generation efficiency, based on acid conversion yield. The mechanism of the photo-cleavage is currently under more detailed investigation.

In the case of MFVT, no acid was detected after 4 hours irradiation. This surprising result is supported by data from Cameron and coworkers who reported a lower acid generation quantum yield of Φ_a = 0.009 - 0.013 in acetonitrile upon 308 nm exposure for 2-[2-(furan-2-yl)vinyl]- 4,6-bis(trichloromethyl)-1,3,5-triazine.[11] The chloromethyl triazine is a close analog to MFVT used in this study for comparison.

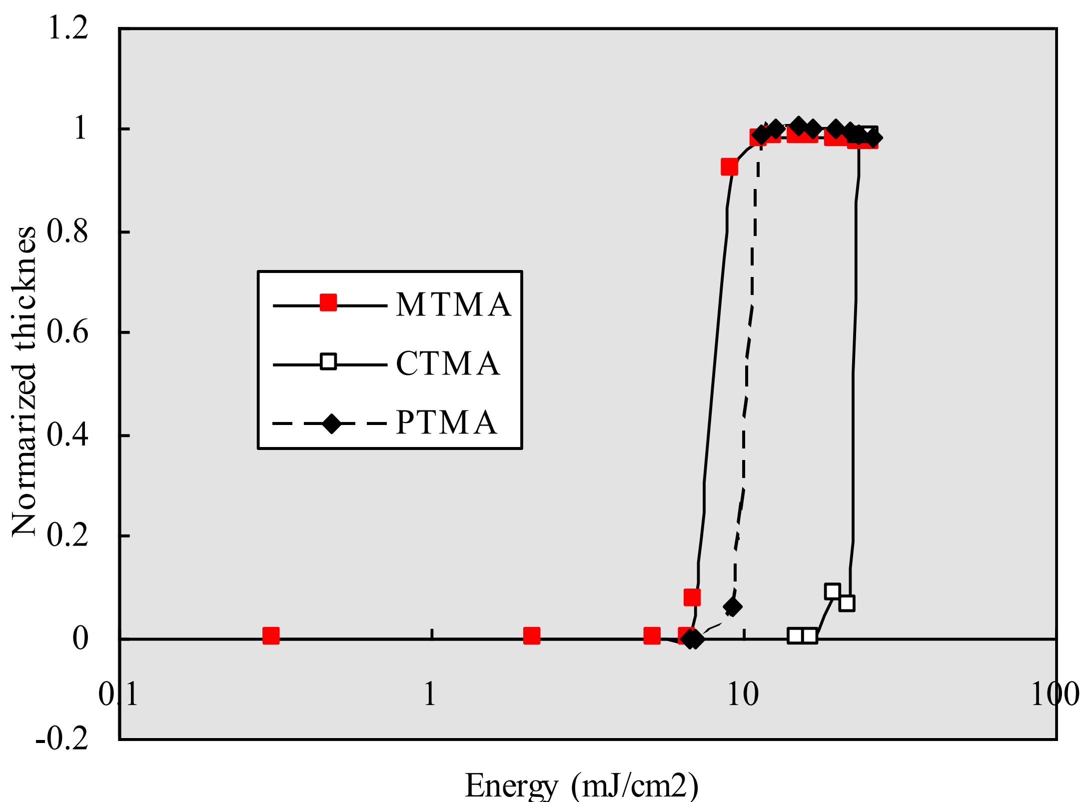

Fig. 6. Contrast curves of MTMA, CTMA and PTMA in a negative tone photoresist upon exposure at g-line

Photosensitivity. Fig. 6 shows the contrast curves of MTMA CTMA, and PTMA in the negative tone model photoresist exposed at g-line. Excellent cross-linking and high contrast were obtained, indicating the potential for practical use in negative photoresists. With increasing size of the acid moiety from methyl to propyl and finally camphoryl, the resist sensitivity was reduced. The camphoryl group resulted in the most significant shift of the contrast curve towards higher dose. Considering that the quantum yield differences between CTMA and the methyl and propyl analogs are within 20%, the sensitivity differences between CTMA and others must be mainly caused by the different diffusion rates of the corresponding acids in the resist layer.

Table 5 summarizes the sensitivity data derived from the contrast curves. As a measure for sensitivity, dose to clear (E_0) was used for the positive resist and the dose necessary to obtain full resist thickness (E_1) was used for the negative resists. The positive DUV model resist was exposed at 254 nm and the negative near-UV model resists were exposed at i-line and g-line through narrow bandpass filters. The photosensitivity of MTMA in *t*-BOC type-resist DUV formulation was similar to the one with TPST. In addition, high photospeed, close to the one of MFVT was obtained in

negative tone formulations with both, i-line and g-line exposures. Also PTMA gave comparable sensitivity to TPST in *tert*-butyl acrylate-type positive DUV resist, exposed at 254 nm. BCSD showed the poorest sensitivity among the evaluated PAG's, probably due to its low absorption at 254 nm. It appears that the low acid formation quantum yield of the chloromethyl triazines is compensated by high diffusion of the relatively small and mobile hydrochloric acid molecules in the resist matrix and its higher acid strength.

Table 5. Sensitivity

Compound	Sensitivity : (mJ/cm^2)			
	E_0 /DUV *t*-BOC posi.	E_0 /DUV *tert*-butyl ester posi.	E_1 /i-line nega.	E_1 /g-line nega.
MTMA	12	0.70	14.1	9.3
PTMA	17	0.37	18.3	11.4
CTMA	-	1.76	30.1	23.5
cf.				
TPST	8.2	0.27	>1000	>1000
MFVT	-	-	5.1	6.4
BCSD	-	5.06	-	-

-) not measured.

Dissolution inhibition of PAG. The NR_{min} values, which are a measure of the respective PAGs' dissolution inhibition, is summarized in Table 6. Depending on the type of acid moiety, the NR_{min} value of the PAG's varied in the range from 0.37 to 1.76. MTMA and PTMA showed higher dissolution inhibition (lower NR_{min}) than BCSD. However both were still inferior to that of the ionic PAG, TPST.

Table 6. Dissolution inhibition

Compound	Normalized dissolution rate /NR_{min}
MTMA	0.46
PTMA	0.37
CTMA	1.76
TPST	0.13
BCSD	0.77

Microlithography. As displayed in the microphotograph, Fig. 7, a high aspect ratio image with excellent profiles was obtained for a 1.5 μm 1:1 dense pattern in the model negative resist. The image was contact printed by monochromatic g-line exposure with a Canon mask aligner PLA 501 by contact exposure. The aspect ratio of the pattern is 2.8.

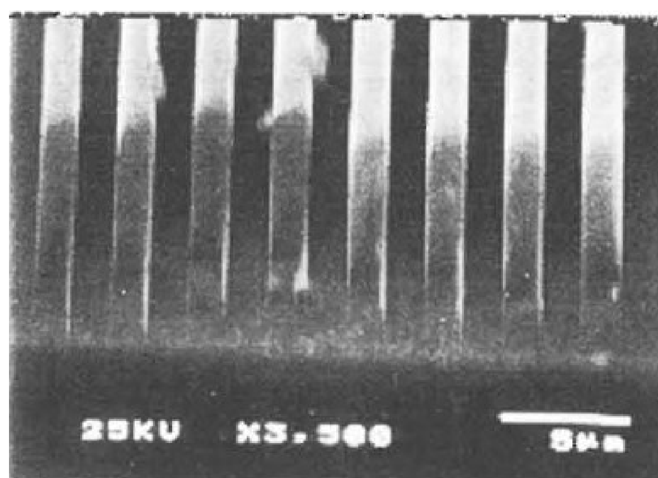

Fig. 7. SEM microphotograph of 1.5 μm line and space pattern.

Conclusion

A new class of PAG's, which are non-ionic, halogen-free, highly soluble in PGMEA and thermally stable up to 140 °C in a phenolic matrix, has been developed. The PAG's exhibit comparable or superior quantum yield to conventional PAG's upon g-line exposure. Photoresists comprising the new PAG's have good sensitivity at DUV, i-line, and g-line exposure. Feasibility for use in chemically amplified positive and negative tone resists was demonstrated.

References

1. For example, R. Dammel, *Diazonaphthoquinone-based Resists,* pp. 9-96, SPIE Optical Engineering Press, Washington, D. C., **1993**.
2. G. Buhr, R. Dammel and C. R. Lindley, *Polym. Mater. Sci. Eng.,* **1989**, *61*, 269-77.
3. W. Brunsvold, W. Montgomery and B. Hwang, *Proc. SPIE,* **1991**, *1466*, 368-76.
4. T. Yamaoka, T. Omote, H. Adachi, N. Kikuchi, Y. Watanabe and T. Shirosaki, *J. Photopolym. Sci. Technol.,* **1990,** *3*, 275-80.
5. G. Berner and W. Rutsch, U.S. patent 4540598.
6. H. Yamato et al., U.S. patent 6004724, **1999**.
7. G. Pohlers, J. C. Scaiano and R. Sinta, *Chem. Mater.,* **1997**, *9*, 3222-30.
8. G. G. Barclay, D. R. Medeiros and R. F. Sinta, *Chem. Mater.* **1995**, *7*, 1315-24.
9. T. X. Neenan, F. M. Houlihan, E. Reichmanis, J. M. Kometani, B. J. Bachman and L. F. Thompson, *Macromolecules,* **1990,** *23*, 145-50.
10. M. Shirai and M. Tsunooka, *Bull. Chem. Soc. Jpn*., **1998**, *71*, 2483-2507.F. Cameron, J. M. Mori, T. M. Zydowsky, D. King, R. Sinta, M. King, J. Scaiano, G. Pohlers, S. Virdee and T. Connolly, *Proc. SPIE,* **1998**, *3333*, 680-91.

Chapter 3

Studies on novel photoacid generator for 248 nm (KrF) exposure

Abstract

The author has developed new class of non-ionic oxime sulfonate PAG. The compounds generate various kinds of sulfonic acids, such as *n*-propane, *n*-octane, camphor and *p*-toluene sulfonic acid under Deep-UV exposure and trifluoromethanesulfonic acid under ArF exposure and are applicable for the corresponding chemically amplified (CA) photoresists. The application-relevant properties of the compounds such as solubility in propylene glycol monomethyl ether acetate (PGMEA), ethyl lactate, ethyl 3-ethoxypropionate, and 2-heptanone, UV absorption, thermal stability with or without poly(4-hydroxystyrene) (PHS), volatility, perfomance in model resist formulations were evaluated. In addition, the microlithography simulation based on the results of DRM results of the trifluoromethanesulfonate was also studied.

Introduction

The higher performance of the micro devices has been achieved by the shrinkage of the resist feature size that was derived from the development of lithography technology. The wavelength of the exposure light has been shorten from g-line (436 nm), i-line (365 nm) to KrF excimer laser (248 nm). In spite of the fact that the conventional diazonaphthoquinone (DNQ) positive resist technology is well established for i-line and g-line resists,[1] DNQ is not employable to KrF photoresist due to its high absorption problem. Thus the chemically amplified (CA) photoresist technology has been established for KrF photoresist. The photoacid generator (PAG) is one of the most important ingredients in photoresist to achieve the desirable resist profiles. In case of KrF CA photoresist, the PAG that releases weak acid, such as alkylsulfonic acid or arylsulfonic acid, is applicable to Deep-UV (DUV) photoresist.

For further miniaturization, ArF exposure system is developed. The ArF photoresist requires strong photoacid, such as perfluorinated alkylsulfonic acid, because the cleavage of ester bonding in binder polymers, i.e., *tert*-butyl methacrylate or 2-methyladamantyl methacrylate, is a key reaction during lithography process. For the ArF resists, several PAGs have been applied, for instance onium salts (iodonium sulfonates,[2] sulfonium sulfonates[3]), imide sulfonates[4] and so on.

The author has been investigating oxime sulfonates type PAGs[5-7] which are adjustable to the target applications and exposure wavelength range by modification of chromophores and acid moieties. Additionally, non-ionic oxime sulfonates show good solubility in various solvents and compatibility with a wide range of polymers in various formulations.

Recently it has been developed another new class of non-ionic oxime sulfonate PAGs (PAG A, PAG B, PAG C, PAG D and PAG E). All of them have an identical chromophore and release propanesulfonic acid, octanesulfonic acid, camphorsulfonic acid, and toluenesulfonic acid for DUV photoresists and trifluoromethanesulfonic acid for ArF photoresists, respectively. In this chapter, the application-relevant properties of this new class of non-ionic PAGs such as solubility in PGMEA, UV absorption, thermal stability with or without poly(4-hydroxystyrene), volatility, photochemical properties in model photoresists and microlithography simulation were described and compared with the conventional ionic and non-ionic PAGs. The compounds exhibit high sensitivity in positive CA resist formulations with DUV or ArF exposure, and good thermal stability.

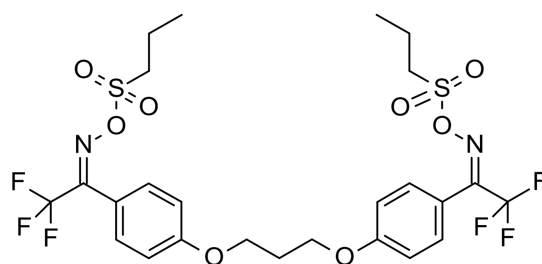

PAG A

Table 1. Acid moiety of new PAGs

Compound	Acid moiety
PAG A	Propanesulfonic acid
PAG B	Octanesulfonic acid
PAG C	Camphorsulfonic acid
PAG D	Toluenesulfonic acid
PAG E	Trifluoromethanesulfonic acid

Experimental

Materials. In polymers, poly-(4-hydroxystyrene), a copolymer of 4-hydroxystyrene, styrene and tert-butyl acrylate (69/22/9 mol-%, Mw=9850, from Maruzen Petrochemical Co., Ltd), and a copolymer of γ-butyrolactone methacrylate and 2-methyladamantyl methacrylate (54/46 mol-%, Mn=7600, from Mitsubishi Rayon Co., Ltd) were purchased and employed as received.

In solvents and developers, propyleneglycol monomethyl ether acetate (PGMEA, from Tokyo Kasei Kogyo Co., Ltd), acetonitrile (from Wako Pure Chemical Industries, Ltd.), ethyl lactate (from Tokyo Kasei Kogyo Co., Ltd), ethyl 3-ethoxypropionate (from Tokyo Kasei Kogyo Co., Ltd), 2-heptanone (from Tokyo Kasei Kogyo Co., Ltd), and 2.38 % aqueous tetramethyl ammonium hydroxide solution (TMAH, from Tokyo Ohka Kogyo Co., Ltd.) were purchased and employed as received.

In chemicals, triphenylsulfonium trifluoromethanesulfonate (TPST, from Midori Kagaku Co., Ltd.), bis(*p*-*tert*-butylphenyl)iodonium trifluoromethanesulfonate (BTIT, from Midori Kagaku Co., Ltd.), 5-norbornene-2,3-dicarboximidyl trifluoromethanesulfonate (NDIT, from Daychem), and a formulation of bottom antireflection coating (AR-19 from Shipley Company L.L.C.) were purchased and employed as received. Bis(cyclohexylsulfonyl)diazomethane (BCSD), (2-propylsulfonyloxyimino-2*H*-thiophen-3-ylidene)-2-methylphenyl-acetonitrile (PTMA), PAG A, PAG B, PAG C, PAG D and PAG E were synthesized internally by the know procedures.[8&9]

Solubility. Solubility of the compounds was determined by UV absorption measurement of the saturated solution in PGMEA. By comparing the absorption with that of the standard concentration, 0.01 g/L , the solubility was determined.

Thermal properties. DSC analysis was carried out under nitrogen to evaluate melting points (T_m) and decomposition temperatures (T_d) with a Mettler DSC 30 system.

T_d was determined as the onset value of the exothermic reaction at a scanning rate of 10 °C/min. These measurements were performed for the neat compounds. TGA was performed with a Mettler TG50 system at the heating rate of 10 °C/min to determine decomposition temperatures. The temperature at 5 % weight loss was recorded as Td^{TGA}.

UV absorption. UV absorption of the compounds was measured in acetonitrile solutions at concentration of 0.01 g/L with a Hitachi U-3300 spectrometer.

Volatility. A photoresist composed of poly(4-hydroxystyrene-*co*-styrene-*co*-*t*-butyl acrylate) (69:22:9 mol%) and 4 % photoacid generator (*Resist*) was spin-coated from PGMEA solution onto silicon wafers. As a detector layer, a film of only the above copolymer (*Detector*) was spin-coated from a solution in PGMEA on another set of Si-wafers, respectively. The wafers coated with *Resist* were baked on a hotplate at a relatively low temperature of 60 °C for 2 minutes in order to make its surface tack-free and to provide high sensitivity for this test. The wafers coated with *Detector* film were baked on a hotplate at 130 °C for 1 minute. Contacting a *Resist* wafer and a *Detector* wafer with their coated sides facing each other, the wafer stack was heated on a hotplate for 5 minutes at 130 °C with the *Resist* wafer contacting the hotplate in order to induce evaporation and to trap evaporated photoacid generator on the *Detector* film surface. The *Detector* film was then flood-exposed with 20 mJ/cm^2, (wavelength range 240 - 260 nm) post-exposure baked at 130 °C, developed with TMAH developer (1.785% TMAH aq) for 1 minute and the percent thickness loss upon development (ΔT) was measured. Additionally, a control experiment was carried out with a *Detector* film-wafer replacing the *Resist* wafer (no PAG present) and the percent thickness loss recorded.

The percentage of thickness loss, (ΔT) % (relative to thickness of the detector film prior to exposure and development), caused by the transfer of photoacid generator from the resist layer to the detector layer was determined as measure for each PAGs' volatility. It is plotted along with the result of the control experiment without PAG, for PAG A, TPST, and BCSD for comparison in Fig. 3.

Photochemical properties in model formulations. Photosensitivity of PAG A, PAG B, PAG C, and PAG D in a resist formulation was measured with a Canon mask aligner PLA 521 for 254 nm (DUV) exposure. For DUV photoresist formulation, a copolymer of (4-hydroxystyrene), styrene and *tert*-butyl acrylate (69/22/9 mol-%, Maruzen Petrochemical Co., Ltd) having a weight average molecular weight of 9850 was employed as a binder polymer. As the resist solvent PGMEA (Tokyo Kasei Kogyo Co., Ltd) was used without further purification. The compositions of the formulations are described in the Table 2.

The resists were spin-coated on silicon wafers and prebaked at 140 °C for 90 sec. After exposure through a multi density mask, a post exposure bake was applied at 140 °C for 90 sec. and the resists were then developed in 1.78% aqueous tetramethyl ammonium hydroxide solution for 60 sec and rinsed 30 seconds in water. Thickness was measured mechanically with an Alpha Step 200 profiler (Tencor Instruments), or optically with an Axiospeed film thickness measurement instrument from Zeiss. For comparison, three PAGs were investigated in terms of sensitivity,

triphenylsulfonium trifluoromethanesulfonate (TPST) as a typical ionic DUV PAG, bis(cyclohexylsulfonyl)diazomethane (BCSD) as a representative non-ionic DUV PAG and (2-propylsulfonyloxyimino-2*H*-thiophen-3-ylidene)-2-methylphenyl-acetonitrile (PTMA), which was developed by ourselves as versatile PAG for wide range of light source from g-line to DUV.

Photochemical properties of PAG E were measured in an ArF model resist formulation with VUVES 4500, Litho Tech Japan, as an exposure tool. The positive tone resist utilized a copolymer of γ-butyrolactone methacrylate and 2-methyladamantyl methacrylate (54/46 mol-%, Mitsubishi Rayon Co., Ltd) having a number average molecular weight of 7600. The composition of the formulation is also described in the Table 2.

The resist was spin-coated at 370 nm thickness on silicon wafers on which the bottom antireflection coating with AR-19 from Shipley Company L.L.C. was applied in advance at 80 nm thickness and prebaked at 120 °C for 60 sec. After exposure with various exposure doses, a post exposure bake was applied at 120 °C for 60 sec and the resist was then developed in 2.38% aqueous tetramethyl ammonium hydroxide solution for 120 sec with monitoring the resist thickness by RDA-790 (Litho Tech Japan).

For comparison, the PAGs shown below were investigated, TPST and bis(*p-tert*-butylphenyl)iodonium trifluoromethanesulfonate (BTIT) as typical ionic DUV PAGs, and 5-norbornene-2,3-dicarboximidyl trifluoromethanesulfonate (NDIT) as a representative non-ionic DUV PAG for ArF photoresists.[10]

The PAGs in the model formulation was coated on MgF_2 plate at 370 nm resist thickness and the transparency of the formulation at 193 nm was measured with VUVES 4500, Litho Tech Japan. From the transparency, the absorption of only PAG at 193 nm in the photoresist was calculated.

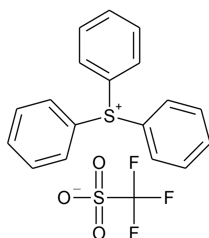

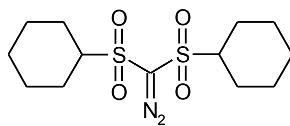

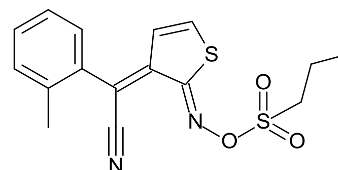

TPST **BCSD** **PTMA**

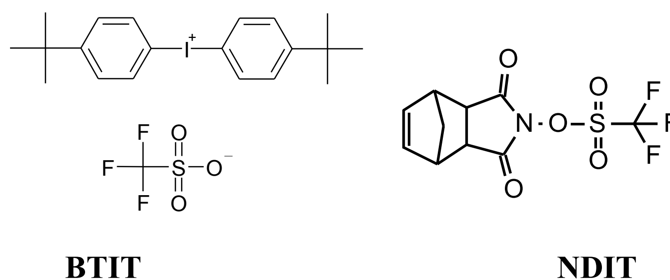

Table 2. Composition of the formulations

Photoresist composition	DUV	ArF
Binder polymer (parts)	100	100
PAG (parts)	4	2
Solvent (parts)	475	600

Microlithography simulation. To investigate the lithographic feasibility of PAG E, a lithography simulator, SOLID-CL, from SIGMA-C GmbH was employed.[11] The dissolution rate of the resist against exposure dose energy, R(E), data of PAG E and TPST acquired by dissolution rate monitoring experiments with RDA-790 was used for the simulation. The employed parameters were listed as below:

Refractive Index of the resist: n = 1.55
Wavelength: 193 nm
NA: 0.68
Exposure: annular
σ : out = 0.8 in = 0.6
Pattern for mask-linearity evaluation: 100 nm ~ 200 nm (10 nm step) line and space (L&S)
Optimum dose for mask-linearity evaluation: 170 nm
Pattern for exposure latitude evaluation: 130 nm L&S
Development time: 60 sec
Software: SOLID-C Ver.6.01

Results and discussion

Solubility. Author previously reported several oxime sulfonate type PAGs such as (2-alkylsulfonyloxyimino-2*H*-thiophen-3-ylidene)-2-methylphenyl-acetonitriles.[6] All of them were solved well over 5% in an organic solvent, PGMEA, which is widely used in photoresists. Similarly all new non-ionic compounds exhibited good solubility (>25%) in PGMEA comparing to TPST (1.2%), which is a representative ionic PAG, as shown in Table 3. The solubility of PAG A in other various solvents was also measured and the data is summarized in Table 4. In all solvents PAG A showed quite high solubility. The high solubility minimizes the risk of particle generation during resist storage and improves formulation flexibility.

Table 3. Solubility in PGMEA

Compound	Solubility (%)
PAG A	25
PAG B	–[1)]
PAG C	> 30
PAG D	> 30
PAG E	>30
TPST	1.2

1) PAG B is liquid and miscible in PGMEA.

Table 4. Solubility of PAG A in various solvents

Solvent	Solubility (%)
PGMEA	25
Ethyl lactate	> 30
Ethyl 3-ethoxypropionate	> 30
2-Heptanone	> 30

Thermal stability. Thermal stability of the new PAGs was evaluated by means of DSC measurements. Fig. 1 shows the DSC curves of PAG A in the presence and absence of PHS matrix.

After the endothermic peak corresponding to the melting (T_m) appeared at 60 °C, the exothermic heat flow corresponding to the decomposition (T_d) started from 204 °C in the absence of PHS. PHS has a harmful effect on the thermal stability of PAG A and decreased T_d by 16 °C. This reduced thermal PAG stability in the presence of phenolic resins was reported for (2-alkylsulfonyloxyimino-2*H*-thiophen-3-ylidene)-2-methylphenyl-acetonitriles previously[6] and well known for a variety of PAGs, independent of their chemical structure.[11] The data of T_m and T_d of the new PAGs is summarized in Table 5. Even if blended with phenolic resin, all PAGs form A to D exhibit quite high thermal stability (> 188 °C) and it was found that they can be employed even in high activation energy type resist which needs high pre- and post-bake processes typically performed in the 100 - 140 °C temperature range.

In the case of PAG E, the melting point was observed at 58 °C as the peak of endothermic heat flow in DSC analysis. The exothermic heat flow due to degradation of PAG E started at 183 °C, T_d. Though the T_d of PAG E was slightly lower than the other new PAGs, this result clearly indicates that PAG E is potentially stable at the baking process temperature in the range mentioned above. Additionally TGA analysis also indicated the similar value of T_d^{TGA} at 185 °C. In conclusion, PAG E was found to be thermally stable and non-volatile up to 180 °C and suitable for chemically amplified resist application.

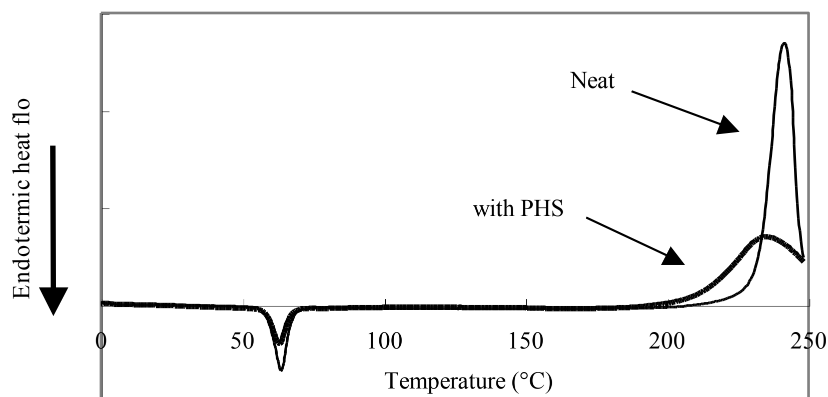

Fig. 1. DSC curves of PAG A in neat state or with PHS

Table 5. Melting point (T_m) and decomposition point (T_d)

Compound	T_m (° C)	T_d neat (° C)	T_d in PHS (° C)
PAG A	60	204	188
PAG B	< r.t.	193	192
PAG C	54	217	197
PAG D	127	205	191
PAG E	58	183	–

–: not measured.

UV absorption. The UV absorption spectra of all the PAGs were measured in acetonitrile. As for the absorption in the range from 190 nm to 245 nm, these PAGs except PAG D have identical absorption spectra, and PAG D exhibits slightly higher absorption comparing to other PAGs due to aromatic absorption of toluene sulfonate moiety. Fig. 2 shows the absorption spectra of PAG A and PAG D as well as TPST, BCSD, and PTMA. As reported previously,[6] PTMA has an enlarged conjugation system, which made the absorption of λ_{max} shifted to 405 nm. Therefore, PTMA was characterized as PAG having a good photosensitivity at the wide range of light sources from g-line to DUV. However, PTMA has a significantly high absorption at 248 nm and TPST has higher absorption. The high absorption prevents from a good light penetration through resist layers, which can be a reason for poor resist profile. On the other hand, BCSD exhibits quite small absorption at 248 nm, which may cause insufficient photosensitivity. PAG A and PAG D do not have an absorption in a range of long wavelength like g-line (436 nm) and i-line (365 nm), and the λ_{max} appears at 280 nm. A valley of absorption spectra of PAG A and PAG D fits to around 248 nm, and its value is small but significant for high photosensitivity. In other words, these new PAGs have the well-balanced absorption at 248 nm between light penetration and photosensitivity.

Fig. 2 also shows the UV absorption spectra of PAG E and the UV absorbance of PAG E at 193 nm is listed in Table 6 with the data of TPST, BTIT, and NDIT as references. The UV absorption profile of PAG E was similar to that of PAG A except for the λ_{max}, of absorption at around 290 nm, which was bathochromic shifted by about 10 nm. The absorbance of PAG E at 193 nm was 0.96 (ε = 69000) in acetonitrile solution. This value is not as low as that of NDIT but it is less than two third of that of TPST, 1.57, and slightly less than BTIT, 1.00. Therefore, this low absorption of PAG E at 193 nm is preferable to make a good resist profile comparing to TPST. Since the maximum loading amount of PAG in the resist is limited by its solubility or absorbance, the low absorption of PAG E will make formulation more flexible.

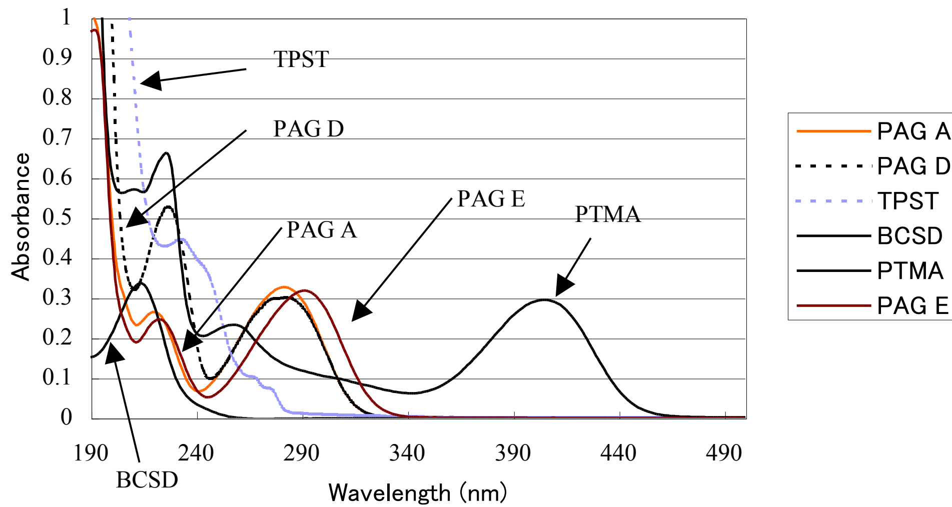

Fig. 2. UV absorption spectra (0.01 g/L, CH_3CN)

Table 6. Absorbance at 193 nm: Abs(193nm)

PAG	Abs(193nm)
PAG E	0.97
TPST	1.57
BTIT	1.00
NDIT	0.55

Volatility. The volatile feature of PAG is not preferable for the resist application, which may cause a reduced PAG concentration at the resist/air interface during the pre-bake process. The volatility was evaluated by transfer of PAG from the resist layer to the detector layer at 130 °C for 5 minutes. If a significant amount of PAG is transferred to the detector layer, the thickness of the detector layer decreases by the development after the flood-exposure. Fig. 3 shows the loss of the detector layer induced by the volatility of PAG A, TPST, and BCSD, respectively. PAG A did not indicate any significant volatile feature as well as TPST, while BCSD exhibited a serious volatile property.

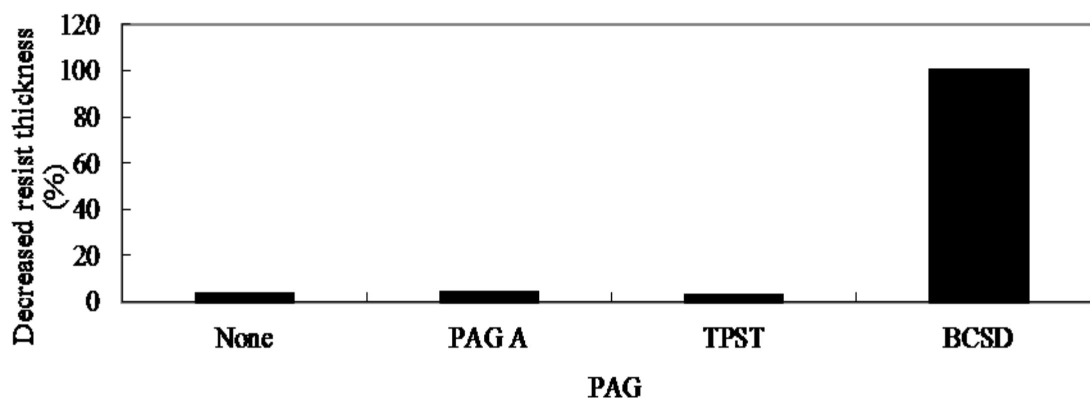

Fig. 3. Volatile property of PAGs

Photosensitivity in DUV model formulation. As described above, the new PAGs showed high thermal stability in PHS matrix up to 188 °C, indicating that these PAGs can be employed in high activation energy resists whose typical pre-bake and post-exposure bake temperatures are around 140 °C. Therefore, photosensitivity measurement of PAGs was carried out using positive tone high activation energy type resist upon monochromatic light irradiation (254 nm) through a multi density mask. The resist thickness after the development was plotted against light energy as shown in Fig. 4. High contrast curves were obtained with PAG A, PAG B, PAG C, and PAG D, indicating the potential for making good positive tone CA photoresists. As a measure for photosensitivity, dose to clear (E_0) was used for comparison. Table 7 summarizes the sensitivity of the new PAGs as well as TPST, BCSD, and PTMA. With increasing size of the acid moiety from propyl (PAG A) to octyl (PAG B) and finally camphoryl (PAG C), the resist sensitivity was reduced. The sensitivity differences between these three PAGs must be mainly caused by the different diffusion rates of the corresponding acids in the resist layer. Although the size of toluenesulfonic acid is larger than that of propanesulfonic acid, PAG D exhibited higher sensitivity than PAG A. This may be attributable to stronger acidity of the aromatic sulfonic acid comparing to the aliphatic sulfonic acid. Comparing to TPST, the sensitivity of the new PAGs is lower, but this high sensitivity is contributed from the high absorption of TPST at 254 nm, which is not preferable from the viewpoint of the light penetration in resist layers. BCSD and PTMA exhibited the decomposition temperature in PHS matrix at 140 °C and 142 °C,[6] respectively. Accordingly, under the conditions of the sensitivity measurement, these PAGs may be partially decomposed and thermally generated acid might contribute to the sensitivity. Additionally the volatile tendency of BCSD reported above might also influence its sensitivity.

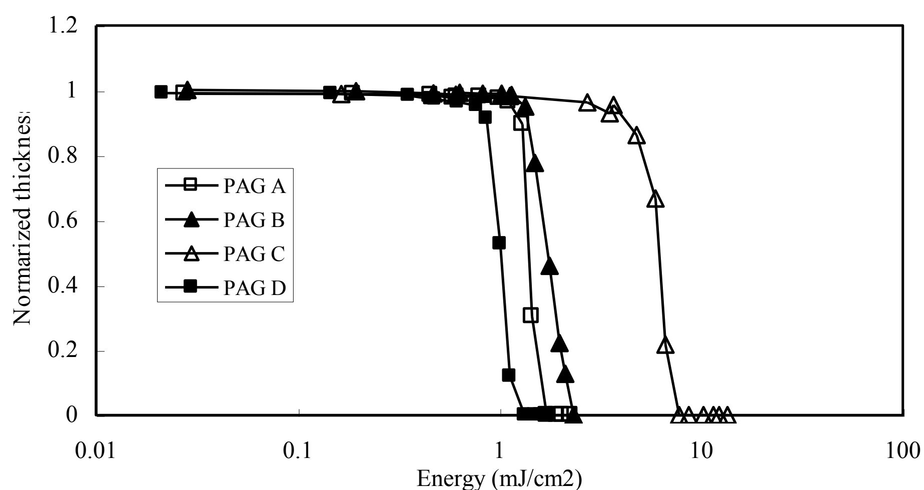

Fig. 4. Contrast curves in a positive tone photoresist

Table 7. Sensitivity with DUV exposure

Compound	Sensitivity (mJ/cm^2)
PAG A	1.73
PAG B	2.26
PAG C	7.02
PAG D	1.19
TPST	0.27
BCSD	5.06
PTMA	1.10

Photochemical properties of PAG E in ArF model formulation. DRM experiment is a well-known method to characterize the resist performance. Fig. 5 shows the dissolution rate vs. exposure dose plots, discrimination curves, of PAG E, TPST, BTIT, and NDIT with ArF exposure. Since the resist thickness is typically in a range between 200 nm and 500 nm and the development time is in a range between 30 sec and 90 sec, the dose value of dissolution rate at around 10 nm/sec is corresponding to the sensitivity, E_0. Hence, the discrimination curves below this critical value (10 nm/sec) include the most important information to characterize the resist performance. In this region PAG E showed the steepest slope (high Tan θ) compared to TPST and comparable to BTIT and NDIT, indicating that PAG E will give a high contrast.

Table 8 summarizes the sensitivity value derived from the experimental data obtained by DRM. As a measure for sensitivity, E_0 at 60 seconds development was determined. PAG E showed higher sensitivity, 2.7 mJ/cm^2, in the model formulation than BTIT, 6.0 mJ/cm^2, or NDIT, 11 mJ/cm^2.

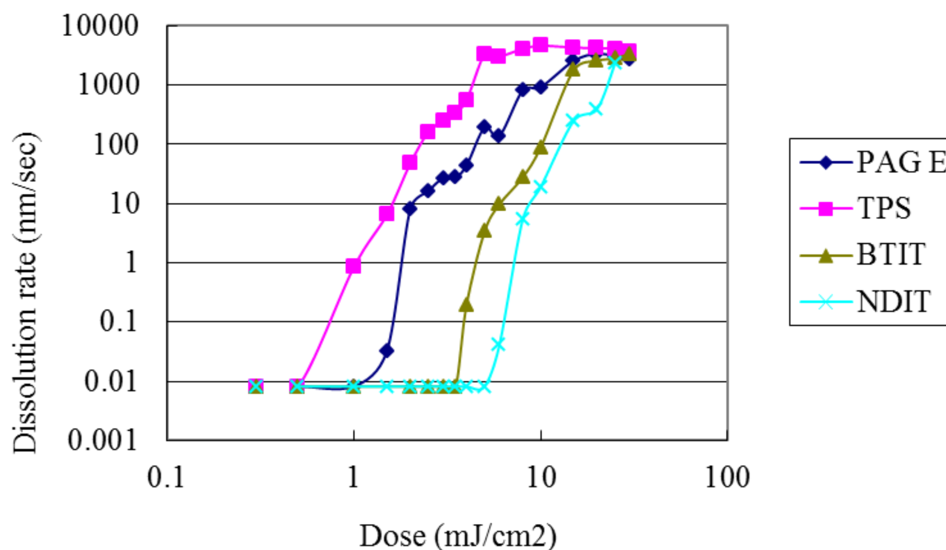

Fig. 5. Dissolution rate vs. exposure dose plot

Recently Pohlers *et al.* introduced P-parameter,[13] which is derived from the following equation:

$$P = E_0 \times [\text{fraction of incident light absorbed by PAG}]$$

In P-parameter, the smaller is the higher efficiency in photoresist lithography. In this chapter, the P-parameter in our model formulation was calculated and employed as a measure for the comparison of PAG efficiency. Please note the absolute values of the P-parameter were affected by the content of photoresist formulations, process conditions, the sort of the generated photoacid and so on. Hence, the values calculated in this chapter can't be directly compared with those of the previous report.[13]

From this evaluation, it was disclosed that the value of P-parameter of PAG E (P=0.5) was smaller than BTIT (P=1.5) or NDIT (P=1.1) and slightly superior to TPST (P=0.6). The observed P-parameter of NDIT is 1.9 times of that of TPST. Interestingly, the ratio of P-parameters between triphenylsulfonium sulfonate and 5-norbornene-2,3-dicarboximidyl sulfonate described in the previous report[13] shows a good agreement with our result.

Table 8. Photochemical properties

PAG	Photochemical properties			
	Tan θ	E_0 (mJ/cm^2)	Abs [1)] (1/μm)	P
PAG E	12.5	2.7	0.18	0.5
TPST	5.7	1.7	0.35	0.6
BTIT	11.9	6.0	0.25	1.5
NDIT	11.2	11	0.10	1.1

1) Absorbance of only PAGs in a resist film

Microlithography simulation. Microlithography simulation was performed with the DRM data of PAG E and TPST by SOLID-CL from SIGMA-C in order to compare the two PAGs each other. Fig. 6 shows mask-linearity of the photoresists containing the two PAGs respectively. PAG E exhibited higher resolution, 100 nm, than TPST, 150 nm, when the exposure dose was optimized at 170 nm L&S pattern. Considering the fact that the same triflic acid was photochemically generated from the PAGs, it became clear that the chromophore of PAG E achieves the higher resolution than that of TPST.

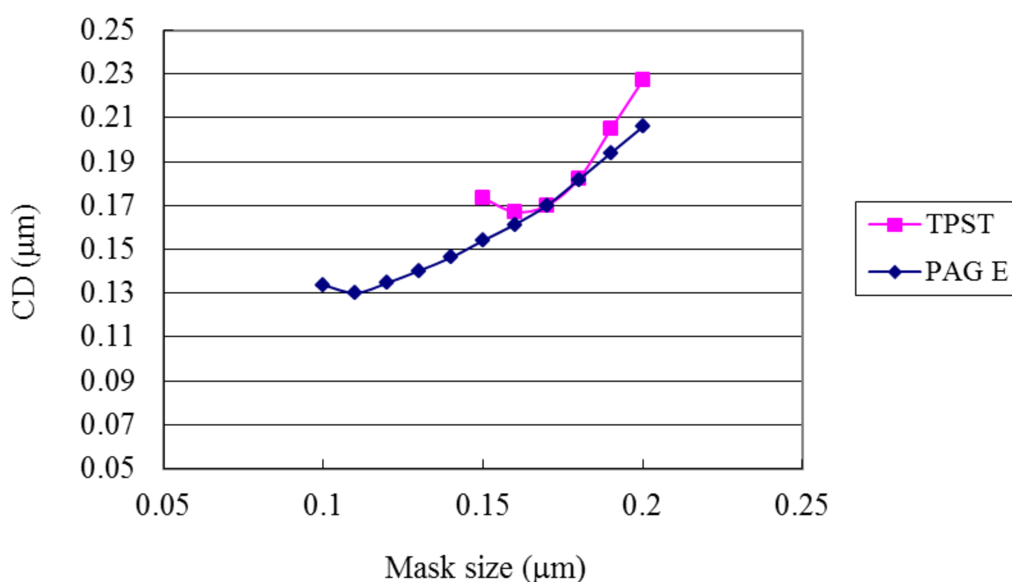

Fig. 6. Mask linearity plot of PAG E and TPST

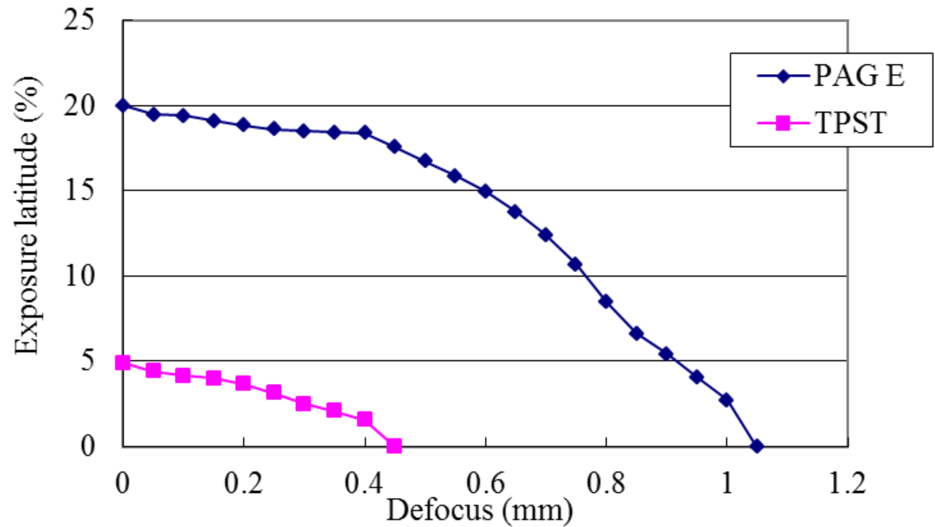

Fig. 7. Exposure latitude vs. defocus plot of PAG E and TPST

In Fig.7, exposure latitude was plotted against defocus. At just focus, PAG E allows 20 % exposure latitude while TPST does 5%. Maximum defocus of PAG E was 1.05 μm and more than twice of that of TPST, 0.45 μm. Fig. 7 clearly revealed the superiority of PAG E in process latitude to TPST.

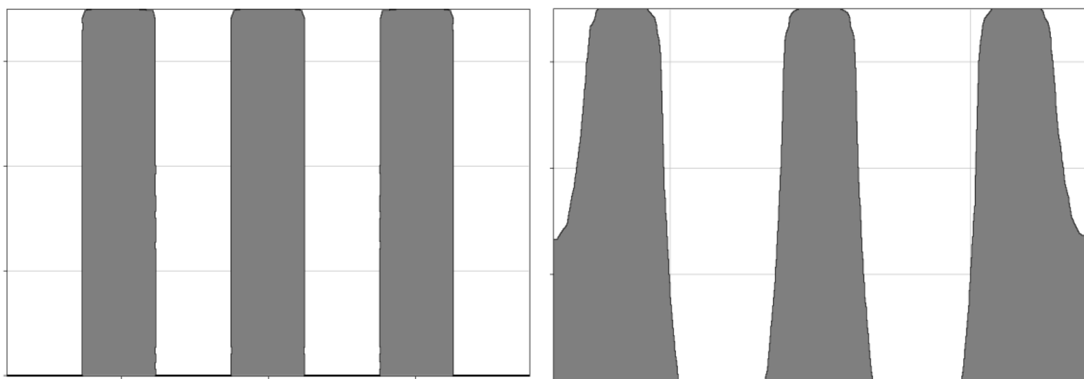

Fig. 8. Cross-sectional view of the resist with PAG E (left, 100 nm L&S) and TPST (right, 130 nm L&S)

Fig. 8 shows the cross-sectional view of the resist containing PAG E and TPST simulated by SOLID-CL, respectively. It is obvious that PAG E gives better resist profile (rectangular shape) and higher resolution than TPST.

Conclusion

A new class of oxime sulfonate PAGs was developed for the CA photoresist application. As reported previously, (2-alkylsulfonyloxyimino-2*H*-thiophen-3-ylidene)-2-methylphenyl-acetonitriles were characterized as high sensitive PAG at the wide range of light source from g-line to DUV and enough thermal stability for the application of low activation energy resist. On the other hand, the new PAGs demonstrated superiority in thermal stability (> 188 °C in phenolic resin) and had an adequate absorption around 250 nm with good sensitivity for DUV light source of 254 nm, indicating feasibility of practical uses in both low activation energy and high activation energy CA resists.

Moreover PAG E, a trifluoromethanesulfonate derivative for ArF photoresists, is also highly soluble in PGMEA and thermally stable up to 180 °C. The PAG exhibits superior efficiency to a conventional ionic PAG, BTIT, and a non-ionic PAG, NDIT, and comparable to TPST upon ArF exposure. Furthermore the microlithography simulator predicted the higher resolution limit and the wider process latitude than TPST.

References

1. For example, R. Dammel, *Diazonaphthoquinone-based Resists,* pp. 9-96, SPIE Optical Engineering Press, Washington, D. C., **1993**.
2. R. D. Allen, G. M. Wallraff, R. A. DiPietro, D. C. Hofer and R. R. Kunz, *Proc. SPIE,* **1995**, *2438*, 474.
3. K. Nozaki, K.watanabe, E. Yano, A. Kotachi, S. Takechi, and I. Hanyu, *J. Photopolym. Sci. Technol*., **1996**, *9*, 509-22.
4. S. Iwasa, K. Maeda, K. Nakano, T. Ohfuji, and E. Hasegawa, *J. Photopolym. Sci. Technol,.* **1996**, *9*, 447-56.
5. G. Berner and W. Rutsch, US patent 4540598.
6. T. Asakura, H. Yamato and M. Ohwa, *J. Photopolym. Sci. Technol.,* **2000**, *13*, 223-30.
7. H. Yamato, T. Asakura, A. Matsumoto and M. Ohwa, *Proc. SPIE,* **2002**, *4690*, 799-808.
8. H. Yamato et al., U.S. Patent 6004724,**1999**;
9. T. Asakura et al., U.S. Patent 6261738 B1, **2001**
10. C. R. Szmanda, R. Kavanagh, J. Bohland, J. Cameron, P. Trefonas and R. Blacksmith, *Proc. SPIE,* **1999**, *3678*, 857-66.
11. A. Sekiguchi, Y. Sensu and Y. Miyake, *Jpn. J. Appl. Phys,.* **2003**, *42*, 16-22.
12. G. G. Barclay, D. R. Medeiros and R. F. Sinta, *Chem. Mater.,* **1995**, *7*, 1315-24.
13. G. Pohlers, Y. Suzuki, N. Chan and J. F. Cameron, *Proc. SPIE,* **2002,** *4690*, 178-90.

Chapter 4

Studies on novel photoacid generator for 193 nm (ArF) exposure

Abstract

In this chapter, a novel oxime sulfonate type of photoacid generator (PAG), 2-[2,2,3,3,4,4,5,5,6,6,7,7-dodecafluoro-1-(nonafluorobutylsulfonyloxyimino)-heptyl]-fluorene (DNH F), which generates a typical strong acid (nonaflic acid) by light irradiation and is applicable to chemically amplified ArF photoresists, was developed. Additionally two DNHF analogues with different fluoroalkyl chains adjacent to the oxime moiety, 2-[2,2,3,3,4,4,4-heptafluoro-1-(nonafluorobutylsulfonyloxyimino)-butyl]-fluorene (HNBF) and 2-[2,2,3,3,4,4,5,5-octafluoro-1-(nonafluorobutylsulfonyloxyimino)-pentyl]-fluorene (ONPF), were prepared and investigated in the structure effect. The change of the fluoroalkyl chain did not have a strong impact on photo-efficiency and transparency at 193 nm and these PAGs demonstrated superiority to triphenylsulfonium nonaflate (TPSNF) with respect to these criteria. On the other hand, different behaviors were observed in the coating property and contact angle measurement of the photoresists containing these PAGs. The hydrogen atom at the end of the fluoroalkyl chains of DNHF and ONPF was found to have a role in improving the coating property. These non-ionic PAGs were less risky for contamination on the surface of the lens due to insolubility in water. In addition, the effect by these PAGs on increasing hydrophobicity of the photoresist surface was identified. These results suggest that the newly developed non-ionic PAGs are suitable for ArF immersion lithography.

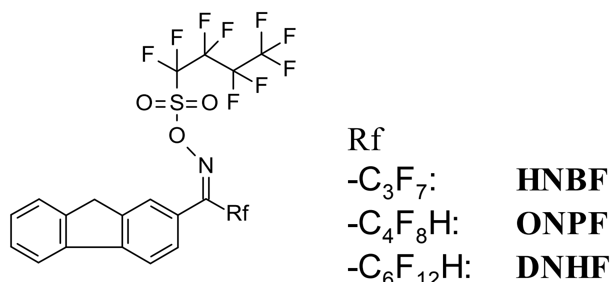

Introduction

The development of ArF immersion lithography is proceeding with an astonishing speed, and has eliminated F_2 lithography from the roadmap of semiconductor manufacturing for design rule of 45nm node (hp 65 nm) and below.[1] This dynamic movement is due to the fact that a lot of key technology components of ArF dry lithography can be utilized in ArF immersion lithography, e.g., lens material and resist materials. However, the critical difference between ArF dry and ArF immersion lies in the contact of the resist layer with a liquid medium in immersion lithography. For the 1st generation of ArF immersion, water is applied as the liquid medium due to its high refractive index (n = 1.44) and high transparency at 193 nm. Hence the interaction of the resist layer with water may cause leaching of hydrophilic resist components, e.g., photoacid generator (PAG) and amine, into water or penetration of water into the resist layer. These potential phenomena raise the concerns of optical property change of the liquid medium and lens contamination by leaching components from the resist layer, and change of resist performance. Owa et al have investigated the influence of chemical contamination on a projection lens under irradiation, and proposed the specifications for the leaching of PAG and amine to be below 2.5 ng/cm^2/s and 1.0 ng/cm^2/s, respectively.[2] One of the approaches to solve the issue is an application of topcoat on the resist layer. There are several studies to develop the topcoat. It is sure that the PAG leaching can be depressed by applying topcoat. However, the topcoat has introduced a new problem in that PAG leaching to the topcoat layer is accompanied by a T-top profile in the resist layer.[3] On the other hand, an interesting result was reported that immersion specific defects were decreased to a large extent by increasing hydrophobicity of the topcoat, indicating that ArF immersion lithography with topcoat is coming close to practical use.[4] However, the lithography with topcoat is not the best option from the view points of cost and throughput, and a topcoat-less process is demanded for future ArF immersion lithography.

For ArF dry lithography, sulfonium salts like triphenylsulfonium (TPS) nonaflate are widely employed. These ionic PAGs were not expected to leach easily to water, but there are several reports on the leaching of sulfonium salts.[5-7] Dammel *et al*. investigated the leaching of TPS with different anions, *i.e.*, triflate, nonaflate, and perfluorooctanesulfonate.[5] They observed a significant amount of leaching of these PAGs and found that more hydrophobic anions can lead to a decrease in saturation concentration. To decrease the PAG leaching, an increase in hydrophobicity of PAG is thought to be effective approach, and a non-ionic PAG looks promising to realize topcoat-less ArF lithography. There are several non-ionic PAGs for KrF lithography such as imidosulfonate, diazomethanedisulfone, and *o*-nitrobenzylsulfonate. However, few non-ionic PAGs are applicable for ArF lithography because a strong acid is needed to catalyze the cleavage of an ester group in a

hydrophobic polymer matrix.[8] It is quite a challenge to make a stable non-ionic PAG that releases strong acid upon light exposure.

The author has been investigating various oxime sulfonates type PAGs,[9-14] which are adjustable to the target applications and exposure wavelength range by modification of chromophores and acid moieties. Additionally, non-ionic oxime sulfonates show good solubility in various solvents. Recently, the author has newly developed and reported a thermally and storage stable non-ionic PAG, DNHF, which can release strong acid, i.e., perfluorobutanesulfonic acid.[12-14] In this chapter, a series of DNHF analogues with different fluoroalkyl chains adjacent to the oxime moiety is prepared and investigated in influence of the structure on resist sensitivity, coating property and hydophobicity of the resist formulation.

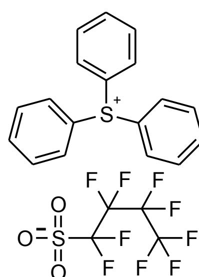

TPSNF

Experimental

Materials. In polymers, a copolymer of (4-hydroxystyrene), styrene and tert-butyl acrylate (69/22/9 mol-%, Mw=9850, from Maruzen Petrochemical Co., Ltd), and a copolymer of γ-butyrolactone methacrylate and 2-methyladamantyl methacrylate (62/38 mol%, Mn=11800, Mitsubishi Rayon Co., Ltd) were purchased and employed as received. Polymer B (Mw=14900) was radically polymerized in-house from the corresponding monomers, 2-ethyladamantyl acrylate (from Osaka Yuki), hydroxyadamantyl acrylate (from Idemitsu) and 5-acryloyloxy-6-hydroxynorbornane-2-carboxylic 6-lactone (from Daicel) by the know procedures.[15&16]

In solvents and developers, propyleneglycol monomethyl ether acetate (PGMEA, from Tokyo Kasei Kogyo Co., Ltd) and 2.38 % aqueous tetramethyl ammonium hydroxide solution (TMAH, from Tokyo Ohka Kogyo Co., Ltd.) were purchased and employed as received.

In chemicals and surfactants, triphenylsulfonium nonaflate (TPSNF, from Midori Kagaku Co., Ltd.), bis(p-tert-butylphenyl)iodonium nonafluorobutanesulfonate (BTINF, from Midori Kagaku Co., Ltd.), a formulation of bottom antireflection coating (ARC-29, from Nissan Chemical Industries, Ltd.), Megafac (from DIC Corporation), Surflon (from AGC Seimi Chemical Co., Ltd.), Fluorolink (from Solvay), and Eftop (from Jemco Inc.) were purchased and employed as received. DNHF, HNHF, and ONHF were synthesized internally by the know procedures.[17]

Photochemical properties in model formulations.

Evaluation in ArF model formulation. Photochemical properties, such as sensitivity and DRM, were measured in an ArF model resist formulation with VUVES 4500 mini, Litho Tech Japan, as an exposure tool. The positive tone resist utilized a copolymer of γ-butyrolactone methacrylate and 2-methyladamantyl methacrylate (62/38 mol%, Mitsubishi Rayon Co., Ltd) having a weight average molecular weight of 11800. The composition of the formulation is described in Table 1-1.

The resist was spin-coated at 370 nm thickness on silicon wafers on which the bottom antireflection coating with ARC-29, Nissan Chemical, was applied in advance at 82 nm thickness and prebaked at 120 ºC for 60 seconds. After exposure with various exposure doses, a post exposure bake was applied at 120 ºC for 60 seconds and the resist was then developed in 2.38% aqueous tetramethyl ammonium hydroxide, TMAH, solution for 120 seconds.

The PAGs in the model formulation were coated on quartz plates at 370nm thickness and the absorbance of the formulation at 193nm was measured with an Hitachi U-3300 spectrometer.

Dissolution rate monitoring (DRM) was carried out with the ArF model resist formulation described above. The resist was exposed with VUVES 4500 mini under dry condition. After post exposure bake, dissolution rate of the resist was monitored by RDA-790, Litho Tech Japan.

.

Table 1-1. Composition of the formulation

Components	Parts
Binder polymer	100
PAG	2
PGMEA	700

Evaluation in EB model formulation. Photo speed and dark erosion were measured in an EB model resist formulation with JBX-5000SI, JEOL, as an EB exposure tool. The positive tone resist utilized a copolymer of a copolymer of 4-hydroxystyrene, styrene, and *tert*-butyl acrylate (69/22/9 mol%, Maruzen Petrochemical Co., Ltd) having a weight average molecular weight of 9850. The composition of the formulation is described in Table 1-2.

The resist was spin-coated at 200nm thickness on silicon wafers treated with hexamethyldisilazane and prebaked at 120 ºC for 60seconds. After exposure with various strength of electron beam (e-beam), a post exposure bake was applied at 120 ºC for 60 seconds and the resist was then developed in 2.38% aqueous TMAH solution for 60 seconds.

Remaining thickness of the resist was measured optically with an Axiospeed film thickness measurement instrument from Zeiss. The resist comprising ONPF was compared with TPSNF and bis(*p*-*tert*-butylphenyl)iodonium nonafluorobutanesulfonate (BTINF)

Table 1-2. Composition of the formulation

Components	Parts
Binder polymer	100
PAG	4
PGMEA	1175

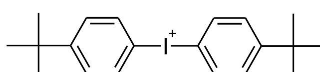

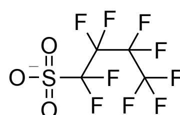

BTINF

Coating property. For the evaluation of coating property of the photoresist formulations containing these PAGs, the ArF model formulation mentioned above was employed except for a PAG loading of 6parts instead of 2parts. In order to investigate the effect of surfactants on the coating property, 0.07 parts of a surfactant was added into the formulation. The formulation was spin-coated at a 370 nm thickness on silicon wafers on which ARC-29 was applied and prebaked as described above. The evaluation of striations was carried out by visual observation.

Contact angle measurement. Water contact angles on the photoresist, which was spin-coated on silicon wafer and prebaked at the condition described above, were measured with contact angle measurement equipment (CA-VE) from Kyowa Interface Science using deionized water at room temperature, ca. 23 ºC.

In case of the contact angle measurement, the two types of base resins as shown below were employed. In addition to Polymer A mentioned above, Polymer B was radically synthesized in-house from the corresponding monomers purchased from Daicel, Idemitsu and Osaka Yuki. The weight average molecular weight of Polymer B was 14900. PAG content was 10% of resin.

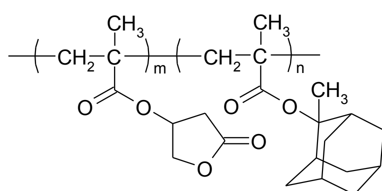

Polymer A

(m: n = 62: 38)

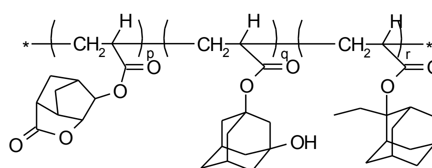

Polymer B

(p: q: r = 50: 20: 30)

Chemical contamination under exposure. Five mg of PAG was put into 1 mL of deionized water and stirred overnight. In the case of TPSNF, the PAG was completely dissolved to give a clear solution at the concentration of 0.5 wt%. In contrast, there remained insoluble PAG in water in the case of HNBF, ONPF, and DNHF. The residual PAG was removed by filtration with a 0.2 µm membrane filter and the filtrate saturated with PAG was employed for the experiment of contamination under exposure.

On a 1-inch quartz plate, an o-ring (Echo®-Oring P-20 from AWI MACH) made with fluoro resin was set. Then the solution was poured into the ring, covered with a 1-inch quartz glass and exposed with an ArF eximer laser at 1 mW intensity for 30 minutes. The evaluation of contamination was carried out by visual observation.

Results and discussion

Absorption and sensitivity in ArF model formulation. In order to investigate the physical and photochemical property of a PAG for resist application, each PAG was formulated in an ArF model formulation with 2 wt% against polymer. As the polymer matrix, a polymethacrylate platform was employed, which has high transparency at 193 nm. The resist layer was exposed by ArF laser (193 nm) for the estimation of sensitivity. In lithography studies, the "Dose to Clear" (E_0) is commonly used as a measure of resist sensitivity. The E_0 is the dose just sufficient to completely remove the resist film with 60 seconds development. A smaller required dose means the resist formulation is more sensitive. The three non-ionic PAGs, HNBF, ONPF, and DNHF, showed similar sensitivity but are less sensitive than TPSNF as shown in Table 2. The higher sensitivity of TPSNF is probably attributable to the high absorption of the formulation. The non-ionic PAGs show superiority in transparency at 193 nm compared with TPSNF and their absorption in the formulation is about one-third that of TPSNF.

As mentioned above, the high sensitivity of TPSNF is due to its high absorption. However, the photochemical efficiency of a PAG cannot be determined only by sensitivity because the light intensity absorbed by each PAG is not identical. In order to estimate a relative photo-efficiency of a PAG in the formulation, the P-parameter is a simple and useful index, which was introduced by G. Pohlers *et al.*[18] The P-parameter is derived from the equation: $P = E_0 \times$ [fraction of incident light absorbed by PAG]. A smaller P-parameter indicates higher photo-efficiency of the resist formulation. It is obvious from Table 2 that the three non-ionic PAGs more effectively generate acid in the formulation than TPSNF. ONPF showed less photo-efficiency than the other two non-ionic PAGs to a small extent but the reason has not been elucidated.

Table 2. Absorbance, E_0, and P-parameter

PAG	E_0 (mJ/cm^2)	Abs(193 nm) in formulation (μm^{-1})	P-parameter
HNBF	2.7	0.08	0.22
ONPF	2.9	0.10	0.29
DNHF	3.0	0.07	0.21
TPSNF	1.6	0.29	0.46

DRM measurement. For the evaluation of the photoresist performance without a stepper, dissolution rate monitoring (DRM) is a good tool to predict the photoresist profile. In addition, DRM is useful to analyze the dissolution property of the photoresist from a fundamental viewpoint.

The DRM measurements were conducted for the ArF model formulations composed of the typical polymethacrylate polymer with HNBF, ONPF or DNHF, respectively. Fig. 1 represents the dissolution rate of the photoresists as a function of the exposure dose. A significant difference was not observed in R_{max}, R_{min}, and the slope of the discrimination curves in the current model formulation, suggesting that the three non-ionic PAGs give a similar photoresist performance.

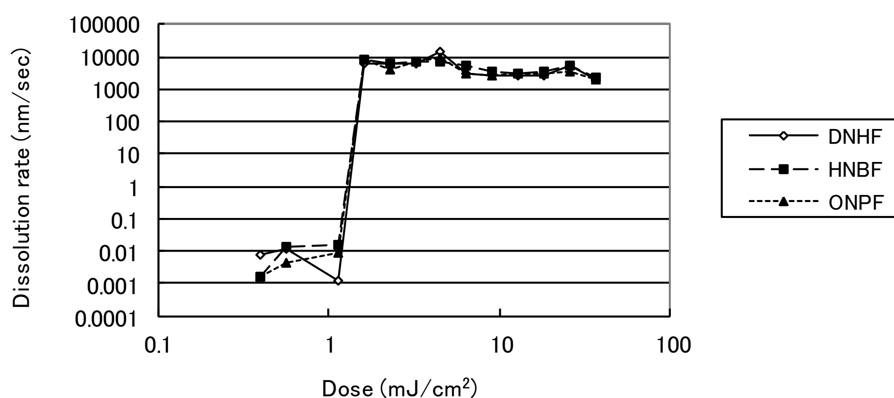

Fig. 1 DRM results of ArF model formulations with non-ionic PAGs

Sensitivity in EB model formulation. In order to investigate the applicability of a PAG into EB resist application, the three PAG, ONPF, TPSNF, and BTINF, was formulated in a model formulation. As for the polymer matrix, a copolymer of (4-hydroxystyrene), styrene and *tert*-butyl acrylate commercially available from Maruzen Petrochemical Co., Ltd was employed, which is known as a base polymer for DUV resists. In this case of the EB resist, E_0 is used as a measure of resist sensitivity as well. The experimental results, contrast curves, were shown in Fig. 2. The remaining resist thickness was plotted against the applied energy of e-beam. Among the three PAGs, TPSNF showed highest sensitivity. ONPF and BTINF, showed similar sensitivity but dark erosion of ONPF is more than that of BTINF. This erosion would be decreased by employing more hydrophobic polymer matrix, such as a copolymer with more ratio of *tert*-butyl acrylate. Interestingly Fedynyshn et al. found that the dissolution inhibition effect of PAG is responsible for the increase of the innate material roughness in the ESCAP type of photoresist as employed here.[19] Therefore the less dissolution inhibition with ONPF than BTINF observed here might positively affect lithography profile in terms of roughness.

Szmanda *et al*. reported the evaluation results of several PAGs in the exposure of EUV and e-beam.[20] In the report, EUV exposures yielded very similar trends to those seen in e-beam irradiation. Thus the fact that ONPF is sensitive to EB tells us that the oxime sulfonates would be applicable to the resists for EUV lithography.

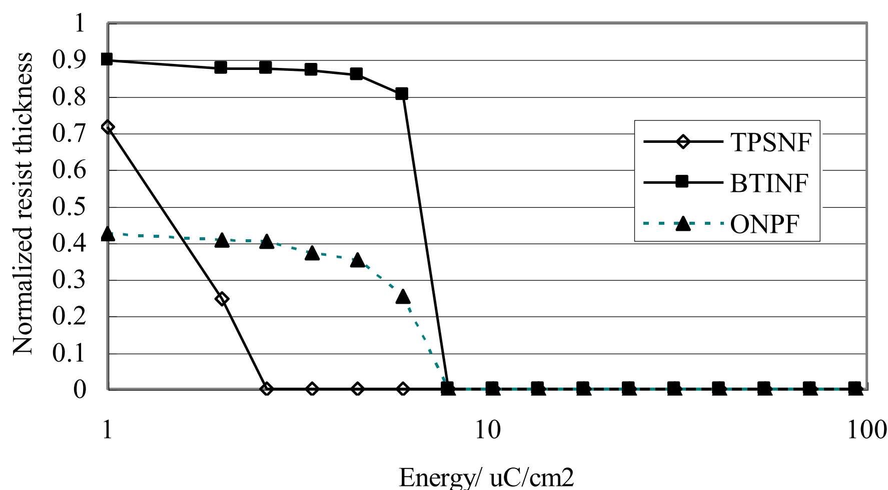

Fig. 2 Sensitivity measurement of PAGs in EB model formulations

Coating property. Solubility of PAG in common organic solvents employed for resist application is one of the basic criteria. As reported previously, DNHF showed very high solubility (> 30 wt/v%) in PGMEA, ethyl lactate, and cyclohexanone. Similarly, HNBF and ONPF were very soluble in these solvents as summarized in Table 3. The high solubility of PAG in the organic solvents enlarges the flexibility of formulation and reduces a risk of particle generation during resist storage. However, it was found that a high loading amount of DNHF in the formulation with Polymer A caused an issue in coating property, *i.e.*, a few striation patterns appeared by spin-coating of the formulation at the loading amount of 6% against polymer content, while no striation was observed at the loading amount of 2 and 4%. The coating property of HNBF and ONPF (Fig. 3) was also examined at the loading amount of 6% in the combination of Polymer A. A similar result was obtained when comparing an ONPF containing film to a film with DNHF. However, a film with HNBF clearly showed much striation under the same condition as shown in Fig. 3(b). The difference of HNBF from the other two PAGs is the lack of a hydrogen atom at the end of the fluoroalkyl chain. Hence, it is assumed that this hydrogen atom has a critical role to improve the compatibility of PAG with Polymer A.

Generally speaking, the coating property of the resist layer can be improved by the addition of a small amount of surfactant and/or leveling reagents. The effect of commercially available surfactants on the coating property has been investigated. One example is displayed in Fig. 3(c), which obviously demonstrates that the poor coating property of HNBF is improved by the addition of the small amount of Fluorolink L in the formulation. Other results are summarized in Table 4. Several surfactants have been found to be effective in improving the coating property. Although the information on chemical structures of almost all surfactants is not available, the structures of

Fluorolink are published as shown in the scheme below, which have fluoroalkyleneoxide units as the main component.

Table 3. Solubility in organic solvents

PAG	PGMEA	Ethyl lactate	Cyclohexanone
HNBF	> 30 %	12 %	> 30 %
ONPF	> 30 %	> 30 %	> 30 %
DNHF	> 30 %	> 30 %	> 30 %

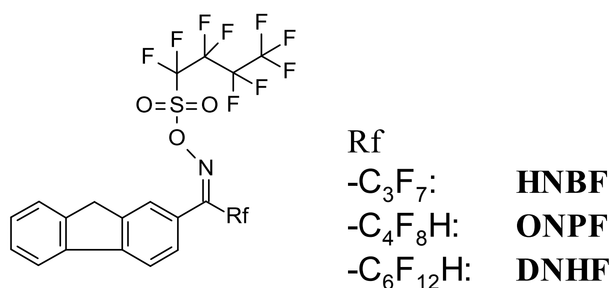

(a) ONPF without surfactant **(b)** HNBF without surfactant **(c)** HNBF with Fluorolink L

Fig. 3 Coating property of photoresist formulations

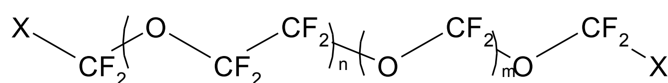

Surfactant	X group	Molecular weight
Fluorolink A10	$-CONHC_{18}H_{37}$	1200 – 2000
Fluorolink L	$-COOCH_3$	1900 – 2300
Fluorolink L10	$-COOCH_3$	1000 – 1500
Fluorolink T	$-CH_2OCH_2CH(OH)CH_2OH$	2200 – 2400

Structures of Fluorolink

Table 4. Coating property of formulations including PAG

Surfactant	PAG		
	HNBF	ONPF	DNHF
None	NG	Moderate	Moderate
Megafac R-08 (DIC)	NG	Good	Good
Megafac R-30 (DIC)	NG	Good	Good
Surflon KH-40 (Seimi Chem)	NG	Good	Moderate
Surflon S-381 (Seimi Chem)	NG	Good	Good
Surflon S-393 (Seimi Chem)	NG	Good	Good
Surflon S-141 (Seimi Chem)	NG	Moderate	Moderate
Surflon S-145 (Seimi Chem)	NG	Moderate	Moderate
Fluorolink A10 (Solvay)	Moderate	Good	Good
Fluorolink L (Solvay)	Moderate	Good	Good
Fluorolink L10 (Solvay)	Moderate	Good	Good
Fluorolink T (Solvay)	Moderate	Good	Good
Eftop EF-351 (Jemco)	NG	Good	Good
Eftop EF-352 (Jemco)	NG	Good	Good
Eftop EF-802 (Jemco)	NG	Good	Moderate

Good, no visible striation; Moderate, moderate striation; NG, much striation.

Contact angle measurement. On the development of immersion lithography, defect generation is one of the most critical issues. Water droplets that remain on the surface of resist or topcoat materials after exposure and stage scanning is one of the causes for the immersion specific defects. Hydrophobicity of the resist and topcoat surface has been found to play an important role in reducing the immersion specific defects. In addition, the high hydrophobic property of the surface enables high stage scan speed, leading to high throughput. Hence the effect of the non-ionic PAGs on the resist surface property has been investigated.

Three non-ionic PAGs, HNBF, ONPF, and DNHF, and ionic PAG, TPSNF, were each formulated with two polymer systems. Compared to Polymer A, Polymer B is less hydrophobic due to a hydroxyl group on the adamantyl moiety. The hydrophobicity of the resist surface was estimated by the contact angle of a water droplet on the surface. The results are represented in Fig. 4(a) and 4(b). In the case of Polymer A, the effect to increase the hydrophobicity by the addition of a non-ionic PAG was observed but was not so large because the hydrophobicity of Polymer A itself was rather high. On the other hand, in the case of Polymer B, the impact of the non-ionic PAG on

the surface property was significant. The hydrophobicity was drastically increased especially by the addition of HNBF. The other two non-ionic PAGs have a smaller effect on the hydrophobicity compared with HNBF. This suggests that the hydrogen atom on the end of the fluoroalkyl chain of ONPF and DNHF has an influence to reduce the hydrophobicity of the fluoroalkyl chain. TPSNF was confirmed to have the effect of decreasing the hydrophobicity by its ionic characteristic in the formulation with Polymer A. However, the hydrophobicity of Polymer B itself was not so high that the decrease of hydrophobicity by the addition of TPSNF was not substantial. It was found that novel non-ionic PAGs work well to increase the hydrophobicity of the resist surface, especially when the resist is comprised of a hydrophilic polymer matrix.

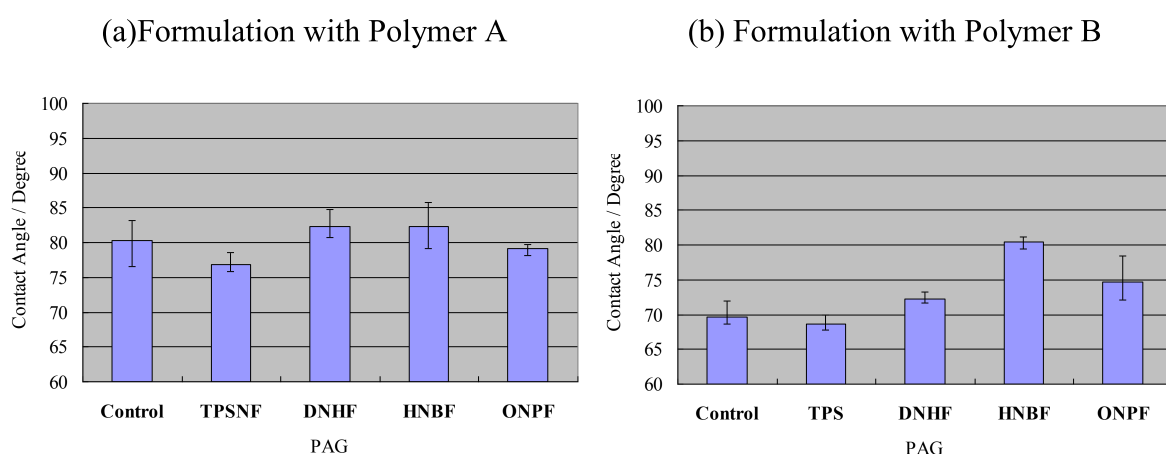

Fig. 4 Contact angle of water on ArF model formulations

Chemical contamination under exposure. There still remains the concern that chemical components may come out of the resist into a liquid medium, resulting in a contamination on the surface of the bottom lens of the exposure tool. Since the leaching components are water-soluble, they may be washed out by water flow and thereby avoid contamination of the exposure tool. However, the products derived from decomposition of the leaching components by light exposure may contaminate the lens surface. The chemical contamination on the quartz glass substrate by a PAG has been investigated under light exposure. TPSNF was dissolved in water with the concentration of 0.5% and monochromatic 193 nm light was exposed to the solution through quartz glass. After the light of 1 mW intensity was applied for 30 minutes, contamination was observed on the quartz substrate as shown in Fig. 5. It seems that TPSNF decomposed by light to produce water-insoluble materials, which adhered to the surface of the quartz glass. On the other hand, the non-ionic PAGs, HNBF, ONPF, and DNHF, do not dissolve in water at the concentration of 0.5%.[12]

Hence, the water solutions saturated with each non-ionic PAG were prepared and the monochromatic light was exposed to each one separately. However, no contamination was observed on the surface of the quartz. As reported previously,[13,14] any significant leaching of HNBF and DNHF was not detected in the water medium from a model formulation (< 2.6 x 10^{-12} mol/cm^2: detection limit). These results suggest a low risk of chemical contamination on the surface of the bottom lens by the newly developed non-ionic PAGs.

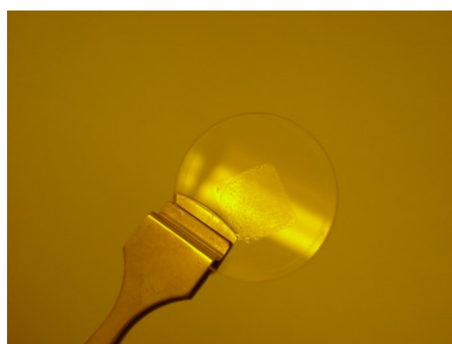

Fig. 5. Contamination on quartz by TPSNF after light irradiation

Conclusion

The oxime sulfonate type of PAGs, HNBF, ONPF, and DNHF, were found to be superior to the conventional ionic PAG, TPSNF, with respect to transparency and photo-efficiency at 193 nm. In addition, these non-ionic PAGs have the effect to increase the hydrophobicity of the photoresist formulation, and they are less risky for contamination on the surface of the lens due to insolubility in water. Our results suggest that these non-ionic PAGs are suitable for ArF immersion lithography. They have different fluoroalkyl chains adjacent to the oxime moiety. This difference did not have a strong effect on photo-efficiency and transparency at 193 nm. However, the hydrogen atom at the end of fluoroalkyl chains of DNHF and ONPF played a role in improving the coating property.

References

1. B. J. Lin, *Proc. SPIE* **4688** (2002) 11-24.
2. a) S. Owa, H. Nagasaka, Y. Ishii, K. Shiraishi and S. Hirukawa, *Proc. SPIE* **5754**(2005) 655-668, b) S. Owa, Presentation of the 2nd International Symposium on Immersion Lithography, held in Brugge (SEMATECH, IMEC, Selete), October (2005).
3. S. Kanna, H. Inabe, K. Yamamoto, S. Tarutani, H. Kanda, K. Mizutani, K. Kitada, S. Uno and Y. Kawabe, *Proc. SPIE* **5753** (2005) 40-51.
4. H. Nagasaka, Presentation of SEMI Technology Symposium, held in Chiba (SEMI), December (2005).
5. R. R. Dammel, G. Pawlowski, A. Romano, F. M. Houlihan, W.-K. Kim, R. Sakamuri and D. Abdallah, *Proc. SPIE* **5753** (2005) 95-101.
6. H. Tsuji, M. Yoshida, K. Ishizuka, T. Hirano, K. Endo and M. Sato, *Proc. SPIE* **5753** (2005) 102-108.
7. W. Conley, R. J. LeSuer, F. F. Fan, A. J. Bard, C. Taylor, P. Tsiartas, G. Willson, A. Romano, R. Dammel, *Proc. SPIE* **5753** (2005) 64-77.
8. G. Pohlers, G. Barclay, A. Razvi, C. Stafford, T. Barbieri and J. Cameron, *Proc. SPIE* **5376** (2004) 79-93.
9. T. Asakura, H. Yamato and M. Ohwa, *J. Photopolym. Sci. Technol.* **13** (2000) 223-230.
10. H. Yamato, T. Asakura, A. Matsumoto and M. Ohwa, *Proc. SPIE* **4690** (2002) 799-808.
11. T. Asakura, H. Yamato, A. Matsumoto, P. Murer and M. Ohwa, *Proc. SPIE* **5039** (2003) 1155-1163.
12. H. Yamato, T. Asakura, T. Hintermann and M. Ohwa, *Proc. SPIE* **5376** (2004) 103-114.
13. T. Asakura, H. Yamato, T. Hintermann and M. Ohwa, *Proc. SPIE* **5753**, (2005) 140-148.
14. T. Asakura, H. Yamato, T. Hintermann and M. Ohwa, *J. Photopolym. Sci. Technol.* **18** (2005) 407-414.
15. N. Dazai et al., Japanese Patent Publication, 2008-308520A;
16. N. D. Jarnagin et al., *J. Photopolym. Sci. Technol.*, **19** (2006) 719-725.
17. H. Yamato et al., U.S. Patent 7399577B2, (2008).
18. G. Pohlers, Y. Suzuki, N. Chan and J. F. Cameron, *Proc. SPIE* **4690** (2002) 178-90.
19. T.H. Fedynyshyn, R. F. Sinta, D. K. Astolfi, A. Cabral, J. Roberts and R. Meagley, *Proc. SPIE* **6153**, 615315 (2006).
20. C. R. Szmanda, R. L. Brainard, J.F. Mackevich, A. Awaji, T. Tanaka, Y. Yamada, J. Bohland, S. Tedesco, B. Dal’Zotto, W. Bruenger, M. Torkler, W. Fallmann, H. Loeschner, R. Kaesmaier, P. M. Nealey and A. R. Pawloski, *J. Vac. Sci. Technol. B* **17** (1999) 3356-3361.

Chapter 5

Studies on novel photoacid generator for 193 nm (ArF) immersion exposure

Abstract

The author has developed novel non-ionic photoacid generators (PAGs), 2-[2,2,3,3,4,4,5,5,6,6,7,7-dodecafluoro-1-(nonafluorobutylsulfonyloxy-imino)-heptyl]-fluorene (DNHF) and 2-[2,2,3,3,4,4,4-heptafluoro-1-(nonafluorobutylsulfonyloxyimino)-butyl]-fluorene (HNBF), which generate a strong acid (perfluorobutanesulfonic acid) by light irradiation and are applicable to chemically amplified ArF photoresist. The studies on quantum yield of this chemistry under 193 nm exposure in an ArF model formulation and in a solution comparing with the ones of ionic PAGs, triphenylsulfonium perfluorobutanesulfonate (TPSPB) and bis(4-*tert*-butylphenyl)iodonium perfluorobutanesulfonate (BPIPB) revealed that these novel PAGs are superior in photo efficiency to the others. PAG leaching into water from the resist during a model immersion process was investigated in detail. No leaching of DNHF and HNBF was observed under the immersion process while significant amount of TPSBP was eluted. Dissolution rate of the resist including DNHF prepared under a model condition of ArF immersion exposure was monitored. No clear difference against dry condition was observed.

DNHF **HNBF**

Introduction

ArF photoresist lithography is expecting to become the major technology for semiconductor fabrication with design rule at 65 nm node and below. In addition to the conventional dry ArF lithography, it was decided that ArF immersion lithography is the next generation lithography at 45 nm node and below.[1] Regarding the development of new materials for ArF photoresist, main attention was paid for polymer matrix so far. Phenolic polymer is employed for KrF photoresist application but this type of polymer can't be applied for ArF photoresist because of its high absorption at 193 nm. Aliphatic polymers were intensively investigated for high transparency. Afterward it was found that aliphatic polymers synthesized so far were insufficient in etching resistance. The etching resistance was improved later by introduction of aliphatic cyclic unit, such as adamantane group, into polymer. There are a lot of reports for new polymers for ArF photoresist applications, and several polymer platforms were proposed, *e.g.*, poly(methacrylate), poly(cyclic olefins), COMA, VEMA, and so on. On the other hand, there have been few quests for suitable photoacid generator (PAG) for ArF photoresist. In case of KrF photoresist, the PAG which releases weak acid, such as alkylsulfonic acid and arylsulfonic acid, is applicable to so-called low activation energy resist, *i.e.*, acetal resists, and the PAG which releases strong acid, such as perfluoroalkylsulfonic acid, is employable to both so-called high activation energy resist and low activation energy resist. The ArF photoresist requires strong photoacid because the cleavage of tertiary ester bonding in binder polymers, *e.g.*, *tert*-butyl methacrylate or 2-methyladamantyl methacrylate, is a key reaction during lithography process. For this application onium salts such as TPSPB, are widely investigated as PAG releasing strong acid. However, TPSPB has a strong absorption at 193 nm, and there are lots of demands for new PAGs for ArF photoresist, which are highly transparent at 193 nm. On the other hand, few non-ionic PAGs were reported for ArF photoresist applications because it is quite difficult to make stable non-ionic PAGs, which can release strong acid by light irradiation.

The author has been investigating oxime sulfonates type PAGs,[2-5] which are adjustable to the target applications and exposure wavelength range by modification of chromophores and acid moieties. Additionally, non-ionic oxime sulfonates show good solubility in various solvents. Recently it has been developed and reported that a thermally and storage stable non-ionic PAG, DNHF, can release strong acid, *i.e.*, perfluorobutanesulfonic acid.[5] In this chapter, the evaluation results of the novel PAGs, DNHF and HNBF, in terms of photo efficiency, *i.e.*, quantum yields, in solution and in formulation are reported. As for immersion lithography relevant properties, PAG leaching from the resist during a model process of immersion lithography was investigated in detail. Additionally dissolution rate of the resist prepared under the immersion condition exposure was

monitored and discussed.

For comparison, the PAGs shown below were also evaluated; TPSPB and BPIPB as typical PAGs.

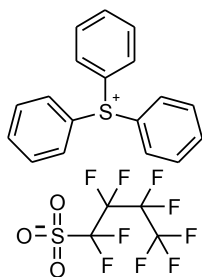

TPSPB

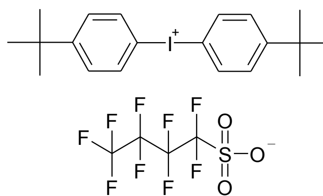

BPIPB

Experimental

Materials. In polymers, a copolymer of γ-butyrolactone methacrylate and 2-methyladamantyl methacrylate (62/38 mol%, Mn=11800, Mitsubishi Rayon Co., Ltd) was purchased and employed as received. Polymer B (Mw=14900) was radically polymerized in-house from the corresponding monomers, 2-ethyladamantyl acrylate (from Osaka Yuki), hydroxyadamantyl acrylate (from Idemitsu) and 5-acryloyloxy-6-hydroxynorbornane-2-carboxylic 6-lactone (from Daicel) by the know procedures.[6&7]

In solvents and developers, propyleneglycol monomethyl ether acetate (PGMEA, from Tokyo Kasei Kogyo Co., Ltd), acetonitrile (from Wako Pure Chemical Industries, Ltd.), distilled water (from Wako Pure Chemical Industries, Ltd.), and 2.38 % aqueous tetramethyl ammonium hydroxide solution (TMAH, from Tokyo Ohka Kogyo Co., Ltd.) were purchased and employed as received.

In chemicals, 1-piperidineethanol (from Tokyo Kasei Kogyo Co., Ltd), triphenylsulfonium perfluorobutanesulfonate (TPSPB, from Midori Kagaku Co., Ltd.), bis(p-tert-butylphenyl)iodonium perfluorobutanesulfonate (BPIPB, from Midori Kagaku Co., Ltd.) and a formulation of bottom antireflection coating (ARC-29, from Nissan Chemical Industries, Ltd.) were purchased and employed as received. DNHF, and HNHF were synthesized internally by the know procedures.[8]

Photodecomposition in solution. PAG was dissolved in acetonitrile at 0.01 mg/mL concentration and the solution was put in an optical cuvette (quartz) with 1 cm optical path-length. The solution was exposed with dose at 193 nm wavelength. Absorption of the solution was measured with exposure by a Hitachi U-3300 spectrometer. Additionally concentration of PAG was monitored by HPLC measurement to determine quantum yield in solution. The HPLC condition is as follows;

Phase: Reverse phase
Column: Shim-pack CLC-Phenyl (M),
Eluent: Acetonitrile/phosphate buffer (pH: 3.6) = 60/40 by volume
Flow rate: 1.0 mL/min
Detection: UV absorption at 254 nm.

Photochemical properties in ArF Model formulation. Photochemical properties were measured in an ArF model resist formulation with VUVES 4500 mini, Litho Tech Japan, as an exposure tool. The positive tone resist utilized a copolymer of γ-butyrolactone methacrylate and 2-methyladamatyl methacrylate (62/38 mol%, Mitsubishi Rayon Co., Ltd) having a weight average molecular weight of 11800. The composition of the formulation is described in the Table 1. In case of determination

of the quantum yield in the formulation, the amine quencher, 1-piperidineethanol, was added by 0, 2, and 4 mol % (0 - 0.08 parts) against PAG.[9&10] When dissolution rate was monitored, no quencher was applied.

The resist was spin-coated at 370 nm thickness on silicon wafers on which the bottom antireflection coating with ARC-29, Nissan Chemical, was applied in advance at 82 nm thickness and prebaked at 120 °C for 60 sec. After exposure with various exposure doses, a post exposure bake was applied at 120 °C for 60 sec and the resist was then developed in 2.38% aqueous tetramethyl ammonium hydroxide, TMAH, solution for 120 sec.

The PAGs in the model formulation were coated on quartz plates at 370 nm thickness and the absorbance of the formulation at 193 nm was measured with Hitachi U-3300 spectrometer.

Table 1. Composition of the formulation

Components	Parts
Binder polymer	100
PAG	2
Solvent (PGMEA)	700
Quencher	0 ~0.08

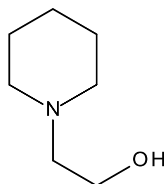

1-Piperidineethanol as the quencher

Model experiment of immersion lithography. Onto photoresists coated on a 4-inches wafer as described above, an o-ring (4D G-95 from ARAM) made with fluoro resin was set. Then 20 ml of distilled water purchased from Wako Chemical was poured into the ring and covered with 4-inches quartz glass.

In case of the determination of PAG leaching from photoresist, two types of base resins as shown below were employed. Polymer A was purchased from Mitsubishi Rayon and Polymer B was radically synthesized in-house from the corresponding monomers purchased from Daicel, Idemitsu and Osaka Yuki. PAG was employed by 10 % against resin.

Dissolution rate was measured in the ArF model resist formulation without amine quencher as described above. The resist was exposed with VUVES 4500 mini under dry/immersion condition. After post exposure bake, dissolution rate of the resists was monitored by RDA-790, Litho Tech Japan.

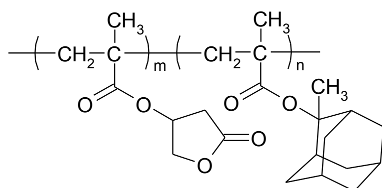

Polymer A

(m: n = 62: 38)

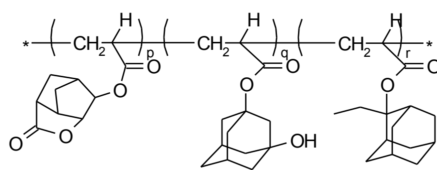

Polymer B

(p: q: r = 50: 20: 30)

Results and discussion

Photodecomposition in solution

UV absorption change. In order to investigate the fundamental photochemical property, one of the novel PAGs, DNHF, dissolved in acetonitrile solution was exposed at 193 nm and the UV absorption of DNHF during the exposure was measured and plotted in Fig. 1. The absorption profile was changed with the exposure. Isosbestic points were clearly observed. Thus it suggests that photodecomposition of DNHF yields only one product.

Because the absorption change at 193 nm was small, within ca. 0.01, between before and after exposure, it is expected that the high transparency of the photoresist including DNHF is kept under lithography process. However the change of UV absorption profile was too small to figure the proceeding of photochemical reaction. The HPLC analysis of the resulting solution was conducted to determine the quantum yields.

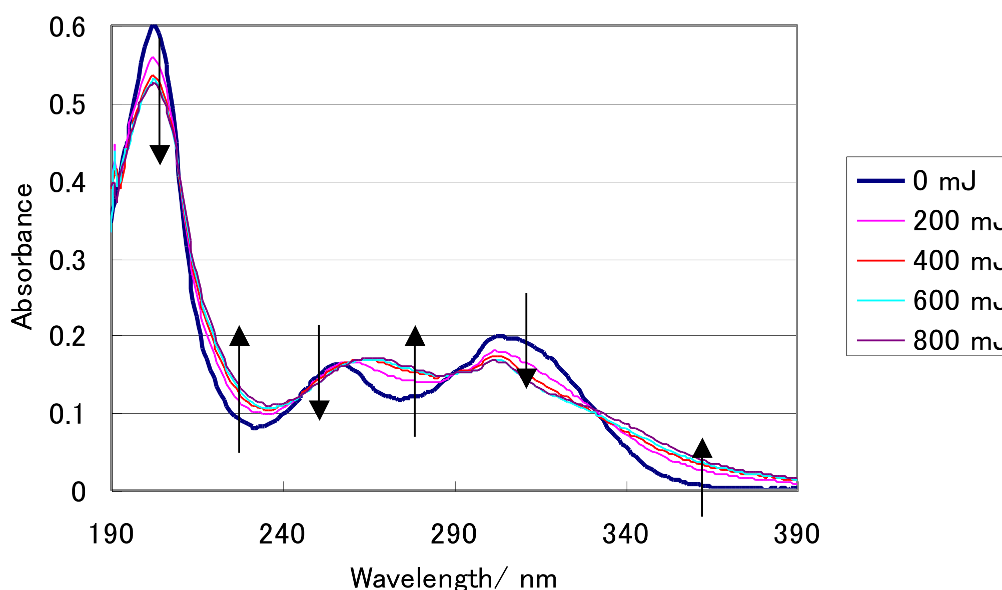

Fig. 1. UV absorption change of DNHF during exposure

Quantum yield measurement of PAG in solution. During the exposure, remaining amount of three PAGs, DNHF, TPSPB, and BPIPB, was monitored by HPLC analysis to study the photo efficiency. The decomposed amount of PAG was plotted against absorbed dose energy, which was calculated from the absorbance and applied dose energy, in Fig. 2. The slope of the fitting line on each PAG gives the quantum yield. The slopes and the quantum yields are listed in Table 2. Additionally normalized ratio calculated from the value of the quantum yield of TPSPB is also

listed. The highest slop of DNHF gave the highest quantum yield, 0.27, among the three PAG evaluated here. The superiority to TPSPB was by 46% from the normalized ratio. BPIPB showed the lowest quantum yield, 0.06, among them. Considering that the same acid, perfluorobutanesulfonic acid, generates under ArF exposure, there is no doubt that the oxime chromophore of DNHF is superior to sulfonium and iodonium chromophores in efficiency on acid generation at 193 nm.

Table 2. Quantum yield of PAG in solvent

PAG	Slope (mol mJ^{-1})	Quantum Yield	Normalized ratio
DNHF	4.3×10^{-10}	0.27	1.46
TPSPB	3.0×10^{-10}	0.18	1
BPIPB	9.1×10^{-11}	0.06	0.31

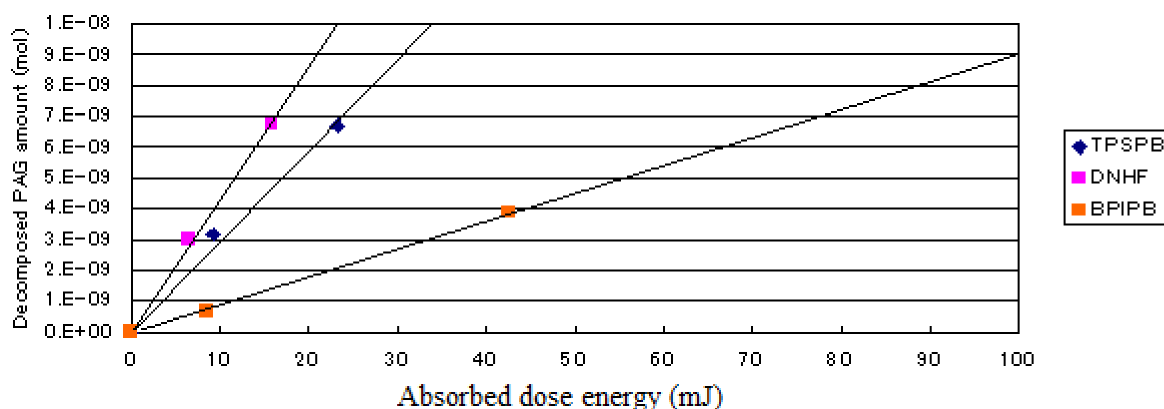

Fig. 2. Photochemical decomposition of PAG

Photodecomposition in formulation

Quantum yield measurement of PAG in formulation. In addition to the fundamental study of PAG efficiency with quantum yield measurement in solution, quantum yields of the PAGs in a model formulation were investigated from application relevant point of view.

Regarding quantum yield measurement of PAG in ArF resist formulation, some measurement methods and techniques have been introduced so far.[9-12] Especially the standard addition method by Szmanda is simple and requires no special experimental setup nor computer simulation calculation but conventional sensitivity measurement.[9]

Thus the method for quantum yields measurement of the PAGs in a model formulation was

chosen. The mole ratio of amines added in the formulation against the PAG was plotted against E_0, sensitivity of the resist. From the slope of the fitted line, the Dill's C-parameter and the quantum yields were calculated and listed in the Table 5. DNHF and HNBF showed the high quantum yield, 0.22 and 0.25. The value of TPSPB, 0.13, was very close to value of triphenylsulfonium trifluoromethanesulfonate, 0.11 ~ 0.13, reported previously.[11] Even though the difference of C-parameter between the novel PAGs and TPSPB was small only by 0.01 to 0.02, the quantum yield of them was bigger. This was due to the higher transparency of DNHF and HNBF than TPSPB at 193 nm. BPIPB, iodonium salt, showed the lowest quantum yield, 0.03. This result is also close to the reported value of the triflates, 0.04 ~ 0.05.[11] C-parameters obtained here were far from the value reported previously. The reason may be due to the difference of matrix resin system, such as transparency at 193 nm.

Quantum yields of all PAGs in formulation are lower than that in solution. It is think this is due to matrix effect of acrylate polymer. The polymer matrix disturbs the diffusion of the generated acid and promotes probability of recombination.

Table 3. Quantum yield of PAGs in formulation

PAG	Slope (mJ^{-1} cm^2)	C-parameter ($mJ^{-1}cm^2$)	Quantum Yield	Normalized ratio
DNHF	0.1429	0.16	0.22	1.68
HNBF	0.1481	0.17	0.25	1.92
TPSPB	0.1243	0.15	0.13	1
BPIPB	0.0151	0.02	0.03	0.23

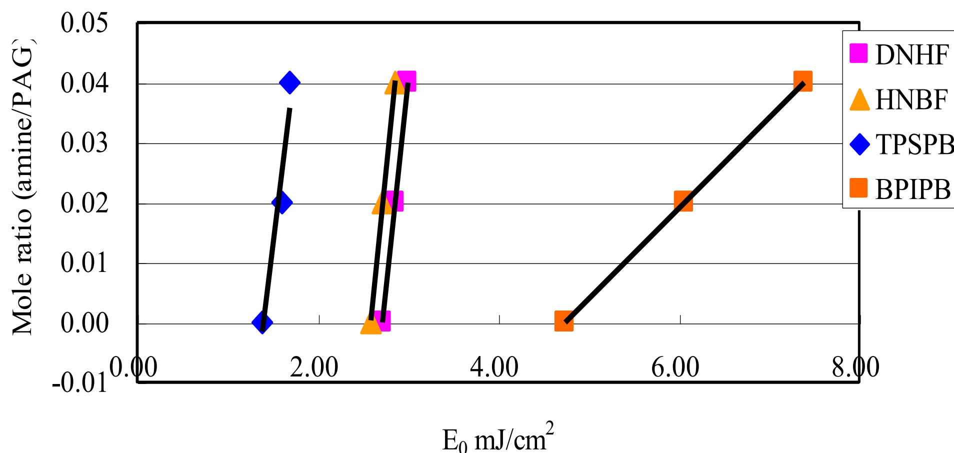

Fig. 3. Relation between amine/PAG ratio and sensitivity

Comparison of quantum yields measured in solution and in formulation. The normalized ratio of PAGs measured in solution and in formulation was plotted in the Fig. 4. The both showed the good agreement each other. This result tells us the photochemical behavior of PAGs measured here is the same in solution and in formulation. In other words, there are no special effects, such as energy transfer form resist matrix shown in DUV resists, were occurred here.

The results in quantum yield measurement obtained here is in relative good agreement on order with P-parameter calculated from E_0, sensitivity and PAG absorbance in resist.[13] DNHF and HNBF show higher efficiency and sensitivity than the others, TPSPB is moderate and BPIPB is the PAG of the poorest efficiency and requires the highest dose of energy for lithography among the PAGs.

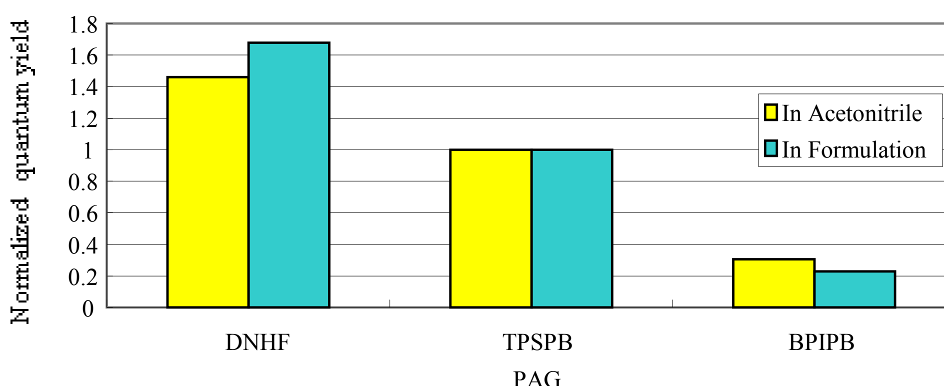

Fig. 4. Comparison of the normalized ratio

Table 4. P-parameter of PAG

PAG	P-parameter
DNHF	0.33
HNBF	0.34
TPSPB	0.45
BPIPB	0.59

Model experiment of Immersion lithography

PAG leaching to immersion media. It is believed that ArF immersion lithography is the up-coming next generation lithography for 45 nm node and the shorter and that water is employed as the immersion media due to the high transparency and the high refractivity at 193 nm. However leaching of the materials into water during immersion process is recognized as one of the most

critical issues of this technique. Thus materials do not elute to water is desirable.

The leaching of PAG during immersion process was investigated in our model immersion process. The employed materials, soaking time and leaching result of PAG were listed in Table 5. While TPSPB exhibited significant leaching behavior, 2 ~ 9 x 10^{-11} mol/cm^2, in any experiments, no leaching of DNHF and HNBF was observed, < 2.6 x 10^{-12} mol/cm^2. This result agrees with PAG solubility in water reported previously[5] (TPSPB: 0.34%, DNHF: <0.001%) and clearly indicates that DNHF and HNBF are the more preferable PAGs in up-coming immersion lithography from view point of leaching than TPSPB which is popular in current dry ArF photoresists. The observed leaching value of TPSPB form polymer B, 8 - 9 × 10^{-11} mol/cm^2, showed excellent agreement with the value previously reported by Sato, 6 × 10^{-11} mol/cm^2.[14&15]

In comparison of polymers, three to four times larger amount of TPSPB was eluted into water from hydrophilic polymer B than from hydrophobic polymer A. In the current ArF dry resist, the hydrophilic polymer, such as polymer B, having good affinity with aqueous alkaline developer tends to be employed to reduce development defects. Thus the less leaching PAGs, such as DNHF and HNBF, will be more desirable in immersion lithography.

The soaking time experiments suggest that TPSPB leaching is fast and almost finishes within 15 seconds (or shorter) after water apply.

Table 5. PAG leaching

PAG	Polymer	Soaking time	PAG leaching (mol/ cm^2)
TPSPB	A	10 min	3×10^{-11}
TPSPB	A	15 sec	2×10^{-11}
TPSPB	B	10 min	9×10^{-11}
TPSPB	B	15 sec	8×10^{-11}
DNHF	A	10 min	$< 2.6 \times 10^{-12}$
DNHF	B	10 min	$< 2.6 \times 10^{-12}$
HNBF	A	10 min	$< 2.6 \times 10^{-12}$
HNBF	B	10 min	$< 2.6 \times 10^{-12}$

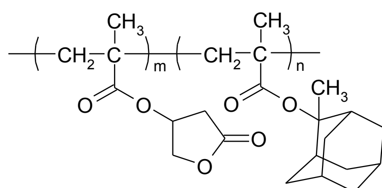

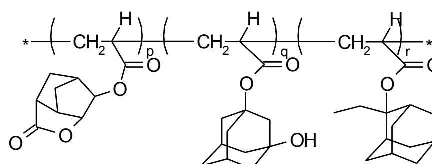

Polymer A (m: n = 62: 38)

Polymer B (p: q: r = 50: 20: 30)

DRM results under dry and immersion exposure. Dissolution rate monitoring (DRM) has been conducted to study the fundamental dissolution property of photoresists including DNHF and to predict the resulting resist profile. In this chapter, dissolution rate of DNHF in a typical poly(methacrylate) type photoresist was measured after dry and immersion exposure process to investigate the difference between them. The experimental results were plotted in Fig. 5. No clear difference between the two exposure conditions was observed. In case that PAG elutes into immersion media, reduction of dissolution rate of the resist is reported.[16] No reduction of DRM results suggests that no DNHF elutes from the resist. Considering that no difference of DRM was reported so far with poly((meth)acrylate) type photoresists, the results obtained here are reasonable.[15&17] The resolution achieved in dry resist can be expected even in immersion condition. Considering the fact that DNHF shows no leaching during immersion process and higher quantum yield, DNHF is a superior PAG to TPSPB for photoresists in up-coming immersion lithography.

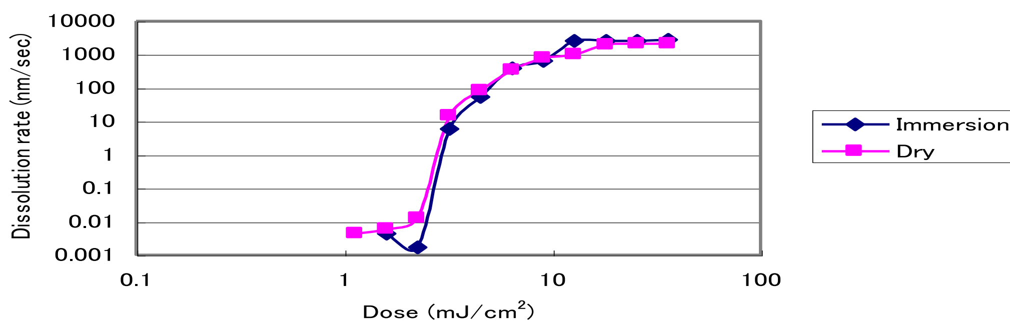

Fig. 5. DRM results of dry and immersion lithography with DNHF

Conclusion

Novel non-ionic PAGs, DNHF and HNBF, developed for ArF photoresist applications are discussed. This chemistry of PAG can release strong acid (perfluorobutanesulfonic acid) by ArF irradiation with higher efficiency in solution and in photoresist formulation comparing to the conventional ionic PAGs, such as TPSPB and BPIPB. Additionally DNHF and HNBF showed no leaching under a model immersion process while significant amount of TPSBP was eluted. It is concluded that DNHF and HNBF are the ideal PAGs not only for dry ArF but also for immersion lithography process.

References

1 B. J. Lin, *Proc. SPIE* ,**2002**, *4688*, 11-24.

2 T. Asakura, H. Yamato and M. Ohwa, *J. Photopolym. Sci. Technol.,* **2000,** *13,* 223-230.

3 H. Yamato, T. Asakura, A. Matsumoto and M. Ohwa, *Proc. SPIE,* **2002,** *4690*, 799-808.

4 T. Asakura, H. Yamato, A. Matsumoto, P. Murer and M. Ohwa, *Proc. SPIE,* **2003,** *5039*, 1155-1163.

5 H. Yamato, T. Asakura, T. Hintermann and M. Ohwa, *Proc. SPIE*, **2004,** *5376*, 103-114.

6 N. Dazai et al., Japanese Patent Publication, 2008-308520A;

7 N. D. Jarnagin et al., *J. Photopolym. Sci. Technol.*, **2006**, *19*, 719-725.

8 H. Yamato et al., U.S. Patent 7399577B2, **2008**.

9 C.R. Szmanda, R. Kavanagh, J. Bohland, J. Cameron, P. Trefonas and R. Blacksmith, *Proc. SPIE,* **1999,** *3678*, 857-866.

10 A. R. Pawloski, P. F. Nealey and J. J. de Pablo, *SRC Program Review* **2001**.

11 J. F. Cameron, N. Chan, K. Moore and G. Pohlers, *Proc. SPIE,* **2001,** *4345*, 106-118.

12 K. Ray, M. D. Mason, R. D. Grober, G. Pohlers, C. Staford and J. F. Cameron, *Chem. Mater.,* **2004,** *16*, 5726-5730.

13 G. Pohlers, Y. Suzuki, N. Chan and J. F. Cameron, *Proc. SPIE,* **2002,** *4690*, 178-190.

14 M. Yoshida, K. Endo, K. Ishizuka and M. Sato, *J. Photopolym. Sci. Technol.,* **2004,** *17*, 603-608.

15 M. Sato, M. Yoshida, K. Ishizuka, and K. Endo, *Polymer Preprints, Japan,* **2004,** *53*, 115-118.

16 S. Kishimura, M. Endo, and M. Sasago, *Proc. SPIE,* **2004,** *5376*, 44-55.

17 A. Sekiguchi, Y. Kono and M. Kadoi, *The Papers of Technical Meeting on Light Application and Visual Science, IEE Japan*, **2004,** 27-32.

Chapter 6

Studies on novel photoacid generator for 13.4 nm (EUV) exposure

Abstract

Extreme Ultraviolet (EUV) has already achieved the initial requirements for 32 nm DRAM half pitch lithography rule and is known as one of the most promising next generation lithography techniques to be realized for 22 nm patterning technology though strict requirements for the power of the light sources, lithographic performance of the photoresist and the manufacturing and inspection of masks are still remaining,.

In this chapter, the author investigated the photolithographic characteristics of photoacid generator (PAG) additive approach in EUV lithography with different polymer platforms and sulfonium-type PAGs compared with other exposure techniques to understand the relationship between lithography results and photoresist materials. Four different sulfonium nonafluorobutanesulfonate; triphenylsulfonium nonafluorobutanesulfonate (**TPS**), tri(4-methoxy-3,5-dimethylphenyl) sulfonium nonafluorobutanesulfonate (**MDP**), tri(4-methoxy-3-methylphenyl)sulfonium nonafluorobutanesulfonate (**MMP**) and tri(4-methoxy-3-phenylphenyl)sulfonium nona-fluorobutanesulfonate (**MPP**) were employed as PAG in order to study the fundamental properties, such as sensitivity, photo-efficiency, lithographic performance , in the two different model formulations, poly(hydroxystyrene) (PHS) type and poly(methacrylates)-type, under three different exposures of 193 nm (ArF), Electron Beam (EB) and EUV.

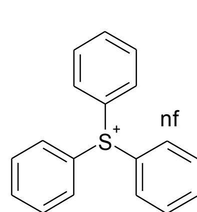

TPS

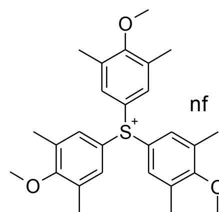

MDP

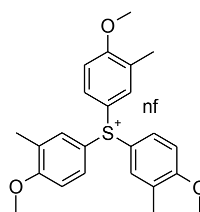

MMP

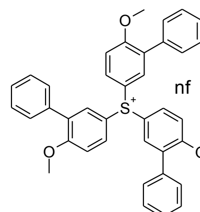

MPP

PAG employed in this study

(nf: nonafluorobutanesulfonic acid)

Introduction

Further miniaturization has always been a duty in semiconductor fabrication and technology developments related to photoresist lithography have been achieved with a drastic speed to meet the demand. The latest technology, which is currently 193 nm (ArF) photoresist lithography, has achieved the semiconductor fabrication with a design rule at 50 nm DRAM half pitch (HP) scaling technology. Though ArF lithography is expected to be extended to the 32 nm scaling rule owing remarkable progress in new technology like double-patterning, the limitation of utilization is also expected due to its high cost and low yield for the complicated manufacturing processes.

Extreme ultraviolet (EUV) has already achieved the initial requirements for 32 nm DRAM HP lithography rule and is known as one of the most promising next generation lithography techniques to realize 22 nm scaling technology though strict requirements for the power of the light sources, lithographic performance of the photoresist and the manufacturing and inspection of masks are still remaining.[1]

Regarding the lithographic performance on EUV exposure, the well-known three serious challenges for photoresists are sensitivity, resolution and linewidth roughness (LWR); target criteria are below 10 mJ/cm^2 in sensitivity, below 40 nm in HP resolution, and below 3 nm (3σ) in LWR simultaneously.[2] To achieve the criteria, many approaches and concepts, such as molecular glass and PAG on polymers, are investigated and developed thus far.[3&4]

In this chapter, the author investigated the fundamental properties of authentic PAG additive approach in EUV lithography with different polymer platforms and different sulfonium-type PAGs compared with other exposure techniques to understand the relationship between lithography results and photoresist materials.

It was utilized that EUV Micro-Exposure Tool (eMET) in Sematech North at Albany in the US for 50 nm line and space (L/S) pattering lithography comparing EUV photoresist model formulations in order to study the basic properties, such as sensitivity, photo-efficiency, exposure latitude and line width roughness.[5] Four different sulfonium nonafluorobutanesulfonates; triphenylsulfonium nonafluorobutanesulfonate (**TPS**), tri(4-methoxy-3,5-dimethylphenyl) sulfonium nonafluorobutanesulfonate (**MDP**), tri(4-methoxy-3-methylphenyl)sulfonium nonafluorobutanesulfonate (**MMP**), and tri(4-methoxy-3-phenylphenyl)sulfonium nonafluorobutanesulfonate (**MPP**) were employed in the two different model formulations, poly(hydroxystyrene) (PHS) type and poly(methacrylates)-type, under three different exposures of ArF, electron beam (EB) and EUV.

Experimental

Materials. In polymers, a copolymer of γ-butyrolactone methacrylate and 2-methyladamantyl methacrylate (62/38 mol%, Mn=11800, Mitsubishi Rayon Co., Ltd) was purchased and employed as received. PHS-type copolymer (Copolymer A) and poly(methacrylates)-type copolymer (Copolymer B) were radically polymerized in-house from the corresponding monomers, 2-ethyladamantyl methacrylate (from Osaka Yuki), γ-butyrolactone methacrylate (from Daicel) and 4-vinylphenyl acetate (from Tokyo Kasei Kogyo Co., Ltd) by the know procedures.[6&7]

In solvents and developers, propyleneglycol monomethyl ether acetate (PGMEA, from Tokyo Kasei Kogyo Co., Ltd), acetonitrile (from Wako Pure Chemical Industries, Ltd.), ethyl lactate (from Tokyo Kasei Kogyo Co., Ltd), and 2.38 % aqueous tetramethyl ammonium hydroxide solution (TMAH, from Tokyo Ohka Kogyo Co., Ltd.) were purchased and employed as received.

In chemicals, N-(1-adamantyl)acetamine (from Aldrich), triphenylsulfonium nonafluorobutanesulfonate (TPS, from Midori Kagaku Co., Ltd.), and a formulation of bottom antireflection coating (ARC-29, from Nissan Chemical Industries, Ltd.) were purchased and employed as received. Tri(4-methoxy-3,5-dimethylphenyl) sulfonium nonafluorobutanesulfonate (MDP), tri(4-methoxy-3-methylphenyl)sulfonium nona-fluorobutanesulfonate (MMP), and tri(4-methoxy-3-phenylphenyl)sulfonium nona-fluorobutanesulfonate (MPP) were synthesized internally by the know procedures.[8]

Photolithographic properties in ArF model formulation. To evaluate the photographic properties of our model formulation, they were irradiated by open frame exposure with VUVES 4500 mini, Litho Tech Japan, as an ArF exposure tool. Our positive tone resist model formulations utilized a copolymer of γ-butyrolactone methacrylate and 2-methyladamantyl methacrylate (62/38 mol%, Mitsubishi Rayon Co., Ltd) having a weight average molecular weight of 11800. The composition of the formulation is described in Table 1.

Table 1. Composition of ArF formulations

Components	Parts (Weight)
Binder polymer	100
PAG	2
PGMEA	1300

The resist was spin-coated at 120 nm thickness on silicon wafers on which the bottom antireflection coating (ARC-29, Nissan Chemical) was applied at 82 nm thickness in advance and prebaked at 200 °C for 60 sec. After exposure with various doses of energy, a post exposure bake was applied at 120 °C for 60 sec and the photoresist was then developed in 2.38% aqueous tetramethylammonium hydroxide solution, TMAH commercially available from TOK, for 60 sec at 23 °C.

Photolithographic properties in EB model formulation. To evaluate the EB sensitivity of our model formulation, the EB model photoresist formulations were irradiated by open frame radiation with JBX-500SI, JEOL, as an exposure tool at Technology Research Institute of Osaka Prefecture. The acceleration voltage for patterning was 50 keV. Our positive tone photoresist model formulations utilized two copolymers, one is PHS-type (Copolymer A) and the other is poly(methacrylates)-type (Copolymer B). The composition of formulations is described in Table 2. As for PAG loading, the same molar amount of PAG is loaded as 4 parts of TPS.

Table 2. Composition of EB/EUV formulations

Components	Parts
Binder polymer	100
PAG	4~5.2
N-1-adamantylacetamine	0.27
PGMEA/Ethyl lactate (7/3 by volume)	3000

The photoresist was spin-coated at 60 nm thickness on silicon wafers on which surface 1,1,1,3,3,3-hexamethyldisilazane commercially available Tokyo Chemical Industry was treated at 40 °C and soft-baked at 110 °C for 60 sec. After radiation process with various doses of energy, a post exposure bake was applied at 110 °C for 60 sec and the photoresist was then developed at 23 °C in TMAH for 60 sec.

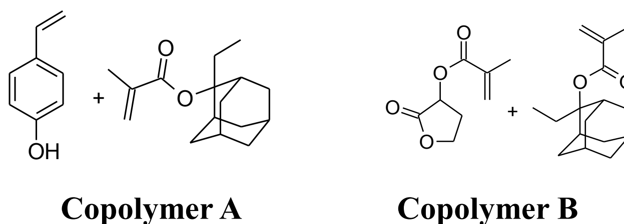

Copolymer A **Copolymer B**

Photolithographic properties in EUV model formulation. To evaluate the EUV photolithographic properties, the 50 nm L/S patterning was performed with the EUV model photoresist formulations by eMET in Sematech North at Albany in the US, as exposure equipment. The composition of the formulation is the same as described in Table 2.

In the lithography process, the photoresist- coating and baking processes are the same as the ones applied in EB evaluation processes. Critical dimension of the obtained line was measured with CD SEM at Sematech North and LWR was determined as an indicator for roughness estimation by software analysis with SuMMIT purchased from EUV Technology, CA, in the US.

UV absorption and transparency measurements. PAGs' UV absorption spectra in acetonitrile with 1 cm optical path-length were taken with a Hitachi U-3300 spectrometer. Absorbance at 193 nm was quantified in a 0.01 g/L solution in acetonitrile.

As for the PAG absorption at 13.5 nm, it was estimated by the calculation method developed by the Center for X-Ray Optics, Lawrence Berkeley National Laboratory in the US.[9]

Results and discussion

Photolithographic properties in ArF model formulation. ArF lithography is the most advanced photolithography technique for high volume production currently. In order to investigate the photolithographic properties of PAG for ArF photoresist applications, each PAG was formulated in an ArF model formulation with 2 wt% against polymer, respectively. As the polymer matrix, a typical poly(methacrylates) platform was employed which has high transparency at 193 nm. The photoresist layer was exposed by ArF laser (193 nm) to determine the sensitivity. In lithography studies, the "Dose to clear" (E_0) is employed as a measure of photoresist sensitivity. The E_0 is the dose of energy just sufficient to remove the photoresist film at the development process completely. As the required dose decreases, the sensitivity of the photoresist formulation increases.

Table 3. Sensitivity (E_0), Absorbance at 193 nm and P-parameter

PAG	E_0 (mJ/cm^2)	Abs. @ 193 nm	P-parameter
TPS	1.6	1.26	2.0
MDP	4.9	0.78	3.9
MMP	5.4	0.72	3.9
MPP	9.9	0.82	8.1

The obtained E_0 for each PAG is listed in the Table 3 with the PAG absorbance at 193 nm, which was obtained in acetonitrile solution at 0.01 g/L concentration with 1 cm optical path-length, and P-parameter.[10] To evaluate PAG photo-efficiency in photoresist formulations, P-parameter, which is defined by the value of sensitivity (E_0) multiplied by PAG absorbance listed in Table 3, was employed here. It is notable that the differences in absorption and P-parameter are only due to PAG's chromophore difference in performance because the same acid, nonafluorobutanesulfonic acid, was generated from each PAG in this study. The smaller P-parameter value indicates the higher photo-efficiency. The P-parameter normalized by the TPS value is plotted in Fig. 1. TPS exhibited the highest photo-efficiency among the PAGs evaluated here. MDP and MMP followed TPS and were superior to MPP in terms of photo-efficiency.

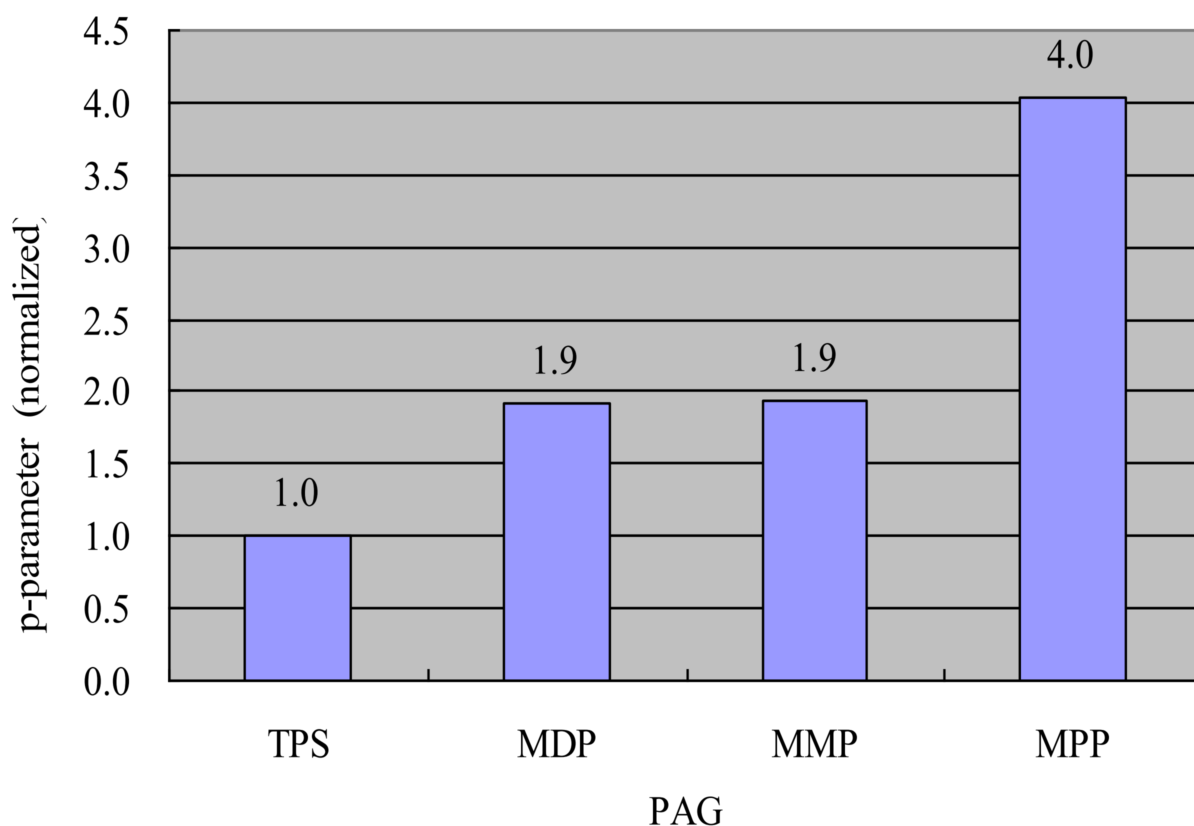

Fig 1. P-parameter (normalized) comparison

Photolithographic properties in EB model formulation. EB radiation chemistry is often studied to interpret the results with EUV lithography results. The photo-sensitivity, E_0, with the EB exposure tool was evaluated. Here one of the important differences between EB radiation lithography and EUV exposure one is energy of doses. While EUV exposure, which is 13.5 nm wavelength, corresponds to 92.5 eV of energy, a typical acceleration voltage in EB lithography, 50 keV, is used here.

The sensitivity results, E_0, in two formulations with different polymer matrices, Copolymer A including PHS and Copolymer B comprising poly(methacrylates), are plotted in Fig. 2. The formulations with Copolymer A showed higher photospeed than the ones with Copolymer B in the presence of any PAGs. Especially in case of MDP, E_0 with Copolymer A was less than half of that with Copolymer B. Kozawa *et al.* chaptered lower acid generation efficiency in poly(methyl methacrylate) (PMMA) than PHS under EB radiation generally because secondary electron generated from polymer matrix is trapped by PMMA itself and because the deprotonation efficiency of PMMA radical cations is lower than that of PHS radical cations.[11] The phenomena observed in PMMA may be one of the reasons why such a drastic sensitivity difference between the two was observed.

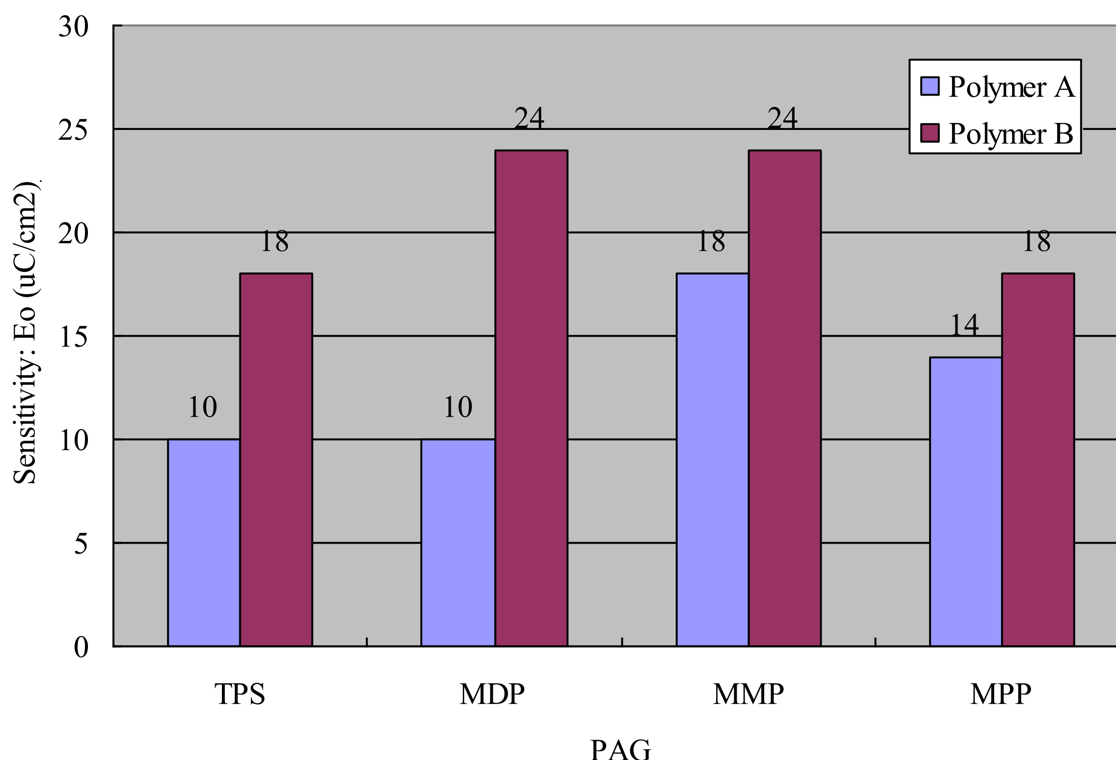

Fig 2. Sensitivity (Eo) comparison

Calculation of UV absorption at 13.5 nm. PAG absorption is a key factor to understand the photolithographic properties under any exposure systems. The PAG absorption at 13.5 nm was calculated by the method developed by the Center for X-Ray Optics (CXRO), Lawrence Berkeley National Laboratory in the US and used to evaluate the photo-efficiency.[9] The gas phase transmission of PAG at 295 degree Kelvin under 30 Torr with 1 cm optical path length was determined by the calculation at CXRO web-site and transformed to absorbance at 13.5 nm. The absorbance is listed in Table 4 as well as the normalized absorbance with that of TPS.

More introduction of alkyl, alkoxy and phenyl group made chromophore absorption higher at 13.5 nm wavelength.

Table 4. PAG absorption at 13.5 nm

PAG	Gas phase absorbance	Normalized absorbance
TPS	0.718	1.00
MDP	0.888	1.24
MMP	0.861	1.20
MPP	0.988	1.38

Photolithographic properties in EUV model formulation. EUV has already achieved the initial requirements for 32 nm DRAM HP lithography rule and is known as one of the most promising next generation lithography techniques to be realized for 22 nm patterning technology.[1] In this chapter, the author utilized eMET at Sematech North for 50 nm L/S pattering lithography comparing several EUV photoresist model formulations in order to investigate the basic photolithographic properties of PAGs, such as sensitivity, photo-efficiency, exposure latitude, and line width roughness (LWR).

Sensitivity under EUV exposure. As publically known well, the three severe challenges for EUV lithography are sensitivity, resolution and LWR; the target criterion for each is below 10 mJ/cm^2 in sensitivity, below 40 nm in HP resolution and below 3 nm (3σ) in LWR simultaneously.[2]

In the experiments here, E_{size}, which is a required dose to achieve the desirable 50 nm L/S pattern lithography, is employed to evaluate the sensitivity for each photoresist. Prior to determination of E_{size}, the critical dimension of the obtained line pattern was determined by CD SEM observation and plotted against the applied dose of energy. From the trend line of the plot, the energy to perform 50 nm L/S patterning was determined and utilized it as E_{size} here.

The obtained results are listed in Table 5 and plotted in Fig. 3.

Table 5. Sensitivity (E_{size}) and P-parameter under EUV exposure

PAG	E_{size} (mJ/cm^2)		P-parameter (mJ/cm^2)	
	A	B	A	B
TPS	11.0	12.0	11.0	12.0
MDP	9.3	9.8	11.5	12.1
MMP	10.8	9.8	13.0	11.8
MPP	11.0	11.5	15.1	15.8

While the significant difference in EB sensitivity was observed between the two formulations, it was interestingly found that there was no clear difference in EUV sensitivity between the two. The fact indicates that acid generation mechanism of EB radiation and EUV exposure are clearly different each other and that the formulations showing inferior sensitivity in EB lithography might perform well in sensitivity under EUV lithography process.

In case of Copolymer A, the value of sensitivity was in the range around 11.0 mJ/cm^2 except MDP. Though the reason why MDP is superior in photospeed is not understood yet, it may be brought by the superior ability to accept the electron transferred from polymer matrix; energy level of LUMO, the energy difference between HOMO and LUMO and distance from hydroxyphenyl

moiety are might be key factors in such a case.[12] Further experiments and investigations are necessary to determine the key property in EUV sensitivity results observed here.

Because the reaction of PAGs and thermalized electrons from PHS strongly depends on PAG loading amount and photoresist film thickness in EUV exposure, it is expected optimization of PAG loading amount and photoresist thickness will improve the sensitivity of formulations with Copolymer A.[13&14]

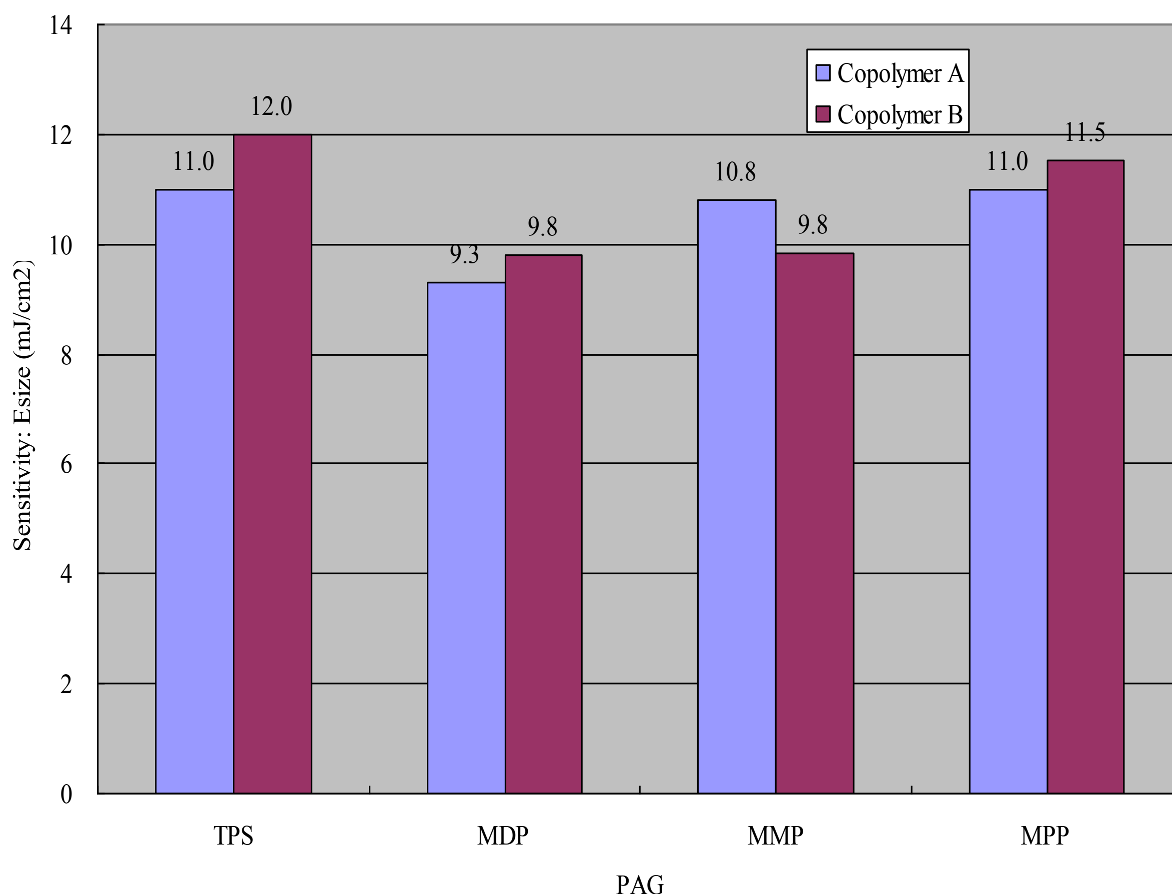

Fig. 3. Sensitivity (E_{size}) comparison

Photo-efficiency under EUV exposure. It is widely proposed that the electrons generated from PHS polymer matrix of photoresists under EUV radiation are involved in the acid generation reaction from PAG.[15] However less information about the acid generation mechanism in poly(methacrylates) matrix is available. To investigate the possibility of direct excitation of PAG under EUV exposure, values of P-parameter with Copolymer A and Copolymer B were calculated and listed in Table 5. In the case of EUV exposure, E_{size} was used instead of E_0 in ArF and calculated P-parameter normalized by the value of TPS was employed instead of absorbance in acetonitrile.

Normalized P-parameter by the value of TPS is plotted in Fig. 4. While the value of TPS, MDP and MMP was varied from 1.00 to 1.18 in case of Copolymer A, the value was interestingly close each other and within the range from 0.98 to 1.01 in case of Copolymer B. Though the reasons of the results observed here are not clear yet, the results may suggest that the acid generation in Copolymer A is related not directly to PAG absorption but to absorption of matrix, that the generation by the direct excitation of PAG by EUV radiation is dominant in Copolymer B matrix and that the acid generation efficiency from the three PAGs is in the same range. The interpretation supports the proposed acid generation mechanism in PHS. In case of MPP, the P-parameter value in Copolymer B is significantly inferior to the others. One possible explanation is that the absorption by additional phenyl group on MPP might not contribute to acid generation.

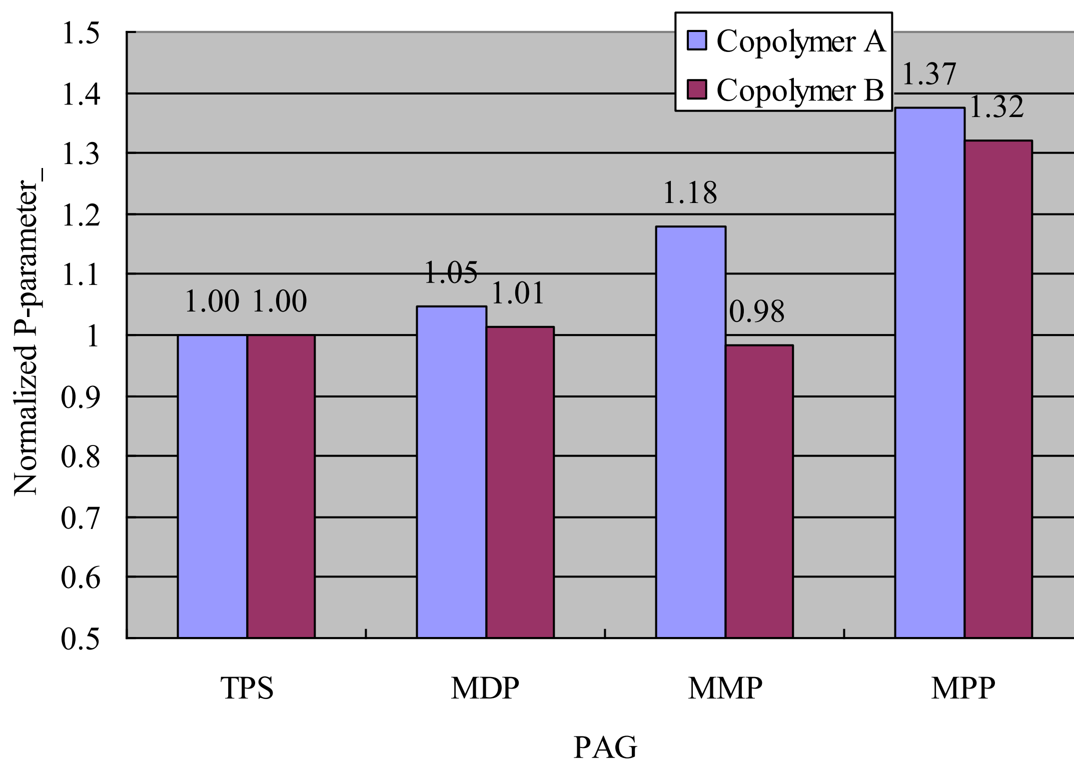

Fig. 4. P-parameter (normalized) in copolymers comparison

Exposure latitude. When the lithography process is executed, process latitude of the utilized photoresist is one of the most important factors to be considered. If it is low, high number of defects on lithography process is projected. As a consequence, yield on device manufacturing becomes poor. During the photolithographic studies with eMET, the applied dose of energy was varied. In the trend line of the critical dimension of line vs. the applied doses plot, the slope of the line was employed as a measure to indicate exposure latitude of the photoresists here. If the line width is affected by dose

change strongly, the trend line becomes steep and the slope becomes big. The smaller slope value means more tolerant and is more preferable in exposure latitude.

The value of the two types of the model formulations are plotted in Fig. 5. It is obvious that exposure latitude of the formulations with Copolymer A is less affected by the sort of PAGs/chromophores and better in performance with any cases except MDP than that with Copolymer B.

One possible explanation for the phenomena observed here is difference in acid generation mechanism as discussed in the sensitivity part; it is known acid generation by the electron transfer from polymer matrix absorbing EUV irradiation is dominant in Copolymer A.[15] In such a case, the acid generation strongly depends on the absorption to PHS matrix. Thus the difference in exposure latitude among PAGs was small. In case of Copolymer B, however, the exposure latitude is affected seriously by the absorption of PAG due to its direct excitation dependency.

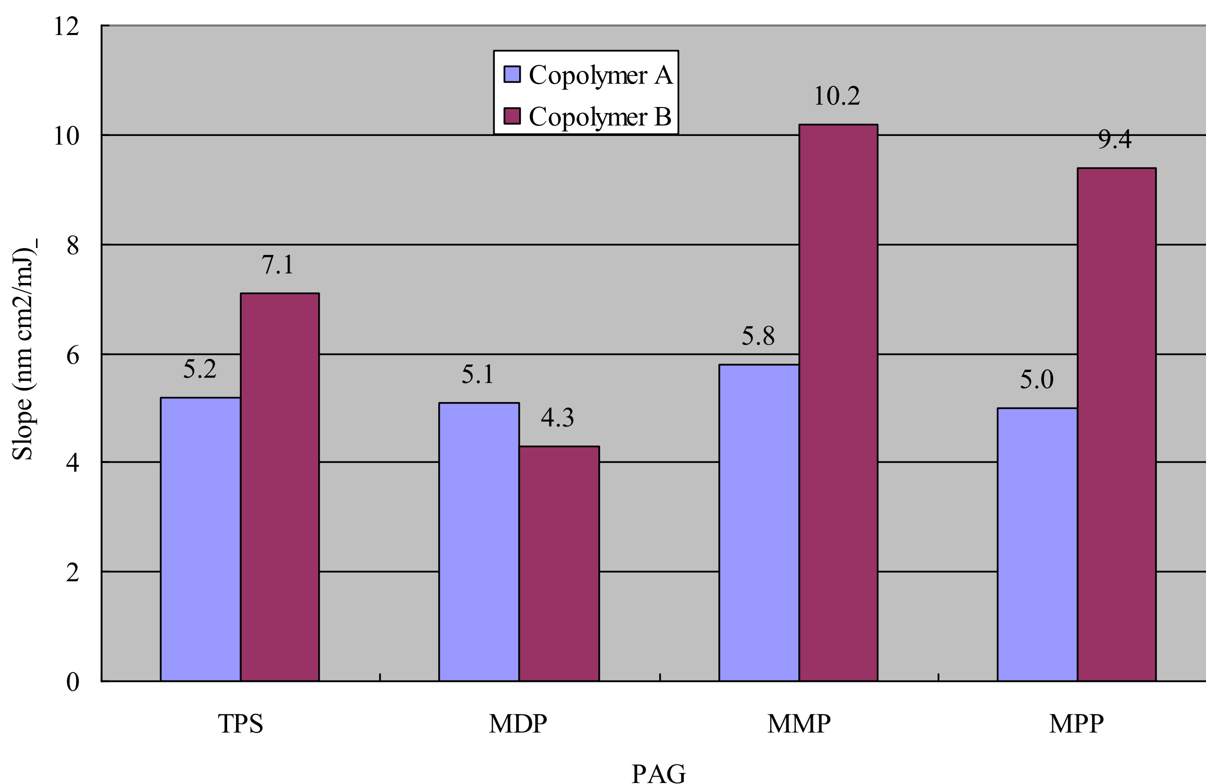

Fig. 5. Exposure latitude (slope of critical dimension vs. exposure dose plot) comparison

Line width roughness. Roughness of the obtained lithography results is becoming a more critical issue with shrinkage of lithography features. In this EUV lithographic study, the resulting Line width roughness (LWR) in the range from 7.9 to 12.0 nm was far above the target value of International Technology Roadmap for Semiconductors (ITRS), below 3 nm. Comparing the LWR results with the determined sensitivity (around 10 mJ/cm^2) and achieved resolution (50 nm L/S pattern), it is clear that this point is the most serious issue remaining on the model formulations. One way to improve this property is to reduce the acid mobility; the results might be improved by changing acid moiety from nonaflic acid to bulky and less movable one.

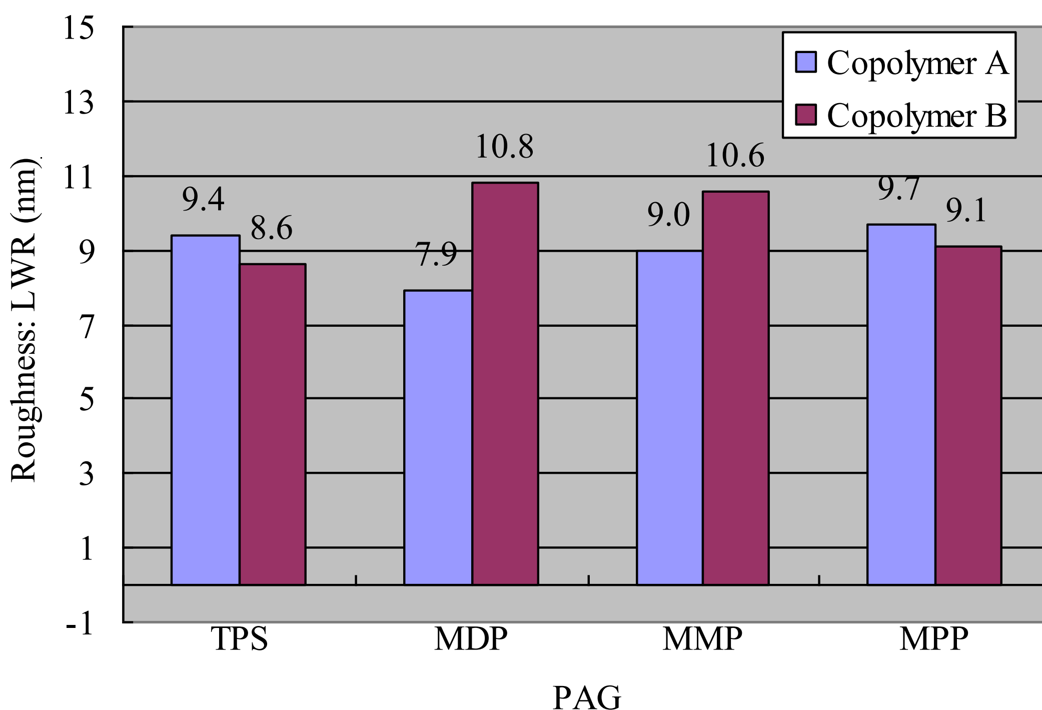

Fig. 6. Roughness (LWR) Comparison

Conclusion

In this chapter, it was investigated the fundamental properties of traditional PAG additive approach in EUV lithography with two different polymer platforms, PHS type and poly(methacrylates) type, and four sulfonium nonafluorobutanesulfonate PAGs, TPS, MDP, MMP, and MPP, compared with ArF and EB exposure techniques to understand the relationship between lithography results and photoresist materials.

While the significant difference in EB sensitivity was observed between the two polymer platforms, it was interestingly found that there was no clear difference in EUV sensitivity between the two. It indicates that acid generation mechanism of EB radiation and EUV exposure are clearly different each other and that the formulations showing inferior sensitivity in EB radiation might perform well in sensitivity under EUV lithography process.

Normalized P-parameter values of TPS, MDP, and MMP in the Copolymer B were interestingly close each other. It suggests the possibilities that acid the generation by the direct excitation of PAG under EUV radiation is dominant in Copolymer B matrix and that the acid generation efficiency from the three PAGs is in the same range.

References

1. J. Park, C. Koh, D. Goo, I. Kim, C. Park, J. Lee, J. Park, J. Yeo, S.-W. Choi and C.-h Park, *Proc. SPIE*, **2009**, *7271*, 727114.
2. INTERNATIONAL TECHNOLOGY ROADMAP FOR SEMICONDUCTORS **2008** UPDATE OVERVIEW, p 36.
3. S. Tanaka, N. Matsumoto, H. Ohno, N. Hatakeyama, K. Ito, K. Fukushima, H. Oizumi and I. Nishiyama, *Proc. SPIE*, **2008**, *6923,* 69231J.
4. C.-T. Lee, M. Wang, N. D. Jarnagin, K. E. Gonsalves, J. M. Roberts, W. Yueh and C. L. Henderson, *Proc. SPIE*, **2007**, *6519,* 65191E.
5. S. Wurm, C. U. Jeon and M. Lercel, *Proc. SPIE*, **2007**, *6517*, 651705.
6. N. Dazai, et al., Japanese Patent Publication, 2008-308520A.
7. N. D. Jarnagin, et al., *J. Photopolym. Sci. Technol.*, **2006**, *19*, 719-725.
8. P. Hayoz, et al., World Intellectual Property Organization, WO 2009/047152 A1.
9. B.L. Henke, E.M. Gullikson, and J.C. Davis, "X-ray interactions: photoabsorption, scattering, transmission, and reflection at E=50-30000 eV, Z=1-92", *Atomic Data and Nuclear Data Tables*, **1993**, *54,* 181-342.
10. G. Pohlers, Y. Suzuki, N. Chan and J. F. Cameron, *Proc. SPIE*, **2002**, *4690,* 178-90.
11. T. Kozawa, S. Tagawa, T. Kai and T. Shimokawa, *J. Photopolym. Sci. Technol.*, **2007**, *20,* 577-83.
12. T. Tsuchimura, K. Shimada, Y. Ishijj, T. Matsushita and T. Aoai, *J. Photopolym. Sci. Technol.*, **2007**, *20,* 621-5.
13. R. Hirose, T. Kozawa, S. Tagawa, T. Kai and T. Shimokawa, *Jpn. J. Appl. Phys*., **2007**, *46,* L979-L81.
14. T. Kozawa, S. Tagawa and M. Shell, *Jpn. J. Appl. Phys.*, **2007**, *46.* L1143-L5.
15. T. Kozawa, S. Tagawa, H. B. Cao, H. Deng and M. J. Leeson, *J. Vac. Sci. Technol. B*, **2007**, *25,* 2481-5.

Chapter 7

General Conclusion

Novel oxime sulfonates were synthesized as photoacid generators (PAGs) for photolithography and their properties were examined in detail. Through this thesis work, following general conclusions were obtained: (1) oxime sulfonates show higher solubility due to their non-ionic character compared with conventional ionic PAGs, (2) photo absorbance characters can be tuned by designing chromophore structure, leading to an optimal total structure for certain wavelength of exposure light, (3) structure and acidity of the acid moiety can be selected, and (4) coating properties, thermal stability, and storage stability can be improved by designing chromophore structure.

In Chapter 2, a new class of PAGs were developed. They are non-ionic, halogen-free, highly soluble in PGMEA and thermally stable up to 140 °C in a phenolic matrix. The PAG's exhibit comparable or superior quantum yield to conventional PAG's upon g-line exposure. Photoresists comprising the new PAG's have good sensitivity at DUV, i-line and g-line exposure. Feasibility for use in chemically amplified positive and negative tone resists was demonstrated.

In Chapter 3, a new class of oxime sulfonate PAGs were developed for the CA photoresist application. As reported previously, (2-alkylsulfonyloxyimino-2*H*-thiophen-3-ylidene)-2-methylphenyl-acetonitriles were characterized as high sensitive PAG at the wide range of light source from g-line to DUV and enough thermal stability for the application of low activation energy resist. On the other hand, the new PAGs demonstrated superiority in thermal stability (> 188 °C in phenolic resin) and had an adequate absorption around 250 nm with good sensitivity for DUV light source of 254 nm, indicating feasibility of practical uses in both low activation energy and high activation energy CA resists.

Moreover, PAG E, a trifluoromethanesulfonate derivative for ArF photoresists, is also highly soluble in PGMEA and thermally stable up to 180 ^{o}C. The PAG exhibits superior efficiency to a conventional ionic PAG, BTIT, and a non-ionic PAG, NDIT, and comparable to TPST upon ArF exposure. Furthermore the microlithography simulator predicted the higher resolution limit and the wider process latitude than TPST.

In Chapter 4, the novel oxime sulfonate type of PAGs, HNBF, ONPF, and DNHF, were developed and found to be superior to the conventional ionic PAG, TPSNF, with respect to transparency and photo-efficiency at 193 nm. In addition, these non-ionic PAGs have the effect to increase the hydrophobicity of the photoresist formulation, and they are less risky for contamination

on the surface of the lens due to insolubility in water. Our results suggest that these non-ionic PAGs are suitable for ArF immersion lithography. They have different fluoroalkyl chains adjacent to the oxime moiety. This difference did not have a strong effect on photo-efficiency and transparency at 193 nm. However, the hydrogen atom at the end of fluoroalkyl chains of DNHF and ONPF played a role in improving the coating property.

In Chapter 5, non-ionic PAGs, DNHF and HNBF, developed for ArF photoresist applications are discussed. This chemistry of PAG can release strong acid (nonafluorobutanesulfonic acid) by ArF irradiation with higher efficiency in solution and in photoresist formulation comparing to the conventional ionic PAGs, such as TPSPB and BPIPB. Additionally DNHF and HNBF showed no leaching under a model immersion process while significant amount of TPSBP was eluted. It is concluded that DNHF and HNBF are the ideal PAGs not only for dry ArF but also for immersion lithography process.

In Chapter 6, it was investigated the fundamental properties of traditional PAG additive approach in EUV lithography with two different polymer platforms, PHS type and poly(methacrylates) type, and four sulfonium nonafluorobutanesulfonate PAGs, TPS, MDP, MMP, and MPP, compared with ArF and EB exposure techniques to understand the relationship between lithography results and photoresist materials.

While the significant difference in EB sensitivity was observed between the two polymer platforms, it was interestingly found that there was no clear difference in EUV sensitivity between the two. It indicates that acid generation mechanism of EB radiation and EUV exposure are clearly different each other and that the formulations showing inferior sensitivity in EB radiation might perform well in sensitivity under EUV lithography process.

Normalized P-parameter values of TPS, MDP, and MMP in the Copolymer B were interestingly close each other. It suggests the possibilities that acid the generation by the direct excitation of PAG under EUV radiation is dominant in Copolymer B matrix and that the acid generation efficiency from the three PAGs is in the same range.

As mentioned above, the author has successfully developed a new class of PAG chemistry, oxime sulfonate, and investigated its photoresist related properties in detail. This type of PAG will be continuously developed and widely employed in the photolithographic systems, e.g., ArF immersion lithography, due to the continuous and strong demand to PAG exhibiting higher lithographic performances than ever.

List of Publication

Chapter 2

1 Novel photoacid generators.

Asakura, T.; Yamato, H.; Ohwa, M..

Journal of Photopolymer Science and Technology, **2000**, *13*, 223-230.

2 Studies on Photodecomposition of an Oxime Sulfonate.

Asakura, T.; Yamato, H.; Tanaka, K.; Takahashi, R.; Kura, H.; Nakano, T..

Journal of Photopolymer Science and Technology, **2014***, 27*, 227-230.

Parts in this chapter are published as a conference proceeding;

3 Novel photoacid generators for chemically amplified resists with g-line, i-line, and DUV exposure.

Asakura, T.; Yamato, H.; Matsumoto, A.; Ohwa, M..

Proceedings of SPIE-The International Society for Optical Engineering, **2001**, *4345*, 484-493.

Chapter 3

4 Novel photoacid generators for chemically amplified resists.

Asakura, T.; Yamato, H.; Matsumoto, A.; Murer, P.; Ohwa, M,.

Journal of Photopolymer Science and Technology, **2003**, *16*, 335-345.

Parts in this chapter are published as a conference proceeding;

5 Novel photoacid generators for chemically amplified resists.

Yamato, H.; Asakura, T.; Matsumoto, A.; Ohwa, M.,

Proceedings of SPIE, **2002**, *4690*, 799-808.

Chapter 4

6 Evaluation of non-ionic photoacid generators for chemically amplified photoresists.

Asakura, T.; Yamato, H; Ohwa, M..

Journal of Photopolymer Science and Technology, **2006**, *19*, 335-342.

Parts in this chapter are published as a conference proceeding;

7 Non-ionic photoacid generators for chemically amplified photoresists: structure effect on

resist performance.

Yamato, H.; Asakura, T.; Ohwa, M..

Proceedings of SPIE, **2006**, *6153*, 61530F/1-61530F/9.

Chapter 5

8 Novel photoacid generators for ArF lithography.

Asakura, T.; Yamato, H.; Hintermann, T.; Ohwa, M..

Journal of Photopolymer Science and Technology, **2005**, *18*, 407-414.

Parts in this chapter are published as a conference proceeding;

9 Evaluation of a novel photoacid generator for chemically amplified photoresist with ArF exposure.

Asakura, T.; Yamato, H.; Hintermann, T.; Ohwa, M.

Proceedings of SPIE, **2005**, *5753*, 140-148.

Chapter 6

10 PAG study in EUV lithography.

Asakura, T.; Yamato, H.; Nishimae, Y.; Okada, K.; Ohwa, M.,

Journal of Photopolymer Science and Technology, **2009**, *22*, 89-95.

Other publications (not included in this thesis)

1 Asymmetric polymerization of methacrylates leading to a one-handed helix.
Okamoto, Y.; Nakano, T.; Mohri, H.; Asakura, T.; Hatada, K..
Polymer Preprints (American Chemical Society, Division of Polymer Chemistry), **1989**, *30*, 437-8.

2 Remarkable influence of tacticity on liquid crystallinity of polymethacrylates with biphenyl moiety as mesogenic group.
Okamoto, Y.; Asakura, T.; Hatada, K..
Chemistry Letters, **1991**, 1105-8.

3 Asymmetric polymerization of optically active phenyl-2-pyridyl-m-tolylmethyl methacrylate and stereomutation of the polymer.
Okamoto, Y.; Nakano, T. ; Asakura, T. ; Mohri, H. ; Hatada, K..
Journal of Polymer Science, Part A: Polymer Chemistry, **1991**, *29*, 287-9.

4 Synthesis of free-standing poly(3,4-ethylenedioxythiophene) conducting polymer films on a pilot scale.
Yamato, H.; Kai, K.; Ohwa, M.; Asakura, T.; Koshiba, T.; Wernet, W..
Synthetic Metals, **1996**, *83*, 125-130.

5 A novel photoacid generator for chemically amplified resist with ArF exposure.
Asakura, T; Yamato, H; Matsumoto, A; Murer, P. ; Ohwa, M.,
Proceedings of SPIE, **2003**, *5039*, 1155-1163.

6 Novel nonionic photoacid generator releasing strong acid for chemically amplified resists.
Yamato, H.; Asakura, T.; Hintermann, T.; Ohwa, M..
Proceedings of SPIE, **2004**, *5376*, 103-114.

7 **Oxime sulfonate chemistry for advanced microlithography.**
Yamato, H.; Asakura, T.; Nishimae, Y.; Matsumoto, A.; Tanabe, J.; Birbaum, J.-L.; Murer, P.; Hintermann, T.; Ohwa, M.,
RadTech Report, **2007**, *21*, 10-16.

8 Oxime sulfonate chemistry for advanced microlithography.

Yamato, H; Asakura, T; Nishimae, Y; Matsumoto, A; Tanabe, J.; Birbaum, J.-L.; Murer, P.; Hintermann, T.; Ohwa, M..

Journal of Photopolymer Science and Technology, **2007**, *20*, 637-642.

9 Non-ionic photoacid generators for chemically amplified photoresists.

Asakura, T.; Yamato, H.; Nishimae, Y.; Ohwa, M..

Proceedings of SPIE, **2007**, *6519*, 65192L/1-65192L/8.

10 Novel photoacid generators for ArF dry and immersion lithography: application-related properties. Asakura, T.; Yamato, H.; Nishimae, Y.; Ohwa, M.,

Journal of Photopolymer Science and Technology, **2007**, *20*, 465-471.

11 Chromophore effect of nonionic photoacid generators on resist performances.

Nishimae, Y.; Yamato, H.; Asakura, T.; Ohwa, M..

Journal of Photopolymer Science and Technology, **2008**, *21*, 377-381.

12 Non-ionic photoacid generators for chemically amplified resists: chromophore effect on resist performance.

Nishimae, Y.; Yamato, H.; Asakura, T.; Ohwa, M..

Proceedings of SPIE, **2008**, *6923*, 69233Q/1-69233Q/6.

ACKNOWLEDGMENTS

The author would like to express his sincere gratitude to Professor Dr. Tamaki Nakano, Catalysis Research Center, Hokkaido University, the academic supervisor of this thesis work, for his helpful and patient guidance, stimulating discussions and warm encouragement.

The research work for this thesis was initiated and was continued in Ciba Specialty Chemicals Ltd., Ciba Ltd. and BASF Ltd. The author wishes to exhibit his thanks to Dr. Masaki Ohwa, the former Head of Amagasaki R& D Center, BASF, the industrial supervisor of this thesis work, for his great support and encouragement at workplace. The experiments for this work were carried out under the direction of Dr. Hitoshi Yamato; the author is deeply grateful to him for his strong leadership and outstanding synthetic work which supported the framework of this thesis.

The author appreciates useful supports, valuable contributions and stimulating discussions from colleagues over the world including Dr. Akira Matsumoto, Dr. Yuichi Nishimae and Dr. Keizou Okada of Ciba Specialty Chemicals Japan K.K., Dr. Peter Murer, Dr. Tobias Hintermann, Dr. Reinhard Schulz and Dr. Hartmut Bleier, of Ciba Specialty Chemicals, Inc., Basel and Dr. Bill Brunsvold and Mr. Nadi Ergenc of Ciba US.

The author would like to express his thanks to Ms. Rumi Yamashita, Ms. Tamaki Kawai, Ms. Midori Masaki, Ms. Mariko Imano, Ms. Yayoi Kakiuchi, Ms. Yuka Kotake, Ms. Masako Takahashi, Ms. Masayo Ogino and Ms. Rumi Okumura for their experimental assistance.

The author appreciates useful support and discussions from Dr. Atsushi. Sekiguchi and Mr. Y. Miyake, Litho Tech Japan. The author would like to express his sincere thanks to Dr. Emil Piscani and Dr. Matt Malloy of Sematech North for their experiments on lithography with eMET.

The author would like to thank Associate Professor Dr. Yasuhito Koyama, Hokkaido University (Nakano group) for his advises on this thesis.

Finally, the author deeply appreciates his family; his wife, Seiko Asakura, his daughter, Kyoko Asakura, his son, Motokage Asakura, and his parents, Yoshikage and Sayoko Asakura, for their kind understanding and continuing emotional support.

This thesis is dedicated to the late Mr. Takushi Yamamoto (deceased August 2010), the author’s best friend.